POWER AND CHANNEL RESOURCE ALLOCATION IN COOPERATIVE MULTIPLE ACCESS SCHEMES

POWER AND CHANNEL RESOURCE ALLOCATION IN COOPERATIVE MULTIPLE ACCESS SCHEMES

By

Wessam Mesbah, B.Sc., M.Sc.

2008

A Thesis

Submitted to the Department of Electrical & Computer Engineering

and the School of Graduate Studies

in Partial Fulfilment of the Requirements

for the Degree of

Doctor of Philosophy

McMaster University

DOCTOR OF PHILOSOPHY (2008) McMaster University

(Electrical & Computer Engineering) Hamilton, Ontario

TITLE:	Power and Channel Resource Allocation in Cooperative Multiple Access Schemes
AUTHOR:	Wessam Mesbah B.Sc. (Communications and Electrophysics), M.Sc. (Communications Engineering), Alexandria University, Alexandria, Egypt.
SUPERVISOR:	Timothy N. Davidson, Associate Professor
NUMBER OF PAGES:	xx, 199

Dedications

To the best of mankind;

the prophet Muhammad, peace and blessings be upon him.

Abstract

In this thesis, we develop efficient algorithms for the jointly optimal power and channel resource allocation in different wireless cooperative multiple access systems. In addition, in some cases insight into the structure of the optimal allocation enables the development of modified cooperation schemes with better performance, and efficient algorithms are developed for jointly optimal power and channel resource allocation for these modified schemes too. The goal of the jointly optimal allocation algorithms developed in this thesis is to maximize the achievable rate regions of the schemes under consideration. Two cooperative channel models are considered; namely, the cooperative multiple access channel, and the multiple access relay channel.

For the cooperative multiple access channel, two relaying strategies are considered; namely decode-and-forward (DF), and amplify-and-forward (AF). For the cooperative multiple access channel with DF relaying, systems with full-duplex nodes and systems with half-duplex nodes are considered. In the case of full-duplex nodes, it is shown that the non-convex formulation of the power allocation problem can be simplified and re-cast in a convex form. In fact, closed-form expressions for the optimal power allocation for each point on the boundary of an achievable rate region are obtained. In the case of half-duplex nodes, we propose a modified version of an existing cooperation scheme that, with jointly optimal power and channel resource allocation, can achieve a large fraction of the achievable rate region of the full-duplex case. An

efficient algorithm for the jointly optimal power and channel resource allocation is also developed for that scheme.

For the cooperative multiple access channel with AF relaying, we consider optimal power and channel resource allocation for a system of two half-duplex source nodes that transmit orthogonal signals, and an efficient algorithm for the optimal power and channel resource allocation is developed. This efficient algorithm is based on a closed-form solution for the optimal power allocation for a given channel resource allocation and on showing that the channel resource allocation problem is quasi-convex. The analysis of the optimal power allocation for a given channel resource allocation shows that the existing scheme that we consider does not use the channel resource efficiently. Therefore, we propose a modified cooperation scheme that maintains the orthogonality property of the original scheme, but provides larger achievable rate regions than those provided by the original scheme.

For the multiple access relay channel, the optimal allocation of the relay power and the channel resource between different source nodes is considered in order to maximize the achievable rate region. Four relaying strategies are used; namely, regenerative decode-and-forward, non-regenerative decode-and-forward, amplify-and-forward, and compress-and-forward. For each of these strategies, an efficient algorithm is developed for the jointly optimal power and channel resource allocation. These algorithms are based on closed-form solutions for the optimal power allocation for a given resource allocation and on proving and exploiting the quasi-convexity of the joint allocation problem. The algorithms developed for the multiple access relay channel can be used for homogeneous (using the same relaying strategy for all users) or heterogeneous (using different relaying strategies with different users) relaying and for any number of users.

Acknowledgements

My first and foremost praise and gratitude is to God, "*Allah*", the Most Merciful, the Most Compassionate. Without the help of *Allah*, none of the work in this thesis would have come to light. However much I may write here, I would not be able to express the extent of gratitude that befits Him. I simply thank Him for allowing me to recognize His bounties and be thankful for them.

God has placed several great people in my life whose presence, love, and contributions have helped me to reach this point. I humbly acknowledge that I am unlikely to succeed in naming all of them or in giving those that I mention full credit for their impact.

I would like to start with a special thanks to my supervisor, Dr. Timothy N. Davidson. During my PhD program, he has helped me a lot in developing my self as an academic, and prepared me to reach further. I have benefited tremendously from his efforts in developing the intellectual and personal growth of his graduate students. As a supervisor, the results in this thesis would not have been possible without his engaged and insightful discussions. He has taught me many things, not least of them is clear technical writing. If my technical writing has been honed, then this is because of his tireless efforts (I am sure that I have missed a comma somewhere here and that he will correct it). As a person, he has always been a friend to his students, provided them with advice, and shown understanding at hard times. There are still many

things to learn from Dr. Davidson. Certainly, he has left an indelible mark.

I would like also to extend my thanks to my supervisory committee members, Dr. K. M. Wong and Dr. Jim Reilly, for their beneficial discussions, suggestions and for their contributions in refining the ideas in this thesis.

From the bottom of my heart I would like to thank my wife, Wafaa. During the the last four years, she has always shown patience, perseverance and continuous understanding. No one has been impacted by this thesis and my PhD studies more than her. She has chosen to live away from her family and move from 30° C, in Egypt, to −30° C, in Canada, just to support and provide me with help. I also want to thank her for writing the best paper in my life; my daughter "Jannah". There are no words that I can use other than "Thank You". I would also like to extend my gratitude to Jannah. Even though she may not be aware of it, but she has been providing me with daily portions of happiness that have had the greatest impact on developing this thesis.

I would also like to sincerely thank my father, Ali, for his continuous help, support, and trust. He has taught me many things. Most importantly, he has taught me how to make my own decisions. My deepest gratitude goes also to my mother, Aisha. Her uninterrupted love and encouragement had helped me tremendously in continuing in the academic track. She had always wished to see this achievement. I ask God to bless her and grant her the highest level of paradise. My thanks go also to my sister, Nermin, and my brother, Sherif. They have supported me all the way before and after graduation, and they have always encouraged me to excel in my studies.

I have been surrounded by numerous great friends that are hard to forget. I would like to thank all of them, including those in the Egyptian community at McMaster, the Muslim Student Association at McMaster, and the Muslim Association of Canada. In particular, I would like to thank Ahmed Khalil, Yaser Elbatawy, Usama Said, Ahmed

Abdelsameea, Omar Omar, and Marwan Abdeen for being very good brothers, and for providing me with help and advice. I would also like to thank Dr. Bakr for his encouragement and support, Muhammad Darwish for our interesting political discussions, Ahmed Kholaif and Ehab Elbadry for the hilarious squash times, Mahmoud Safar for being a good roommate and teaching me how to cook, Ramy Gohary for the hot political, religious, and technical discussions that used to end just before fighting, Muhammad El Tobgy for hosting me for the first week in his room, Muhammad Negm, Muhammad Swillam, Ahmed Farid, Amr Fawzy, Muhammad Rabie, and Nasser Mourad for the good friendship and Yiming Wang for the Chinese flavored friendship. My thanks and gratitude extend to my dear and old friends Ahmed Sadek and Kareem Seddik, of the University of Maryland College Park, for their support, hilarious phone calls, and for the beneficial technical discussions sometimes.

A special thanks to Dr. Y. Haddara. He has always been the elder brother to me and to the Muslim community in general. I want to thank him for his countless efforts to solve other people's problems.

Finally, I am so thankful to all my school teachers, university professors and teaching assistants, and to every individual who has taught me even one thing.

List of Acronyms

AF	Amplify-and-Forward
AWGN	Additive White Gaussian Noise
BC	Broadcast
CF	Compress-and-Forward
CSI	Channel State Information
D-BLAST	Diagonal Bell Labs Space-Time Architecture
DF	Decode-and-Forward
KKT	Karush-Kuhn-Tucker
LAST	LAttice Space-Time
LDPC	Low Density Parity Check
MAC	Multiple Access Channel
MAR	Multiple Access Relay
MARC	Multiple Access Relay Channel
MIMO	Multiple Input Multiple Output
NDF	Non-regenerative Decode-and-Forward
OFDM	Orthogonal Frequency Division Multiplexing
RCPC	Rate Compatible Punctured Convolutional
RDF	Regenerative Decode-and-Forward
SIC	Successive Interference Cancelation
SISO	Single Input Single Output
SNR	Signal-to-Noise Ratio

Contents

List of Figures

Chapter 1

Introduction

The ambition to implement multi-rate multimedia applications over wireless networks has resulted in a continuously increasing demand for high data rates with high quality of service. This demand has initiated a wide range of research toward the development of wireless communication systems that can cope with the requirements of different applications. One research direction that has recently gained significant interest is the development of cooperative wireless communication schemes. In particular, cooperative wireless communication systems have been shown to provide the potential for higher quality of service than conventional communication schemes [38,66]. However, the realization of these quality of service gains is contingent on the choice of the power and channel resource allocations. This thesis develops efficient algorithms for jointly optimal power and channel resource allocation for a variety of cooperation schemes. The objective of these optimal power and channel resource allocations is to maximize the achievable rate region of the scheme under consideration. The proposed algorithms gain their efficiencies from the exploitation of certain structural features of the problem that are not immediately apparent from the direct formulation of the allocation problem.

1.1 Wireless Communications

One of the limitations of wired communication systems is that the terminals must be tethered to the communication infrastructure, and this limits the mobility of the terminals to rather small areas. The recent development and deployment of wireless communication systems, has played a key role in removing this limitation, and has enabled the dramatic development of terrestrial and satellite communication systems for civilian and military applications. However, the advantages of wireless communication are accompanied by challenges that are inherent in the wireless medium.

In addition to the additive noise generated by the receiver components and the interference from other users that share the wireless medium, the key challenge in wireless systems arises from the nature of wave propagation in the wireless medium and the time-varying nature of this medium. In particular, one of the characteristics of wireless systems is that the transmitted signal propagates not only in the direction of the receiver, but also propagates in other directions with relative power dependant on the radiation pattern of the antenna. Due to this spatially dispersive transmission, the transmitted signal may reach the receiver along several different paths due to reflections from buildings and other surrounding objects. The paths have different lengths and different reflection characteristics and hence result in different attenuations, phase changes, and delays. For each frequency component of the transmitted signal, the components of the received signal that propagate along different paths may add constructively, resulting in a stronger signal, or destructively, resulting in a weaker signal. The relationship between the properties of the paths changes with changes in the wireless medium, including changes in the position of the transmitter or the receiver, changes in the position or the nature of the surrounding objects, and the weather conditions, and hence the overall attenuation of the channel varies in

time. This process of fluctuation of the received signal power level is called multi-path fading. In general, it is frequency dependent, since the signals propagating along different paths may add constructively for certain frequencies and destructively for other frequencies. The longer the delay spread (a measure of the difference in delay between different paths), the narrower the coherence bandwidth (the bandwidth over which the channel fading is approximately constant). If the delay spread is relatively short compared to the symbol duration, then all the frequency components of the transmitted signal will experience approximately the same attenuation, and hence the channel is said to be a flat fading channel. The baseband equivalent of a flat fading channel can be described using a single complex scalar. If the delay spread is significant relative to the duration of the transmitted symbols, the channel is said to be frequency selective. The discrete baseband model of a frequency-selective multi-path channel can be represented using a finite impulse response (FIR) filter. Transmission over a frequency-selective channel results in inter-symbol interference, because the symbols are received along different paths that interfere with each other. In order to focus on the design of cooperative communication strategies, the communication environment considered in this thesis will be of the flat fading type.

In addition to multi-path fading, there is another source of fading called large-scale fading. This fading is due to shadowing by large objects; such as buildings and hills. This effect causes the loss of the signal power and is typically frequency independent. The effects of shadowing differs from the effects of multi-path fading in their time scales. While shadowing effects may persist for multiple seconds or even minutes, the effect of multi-path fading changes much faster than that, and hence the shadowing is often called "slow fading" while the multi-path fading is often called "fast fading".

The channel impairments caused by the multi-path fading and shadowing may result in the loss of the information sent over the channel when the channel experiences

a severe fading. In order to combat the effects of channel fading, different diversity schemes have been proposed in the literature. The basic idea that underlies diversity schemes is to provide several independent channels for communication between the source and the destination, so that if some of them suffer from deep fading, the others can be used to detect the data at the destination. As the number of channels provided is increased, the probability that the information is lost is decreased. Diversity techniques may operate over time, frequency, space, or any combination there of. The simplest diversity scheme is repetition coding, in which the same data is repeated over different time slots, different frequency bands, or different transmitting antennas. However, repetition coding does not make efficient use of the degrees of freedom of the channel. For example, in time diversity systems it uses the time of several symbols to send only one symbol. In order to achieve the desired diversity gain and at the same time efficiently use the degrees of freedom of the channel, more sophisticated schemes are required.

Space diversity is of particular interest to this thesis due to its similarity with the diversity inherent in cooperative systems. Space diversity can be used alone or in conjunction with time and/or frequency diversity in order to increase the diversity order. It can be achieved by placing multiple antennas at the transmitter and/or the receiver. Fig. 1.1 depicts the 2×2 case, where there are two antennas at the transmitter and two antennas at the receiver. The separation of the antennas required in order for the paths to be close to being independent is dependent on the local scattering environment and on the carrier frequency. For example, the richer the scattering environment, the shorter distances over which the channels decorrelates (half to one carrier wavelength in the case of rich scattering).

Although space diversity is a technique that can be used to increase the diversity

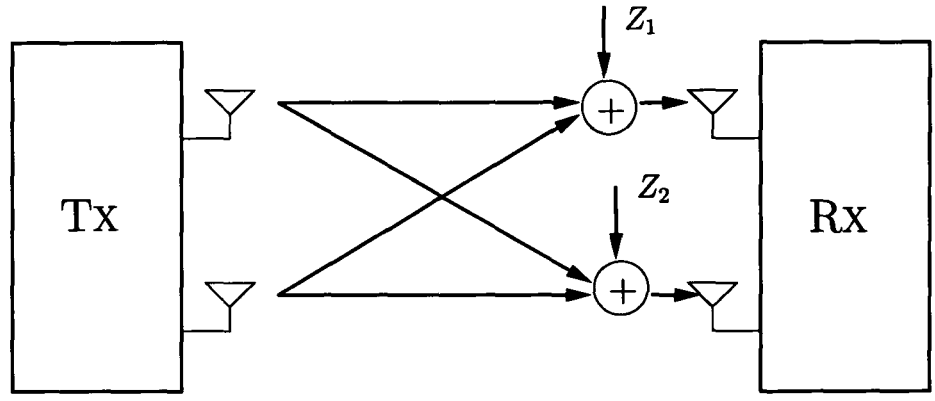

Figure 1.1: Space diversity in 2×2 MIMO system.

order without expending more communication resources (power, time, and bandwidth), it has its constraints. For example, space diversity requires the installation of more than one antenna at the transmitter and/or the receiver. While that may be reasonable at the base station of a cellular system, it may be rather difficult to implement on a mobile device, such as a cell phone, which is required to be of a small size. Therefore, alternatives to multiple antennas ought to be considered. Cooperative communication systems represent one such a technique. These systems can be viewed as providing a virtual antenna array, and hence the same diversity order as a space diversity system can be achieved without having to physically implement the antenna array [4, 38].

1.2 Cooperative Wireless Communications

In conventional wireless systems, the source nodes operate independently in the communication of their messages to their destination nodes. In contrast, in cooperative wireless systems, the source nodes collaborate in the transmission of their messages; e.g., [4, 34, 36, 38, 66, 67]. Moreover, the destination nodes may also collaborate in

decoding the messages transmitted from the source nodes. Such cooperation between source nodes and between destination nodes can improve the quality of service that the whole system is able to provide. The improvements in the quality of service can take the form of an increase in the diversity order, an increase in the achievable rates or a combination of the two [4, 85]. Cooperation between nodes is particularly promising in wireless systems, because the transmitted signals of other nodes can be overheard more or less for free.

The increase in diversity order provided by cooperation can be generally understood by considering the transmission of a single message from multiple nodes instead of only one node, thereby providing multiple paths for the message to be transmitted to the destination. Therefore, we can provide the benefits of space diversity without the need for physical antenna arrays.

To gain some insight into the increase in the achievable rate, consider a case in which one of a pair of nodes wishes to send information using a very small rate. This node does not have to use all of its power to transmit its own message, and hence this node can be viewed as having extra power available. If the extra power of this node is used to help other nodes in the transmission of their messages, then other nodes can transmit using higher rates. Therefore, cooperative systems can provide larger achievable rate regions than those provided by the conventional wireless systems.

Despite the benefits of cooperation for the network in general, relaying for other nodes has two disincentives for the relaying node; namely, energy consumption and possible delay in the transmission of its own data. Nevertheless, mechanisms for encouraging the nodes to relay for each other have been developed, including those based on pricing-and-credit incentives (e.g., [27]), where the network charges the nodes for using the channel and at the same time reimburses them for relaying.

Cooperative wireless systems can take several configurations. Block diagrams of

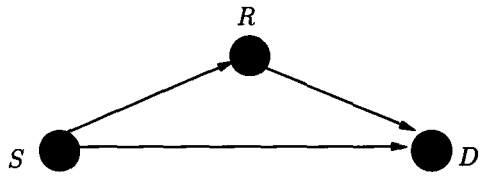

(a) Single relay channel

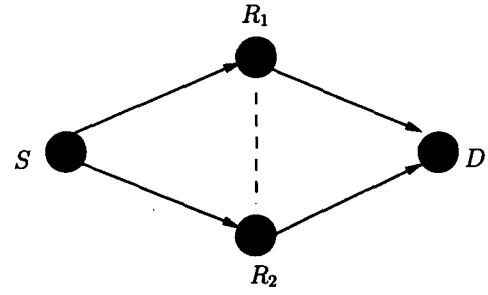

(b) Multiple relay channel

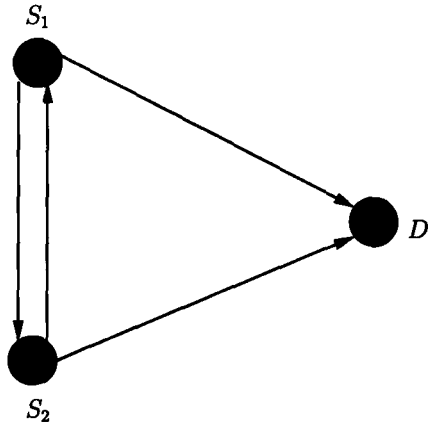

(c) Cooperative multiple access channel

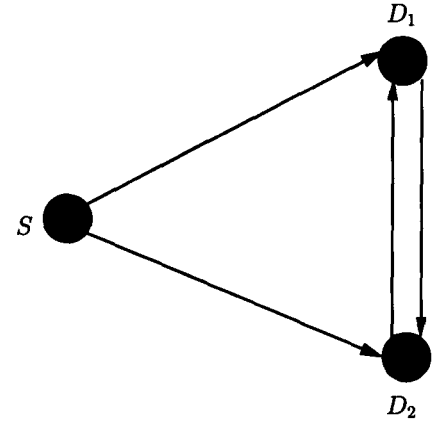

(d) Cooperative broadcast channel

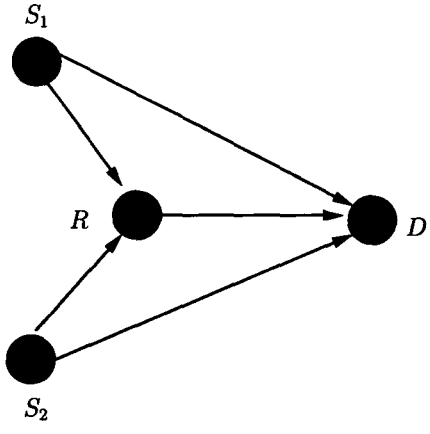

(e) Cooperative multiple access relay channel

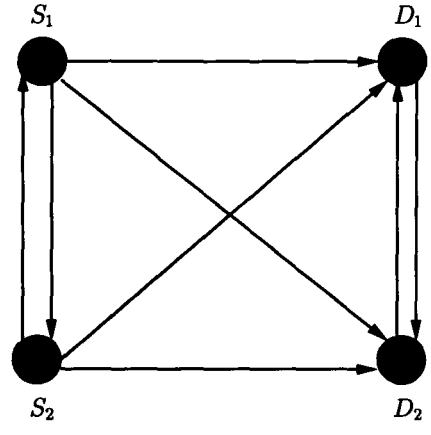

(f) Cooperative interference channel

Figure 1.2: Different cooperative architectures; inspired by [37].

some of these configurations are depicted in Fig. 1.2. These configurations cover, directly or as special cases, most of the known communication scenarios. For example, the simple relay channel in Fig. 1.2(a), encompasses several communication scenarios including the cooperative multi-cast channel, if the relay is also interested in obtaining the information from the source; and the conference channel if all the three nodes have information to transmit and at the same time want to receive information from the other two sources. Figs. 1.2(a) also specialize to conventional point-to-point communication if the relay is removed. In the absence of cooperation, the cooperative multiple access channel in Fig. 1.2(c) and the cooperative broadcast channel in Fig. 1.2(d) specialize to the conventional multiple access and conventional broadcast channels, respectively. Similarly, the multiple access relay channel in Fig. 1.2(e) specializes to conventional multiple access channel if the relay is removed, and the configuration in Fig. 1.2(f) specializes to interference channel if the nodes do not cooperate. The focus of this thesis is on the cooperative multiple-access channel and the multiple access relay channel, Figs 1.2(c) and 1.2(e), respectively. However, as will be explained in Chapter 6, some of the contributions presented herein also apply to more general topologies. In the scenario that are envisioned in this thesis, channel state information (CSI) is assumed to be available at the source nodes. By exploiting this channel knowledge, efficient algorithms for jointly optimal power and channel resource allocation are developed in order to maximize the reliable data rates of the considered communication schemes. The significant gains that joint optimization of power and the channel resource can offer are demonstrated.

1.3 Contributions and Thesis Organization

In this section, the contributions of this thesis are summarized,

1.3.1 Chapter 2

Chapter 2 provides a brief review of the technical foundations of the work presented in the thesis. In particular, the notions of channel capacity and achievable rate region are discussed, and a review of some of the literature on relaying and cooperative multiple access is provided. Finally, for later reference the concepts of convexity and quasi-convexity and the implications of having convex or quasi-convex optimization problems are presented.

1.3.2 Chapter 3

In the first part of Chapter 3, we consider the problem of power allocation in a two-user full-duplex[1] decode-and-forward (DF) cooperative multiple access scheme (see Fig. 1.2(c)) that employs superposition block Markov encoding [81]. In DF cooperation, the relay decodes the information of the source nodes, re-encodes it, and then transmits it to the destination. Although the achievable rate region for this cooperative scheme was obtained in [66], the power allocations that enable the scheme to achieve different points at the boundary of that region were not characterized. The key contribution in the first half of this chapter is the closed-form characterization of the optimal power allocation, for each of the users, required to achieve an arbitrary point on the boundary of the achievable rate region. The direct formulation of this power allocation problem is not convex, and hence can be rather awkward to solve. However, it will be shown that the direct formulation can be transformed into a convex formulation, and that closed-form solutions can be obtained for this convex formulation.

[1]Full-duplex nodes are those nodes that can transmit and receive simultaneously on the same channel.

In the second part of Chapter 3, half-duplex[2] cooperative multiple access schemes are considered. A block-based version of the scheme proposed in [67] is considered and the problem of jointly optimal power and channel resource allocation for that scheme is addressed. Although the power allocation problem for a given resource allocation is convex, the problem of jointly optimal power and channel resource allocation remains non-convex. In this chapter we prove that the jointly optimal power and channel resource allocation problem can be transformed into a quasi-convex problem, and hence, computationally efficient algorithms can be used to obtain the optimal solution. The numerical results show that the proposed half-duplex scheme achieves a large fraction of the achievable rate region of the full-duplex scheme while maintaining the practical constraint that the nodes are half-duplex.

The results of Chapter 3 have been published in [46, 47, 50].

1.3.3 Chapter 4

In the first part of Chapter 4, we consider maximizing the achievable rate region for a two-user orthogonal amplify-and-forward (AF) cooperative multiple access system. In AF cooperation the relay amplifies the signal received from the source nodes and transmits it to the destination. Both users have their own information to communicate in addition to the relaying of the other user's information. In order to avoid interference at the destination, the source nodes employ orthogonal transmission. By using the Karush-Kuhn-Tucker (KKT) optimality conditions to expose some of the structure of the optimal power allocation, it is shown that the problem of jointly optimal power and channel resource allocation for this scheme is quasi-convex. Moreover,

[2]Half-duplex nodes are those nodes that are not allowed to transmit and receive simultaneously on the same channel

we obtain a closed-form solution for the power allocation for a given resource allocation. Therefore, by combining this closed-form solution with the quasi-convexity of the maximum achievable rate in the resource allocation parameter, a simple efficient algorithm for the jointly optimal power and channel resource allocation is obtained.

Using the KKT optimality conditions, it is shown that at optimality both nodes will be idle during at least one of the time slots, and hence the scheme does not use the channel resources efficiently. Therefore, in the second part of Chapter 4, we propose a modified orthogonal amplify-and-forward cooperation scheme that uses the channel resources more efficiently. As expected, with the jointly optimal power and channel resource allocation, the modified scheme is shown to provide a larger achievable rate region than the original scheme. Chapter 4 also includes a discussion in which the available CSI is uncertain and a simple strategy that enables efficient optimization of a guaranteed achievable rate region is developed.

The results of Chapter 4 have been published in [48,49] and will appear in [45].

1.3.4 Chapter 5

In contrast to Chapter 3 and 4 that consider the cooperative multiple access configuration in Fig. 1.2(c), Chapter 5 considers the maximization of the achievable rate region for the orthogonal multiple access relay channel depicted in Fig. 1.2(e). In multiple access relay systems users do not act as relays for each other, rather there is a dedicated relay node that relays the transmitted information of the source nodes. In this chapter, the relay node works in half-duplex mode, and four relaying strategies are considered, namely, regenerative decode-and-forward (RDF), in which the relay re-encodes the information of the source node with the same code book used at the source node, and then transmits it to the destination; non-regenerative decode-and-forward (NDF), in which the relay re-encodes the information of the source node with a code

book that is different from that used at the source node, and then transmits it to the destination; amplify-and-forward (AF), which was described above in Section 1.3.3; and compress-and-forward (CF), in which the relay transmits a compressed version of the signal received from the source nodes. The achievable rate region is maximized by jointly optimizing the power allocation and the channel resource parameter. For regenerative and non-regenerative decode-and-forward strategies it is shown that the problem can be formulated as a quasi-convex problem, while for amplify-and-forward and compress-and-forward it is shown that the problem can be made quasi-convex if the signal to noise ratios of the direct channels are at least -3 dB. Moreover, for a given resource allocation, it is shown that in all cases the problem of power allocation is convex and we obtain a closed-form solution for that problem. The quasi-convexity result, along with the closed-form solutions for the power allocation, enables the development of a simple efficient algorithm for obtaining the jointly optimal power and channel resource allocation at any point on the boundary of the achievable rate region. The numerical results show that the joint allocation of power and the channel resource achieves significantly larger achievable rate regions than those achieved by power allocation alone with fixed channel resource allocation. The numerical results also demonstrate that assigning different relaying strategies to different users together with the joint allocation of power and the channel resources can further enlarge the achievable rate region.

The results of Chapter 5 have been published in [51, 52].

Finally, in Chapter 6 we conclude the thesis and propose some potential research problems for future work.

Chapter 2

Technical Background

This chapter provides a brief summary of some of the principles upon which the work presented in the subsequent chapters will be built. We will begin by discussing the notions of capacity and achievable rate region. Then we will describe the concept of cooperative communications, and will provide a brief literature review. Finally, we will provide a brief overview of convex and quasi-convex optimization.

2.1 Channel Capacity

A fundamental limit on the performance of a communication system is the channel capacity, which is the maximum data rate that can be communicated through the channel with arbitrary small error probability [69]. In the case of additive white Gaussian noise (AWGN) channels, in which the channel gain is constant, the capacity is simple to define. However, in the case of fading channels, the channel gain is a random variable, and hence the instantaneous capacity is also a random variable, and there is no single measure of that random variable that leads to a notion of capacity that is appropriate for all scenarios. The commonly-used notions of capacity

depend on the nature of the random changes of the fading process relative to the delay requirements of the application; that is on whether the fading is fast or slow. They also depend on the amount of channel state information that is available at the receiver and the transmitter.

The capacity of any channel is the maximum mutual information $I(X;Y)$ between the input signal X and the output signal Y, where the maximization is carried over all admissible distributions of the input signal [9]. In the next subsection we define the channel capacity for different single input single output (SISO) channel models. We start with a simple channel; the additive white Gaussian noise (AWGN) channel, and then proceed towards fading channels. Since the thesis focuses on channels whose responses are flat in frequency, the exposition will focus on those channels.

2.1.1 Capacity of SISO point-to-point channels

One of the simplest models for a communication channel is the SISO AWGN channel. The symbol-spaced discrete-time baseband equivalent model for this channel can be written as

$$y(m) = hx(m) + z(m), \tag{2.1}$$

where $x(m)$, $y(m)$, and $z(m)$ are complex scalar sequences that represent the input, the output and the noise at time instant m, respectively, and h is a complex scalar that captures the attenuation and phase rotation of the channel. The noise sequence $z(m)$ is modelled as an i.i.d sequence of zero mean circularly-symmetric complex Gaussian random variables of variance σ^2; i.e., $z(m) \sim \mathcal{CN}(0, \sigma^2)$. If the variance of the transmitted signal is limited to $\bar{P}$, i.e., $\mathbb{E}\{|x(m)|^2\} \leqslant \bar{P}$, then the capacity of the

channel in (2.1) can be shown to be [74]

$$C_{awgn} = \log\left(1+\frac{|h|^2\bar{P}}{\sigma^2}\right), \tag{2.2a}$$

$$= \log\left(1+|h|^2\text{SNR}\right) \qquad \text{bits per channel use,} \tag{2.2b}$$

where the transmission of a single (complex) symbol, $x(m)$, will be called a channel use. The term $\text{SNR} = \frac{\bar{P}}{\sigma^2}$ is the transmitted signal to noise ratio, while the term $\frac{|h|^2\bar{P}}{\sigma^2}$ is the signal to noise ratio of the received signal. The distribution of the input signal $x(m)$ that achieves the capacity in (2.2a) is the circularly symmetric Gaussian distribution with zero mean and variance $\bar{P}$.

In the model of (2.1), the channel gain is constant. While this is appropriate for a large class of narrowband wireline communication systems, in wireless systems the channel gain typically varies with time. This random variation is called fading, and the model in (2.1) can be extended to that case by writing the baseband representation of the channel output as

$$y(m) = h(m)x(m) + z(m), \tag{2.3}$$

where $h(m)$ is the fading process. We will assume that the receiver can perfectly track the fading process, i.e., that the receiver can operate coherently. This is a common assumption, since the coherence time in wireless systems is typically of the order of 100s symbols [74], and hence the channel varies slowly relative to the symbol rate and can be estimated using a training sequence or via a decision directed or an iterative method. Since the channel $h(m)$ changes randomly with time, this will cause random changes of the received SNR, and hence $\log\left(1+|h(m)|^2\text{SNR}\right)$ becomes a random variable. Depending on the channel knowledge at the transmitter and the nature of the channel fading, different measures of this random variable lead to fundamental limits on the data rate at which reliable communication can be achieved.

Fading channels are usually divided into two categories: slow fading channels and fast fading channels, depending on the relationship between the delay requirements of the system and the coherence time of the channel. If the delay requirement is short compared to the coherence time of the channel (i.e., the data should be decoded in periods shorter than the coherence time), then the fading process is said to be slow. (This is sometimes called quasi-static fading.) On the other hand, if the delay constraints are relaxed so that the delay requirements are much longer than the coherence time, then the fading process is said to be fast.

In this thesis, we will focus on the case of slow fading channels, and on systems in which channel state information (CSI) is available at the transmitter. The channel fading is assumed to be slow enough to allow the feedback of the channel gain from the receiver to the transmitter without expending significant amounts of power or the channel resources. Therefore, we will focus our discussion on the capacity measure that is appropriate for this scenario. However, for completeness we will also briefly discuss the capacity measures that are appropriate in slow and fast fading scenarios without channel knowledge at the transmitter.

In the case of slow fading the transmitted data is decoded in periods that are shorter than the coherence time, and hence the channel gain will be roughly static in these periods. Therefore, the capacity of the SISO channel for each channel realization h is $C(h) = \log(1 + |h|^2\text{SNR})$ bits per channel use. In systems in which the source node is aware of this channel realization (or $C(h)$), it can adjust its transmission scheme so as to operate at a rate approaching $C(h)$; [8, 19] Adopting such a scheme, the capacity over L coherence periods will be

$$\frac{1}{L}\sum_{\ell=0}^{L} C(h_\ell), \tag{2.4}$$

where h_ℓ is the channel gain for the ℓ^{th} coherence period and is i.i.d. across different

coherence periods. In the limit as $L \rightarrow \infty$, we obtain, via the law of large numbers, the ergodic capacity of slow fading channels with CSI at the source node:

$$\frac{1}{L}\sum_{\ell=0}^{L} C(h_\ell) \rightarrow \mathbb{E}_h\{C(h)\}, \tag{2.5}$$

where $\mathbb{E}_h\{.\}$ denotes the expectation over h.

In case of slow fading channels without CSI at the source node, there is a non-zero probability that the channel is in deep fade and that any transmitted data is lost. This constitutes a conceptual difference between the AWGN channel and the slow fading channel. In AWGN channel, one can transmit data at a positive rate (any rate $< C$) while making the error probability arbitrary small. In that sense, the capacity of the slow fading channel without CSI at the source node is zero, since there is a non-zero probability that the channel will be in a deep fade. Therefore, it may be more appropriate to consider a different measure for the performance limits of the slow fading channels without CSI at the source node. One such measure is the ϵ-outage capacity C_ϵ, which is the maximum rate at which the transmitter can transmit data while ensuring that the outage probability $P_{\text{out}}(R)$ is less than or equal to ϵ. The probability of outage is defined as

$$\begin{aligned} P_{\text{out}}(R) &= \mathbb{P}\{\log(1+|h|^2\text{SNR}) < R\} \\ &= \mathbb{P}\{|h|^2 < \frac{2^R-1}{\text{SNR}}\}. \end{aligned} \tag{2.6}$$

Solving $P_{\text{out}}(R) = \epsilon$, we obtain the result

$$C_\epsilon = \log(1+F^{-1}(1-\epsilon)\text{SNR}) \qquad \text{bits per channel use,} \tag{2.7}$$

where $F(.)$ is the cumulative distribution function of the random variable $|h|^2$. Therefore, an appropriate criterion for rate-optimal systems in slow fading channels without channel knowledge at the source node is to maximize the the outage capacity C_ϵ.

In contrast to slow fading channels, if the receiver can wait for several coherence periods before decoding the data, the fading scenario can be considered as being fast. When the codeword length spans several coherence periods, time diversity is available and the outage probability can be reduced. Consider the baseband model in (2.3), where $h(m) = h_\ell$ for the ℓ^{th} coherence period and is i.i.d. across different coherence periods. This is the so called block fading model. Suppose that coding is done across L such coherence periods. The capacity of the channel over these L coherence periods is

$$\frac{1}{L}\sum_{\ell=0}^{L}\log(1+|h_\ell|^2\text{SNR}). \tag{2.8}$$

If L is finite, then there will still be a non-zero outage probability for any target rate and we resort to the notion of outage capacity. However, if $L \rightarrow \infty$, the law of large numbers can be used to obtain an expression for the ergodic capacity of fast fading channels. The law of large numbers guarantees that

$$\frac{1}{L}\sum_{\ell=0}^{L}\log(1+|h_\ell|^2\text{SNR}) \;\rightarrow\; \mathbb{E}_h\left\{\log(1+|h|^2\text{SNR})\right\}. \tag{2.9}$$

Therefore, by coding over a large number of coherence periods, the source node can communicate reliably at rates approaching the ergodic capacity of the channel,

$$C = \mathbb{E}_h\{C(h)\} \qquad \text{bits per channel use.} \tag{2.10}$$

2.1.2 Beyond SISO channels

In the case of the simple AWGN SISO channel, closed-form expressions for the capacity of slow and fast fading channels can be obtained. It was shown in Section 2.1.1, that the average capacity of the slow fading channel with CSI at the transmitter (2.5) is equal to the ergodic capacity of the fast fading channel (2.10). However, this is not the case in general. In more complicated communication systems, there is no

closed-form expression for the capacity, rather the capacity is typically expressed in the form of

$$C(h) = \max_{q \in \mathcal{Q}} f(h, q), \tag{2.11}$$

where $f(h, q)$ is a function of the channel h and some design parameters q. For example, the capacity of an AWGN multiple-input multiple-output (MIMO) channel, $\mathbf{y}(m) = \mathbf{H}\mathbf{x}(m) + \mathbf{z}(m)$, can be written as [71]

$$C = \max_{\substack{\mathbf{Q} \succeq 0 \\ \mathrm{Tr}(\mathbf{Q}) \leqslant \bar{P}}} \log\left(\det(I + \mathbf{H}\mathbf{Q}\mathbf{H}^{\dagger})\right), \tag{2.12}$$

where $\mathbf{H}$ is the channel matrix, $\mathbf{Q}$ is the covariance matrix of the input, and $\mathbf{H}^{\dagger}$ is the Hermitian of the channel matrix. Cooperative communication systems fall in this category. Indeed, they resemble multiple antenna systems in which the antennas are not colocated.

In this category of systems, there is a difference between slow fading channels with CSI available at the transmitter and fast fading channels. In slow fading channels with CSI at the transmitter, the transmitter can maximize over the design parameters for each channel realization. Therefore the average capacity can be written as

$$\frac{1}{L}\sum_{\ell=0}^{L} \max_{q \in \mathcal{Q}} f(h_\ell, q) \rightarrow \mathbb{E}_h\left\{\max_{q \in \mathcal{Q}} f(h, q)\right\}. \tag{2.13}$$

In other words, in the case of slow fading and CSI at the source node, the design criteria for a rate-optimal system is based on maximizing the capacity for each channel realization. On the other hand, if the channel fading is fast, the transmitter would choose the design parameters in order to maximize the ergodic capacity; i.e.,

$$\max_{q \in \mathcal{Q}} \frac{1}{L}\sum_{\ell=0}^{L} f(h_\ell, q) \rightarrow \max_{q \in \mathcal{Q}} \mathbb{E}_h\left\{f(h, q)\right\}. \tag{2.14}$$

Therefore, the rate-optimal system design criteria in case of fast fading is to maximize the ergodic capacity. It is interesting to note the difference in the ordering of the

expectation and the max operator between the slow fading with channel knowledge at the transmitter and the fast fading case.

2.1.3 Achievable Rate

While the concept of capacity is used to measure the fundamental limits of a communication system with certain capabilities, the notion of achievable rate is used to capture the performance limits of a particular coding scheme over that system. The achievable rate of a particular scheme is the maximum rate with which that scheme can transmit data with an arbitrary small error probability, and by definition, it is a lower bound on the capacity of the channel. The closer the achievable rate of a certain scheme to the capacity of the channel, the more efficient the coding scheme is deemed to be, and if the achievable rate of a scheme coincides with the capacity of the channel, the scheme is said to be capacity achieving.

In many cases, it is substantially easier to determine the achievable rate of a particular coding scheme than it is to determine the capacity. (The converse of the capacity proof is often the bottleneck.) For example, for relay channels [10] and for cooperative channels [20, 34] an expression for the capacity has, in many cases, remained elusive. However, in cases such as these, the lower bounds on capacity provided by carefully chosen coding schemes and upper bounds obtained by alternative means are often useful guides as to where the capacity lies. In deed, some capacity proofs can be constructed by showing that these upper and lower bounds coincide.

2.1.4 Communication system capabilities

In order to obtain the capacity of a communication system or an achievable rate for a communication scheme, the capabilities of the components of the communication

system have to be taken into consideration. This is often a simple thing to do in single-user systems, but the greater flexibility of multi-user systems means that there are more issues to be considered. Of particular interest in this thesis is whether the relaying nodes operate in full-duplex or half-duplex mode, and whether the receiver is capable of jointly decoding the signals from several transmitters or it uses only per-user decoding. These two issues are discussed below.

Full-duplex nodes are nodes that can simultaneously transmit and receive over the same channel, and hence they efficiently use the communication resources provided by the channel. However, because the transmitted signal typically has much higher power than the received signal, full-duplex cooperation requires a high degree of electrical separation between the transmit and receive modules and may require the use of echo cancelation algorithms to mitigate the effect of the transmitted signal. Therefore, the practical implementation of such nodes is difficult to achieve. On the other hand, half-duplex nodes are nodes that do not simultaneously transmit and receive over the same channel, and hence they divide their available resources between the transmission and reception processes. Although, half-duplex nodes are easier to implement than full-duplex nodes, they do not use the channel resources as efficiently as full-duplex nodes.

Depending on the decoding capabilities of the receiver node, the source nodes of a multi-user system may transmit on the same channel or they may transmit on orthogonal channels. Transmission on the same channel requires a more complicated receiver that is capable of jointly decoding all the transmitted signals from different source nodes. In orthogonal transmission, different source nodes use orthogonal channels (orthogonal time slots or orthogonal frequency bands) to transmit their data and the receiver needs only to perform per-user decoding. While orthogonal transmission reduces the efficiency with which the channel resources are used, it allows for a

simpler receiver structure.

2.1.5 Capacity Region of SISO Multiple Access Channels

In Sections 2.1.1 and 2.1.2, we discussed limits on the data rates of single user systems. In case of systems involving multiple users (e.g., multiple access and broadcast channels), the fundamental limits of the system are described by a capacity region, rather than a scalar value. For an N-user system, the capacity region is the region in $\mathbb{R}^N$ that is the closure of all rate vectors that can be communicated through the channel with arbitrary small error probability. In the same sense, the achievable rate region of a particular multiuser communication scheme represents the closure of all achievable rate vectors of that scheme.

The main focus of this thesis is on cooperative approaches to multiple access communications, in which multiple nodes wish to cooperate in the transmission of their messages to a common destination node. However, it is beneficial to start with the definition of the capacity region of the non-cooperative (conventional) multiple access channel (MAC).

The baseband model for a slow-fading multiple access channel with two users can be written as

$$y(m) = h_1 x_1(m) + h_2 x_2(m) + z(m), \tag{2.15}$$

where x_1 and x_2 are the transmitted signals from Users 1 and 2, respectively, with power constraints $\bar{P}_1$ and $\bar{P}_2$, h_1 and h_2 are the channel gains, and $z \sim \mathcal{CN}(0, \sigma_0^2)$ is the zero-mean circularly symmetric complex white Gaussian noise at the receiver. Since all users share the same bandwidth, there will be a tradeoff between the rates of reliable communication of the users; i.e, if one user needs to increase its rate then the maximum rate of the other user may have to be decreased. The capacity region of this multiple access channel is characterized by all the rate pairs satisfying the

following three constraints [9]:

$$R_1 \leqslant \log\left(1+\frac{|h_1|^2\bar{P}_1}{\sigma_0^2}\right), \tag{2.16}$$

$$R_2 \leqslant \log\left(1+\frac{|h_2|^2\bar{P}_2}{\sigma_0^2}\right), \tag{2.17}$$

$$R_1+R_2 \leqslant \log\left(1+\frac{|h_1|^2\bar{P}_1+|h_2|^2\bar{P}_2}{\sigma_0^2}\right). \tag{2.18}$$

The three constraints have a natural interpretation. The first two constraints state that the rate of any user in the multiple access channel can not exceed the rate that it would achieve in a single-user system (i.e., in the absence of interference from the other user). The constraint in (2.18) states that the sum capacity of both users can not exceed the point-to-point capacity of an AWGN channel with the sum of the received power of both users.

An example of the capacity region of a non-cooperative multiple access channel is plotted with the solid line in Fig. 2.1. As shown in the figure, the three constraints construct three lines that bound the capacity region. Those three lines along with the horizontal and vertical axes give the well known pentagon shape of the multiple access capacity region. Reliable communication at rates on the boundary of the region can be attained by variations on a scheme in which each user encodes its data using a capacity achieving AWGN channel code and the receiver decodes the information from the users using successive interference cancelation (SIC). For example, in Fig. 2.1, Point A can be achieved by first decoding User 1 while considering User 2 as interference, subtracting the component of the received signal arising from the message of User 1, and then decoding User 2. On the other hand, Point B can be achieved by decoding User 2 first. Points on the line segment connecting A and B can be achieved by time sharing between Points A and B.

Fig. 2.1 also shows the capacity region that would be obtained if the users were constrained to transmit on orthogonal channels. Transmission on orthogonal channels

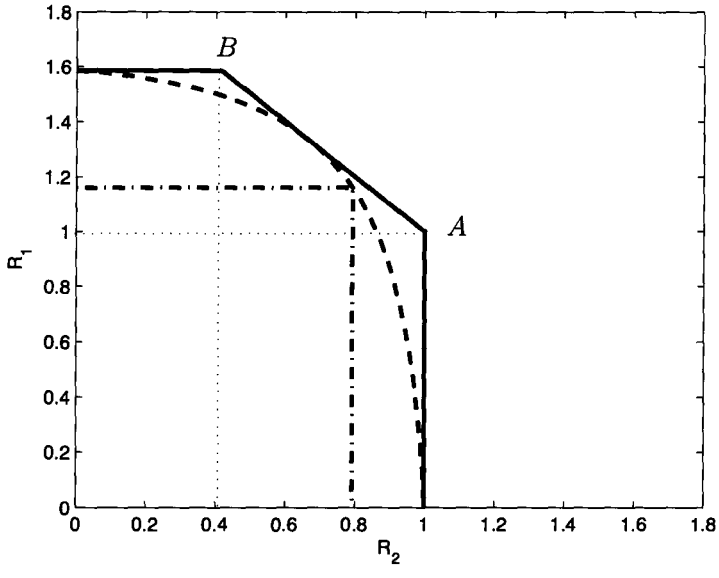

Figure 2.1: Capacity regions for a two-user AWGN multiple access channel with orthogonal (dashed), non-orthogonal (solid) transmission and the achievable rate region of orthogonal transmission with fixed $r = \frac{1}{2}$ (dash-dot), in case of $|h_1| = |h_2| = 1$, $\sigma_0^2 = 1$, $\bar{P}_1 = 2$, and $\bar{P}_2 = 1$.

requires dividing the radio resource (time or bandwidth) between the two users. In that case the capacity region can be characterized with the following two constraints

$$R_1 = r \log\left(1 + \frac{|h_1|^2 \bar{P}_1}{r\sigma_0^2}\right), \tag{2.19}$$

$$R_2 = (1-r) \log\left(1 + \frac{|h_2|^2 \bar{P}_2}{(1-r)\sigma_0^2}\right), \tag{2.20}$$

where $r \in [0,1]$ is the radio resource allocation parameter that determines the fraction of the resource (e.g., time, or bandwidth) that is allocated to Node 1. To obtain each point on the dashed curve, the value of r must be optimized. The dash-dot curve in Fig. 2.1 shows the achievable rate region for the case in which r is fixed to $1/2$. It is clear from Fig. 2.1 that the capacity region of orthogonal transmission is smaller than the capacity region of non-orthogonal transmission. However, it is also clear from Fig. 2.1 that optimization over the radio resource parameter yields much larger achievable rate region than simply setting $r = 1/2$. Furthermore, when orthogonal transmission is employed, optimal decoding can be performed in a per-user fashion and that significantly simplifies the receiver.

Throughout the thesis, the goal will be to maximize inner bounds on the capacity regions (i.e., achievable rate regions) of different cooperative multiple access schemes. In the next section we provide a brief literature review on different cooperative systems and their capacity or achievable rate regions.

2.2 Cooperative Systems

The basic building block of cooperative systems is the three-node relay channel model [77], shown in Fig. 2.2. The general case of this relay channel was first examined in [63, 75, 76]. Later, in [10], the capacity for the class of degraded relay channels was determined. Moreover, in [10] lower bounds (achievable rates) for the

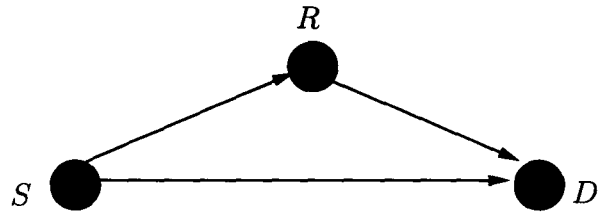

Figure 2.2: Three-node relay channel.

general relay channel were developed using three different coding schemes; namely, facilitation, cooperation (currently known as decode-and-forward), and observation (currently known as compress-and-forward).

Various extensions of the system in Fig. 2.2 to the case of multiple relay channels have appeared in [13,17,18,20,59,64] and in [43,44], where the problem of optimum power and bandwidth allocation for a system of one source, one destination, and many relay nodes was solved for the coherent combining and orthogonal transmission cases. Another variant is the multiple access relay channel (see Fig. 2.3) in which multiple information sources communicate to a single destination with the assistance of a single relay. Some work on this channel has appeared in [34,35,60–62], where bounds on the capacity of such channels were obtained, while in [68] the optimal power allocation for multiple access relay channels was obtained. In Chapter 5 of this thesis (see also [51]), an efficient algorithm for jointly optimal power and channel resource allocation for multiple access relay channels is developed.

Cooperative multiple access systems, in which all nodes have their own data to transmit, but are also prepared to act as relays for each other, were examined late 1970s [33] and early 1980s [6,11,81]. These systems were also called multiple-access channels with feedback. Cover and Leung [11] considered the case of a two-user MAC with the channel output being known to both users and they characterized the achievable rate region for that case. Carlieal [6], and Willems and Van Der Meulen

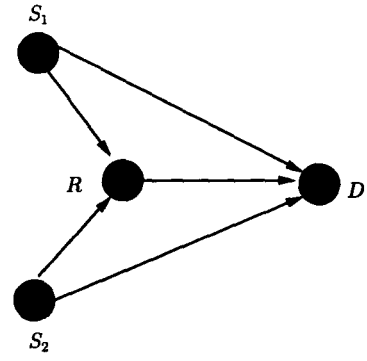

Figure 2.3: Multiple access relay channel.

[79], showed that restricting the feedback of the channel output to only one of the source nodes is sufficient to achieve the same rate region obtained in [11]. The capacity region of a two-user MAC channel with partial cooperation between the users was obtained in [78], while the capacity region of a two-user MAC, in which one or both of the encoders crib from each other and learn the channel input to be transmitted by the other encoder, was obtained by Willems and Van Der Meulen [80]. The capacity of the MAC with cribbing encoders represents an upper bound on the capacity of cooperative multiple access channels, since the cribbed information at both encoders is assumed to be obtained without expending any channel resources. In [81], a communication scheme based on superposition block Markov encoding and backward decoding was proposed for the MAC with generalized feedback and its achievable rate region was shown to improve upon that of [6]. This model can be considered as a generalization of the cooperation coding scheme in [10]. Recently, Sendonaris, Erkip and Aazhang [66] have investigated the application of the generalized feedback model of [81] to fading channels with additive white Gaussian noise. In [66], it was assumed that channel state information for each link is known to the receiver on that link, and the phase of the channel state is also known at the source nodes. The assumption of phase knowledge at the source nodes allows the source nodes to cancel that phase rotation

and obtain a coherent combining gain at the destination node. It was shown that this model achieves significantly larger achievable rate regions than those obtained in the non-cooperative MAC with the same constraints on the users' transmission power. Equivalently, for a give rate vector, cooperative multiple access can cover larger areas than the non-cooperative MAC with the same power, or can cover the same area with lower power.

In [38], different protocols were exploited in conjunction with relaying. The first protocol is "fixed relaying" where the relay always relays the message of the source node with the same relaying strategy, e.g., decode-and-forward (DF), amplify-and-forward (AF), or compress-and-forward (CF). The second protocol is called "selection relaying". In that protocol the source node and the relay are allowed to select between cooperative or non-cooperative transmission based the measured SNR between them. The third protocol is called "incremental relaying" and it improves the spectral efficiency by relaying only when necessary using a limited feedback from the destination to acknowledge success or failure of the reception of the message. Therefore, incremental relaying avoids relaying all the time saving the available resources. In this thesis, it is assumed that cooperation with a certain relaying strategy is selected. Therefore, the algorithms proposed in this thesis can be exploited either in fixed relaying protocol or in the other two protocols when cooperation is selected.

2.3 Approaches to Maximizing The Achievable Rate Region

In point-to-point communications, the achievable rate of a communication scheme is a scalar, and hence the maximization of this scalar is straight forward. In contrast, the achievable rates of multi-user communication systems are vectors with dependent

components. Therefore, there will be a trade-off between different components of those vectors resulting in a region of achievable rates. The achievable rate regions that have been obtained for different cooperative wireless channels can be maximized by optimizing different parameters like the power components and/or the channel resource allocation parameter. There are two approaches that can be used to maximize the achievable rate region of a communication system. The first approach is to maximize a weighted sum of the rates of different users; e.g., for a case of two users,

$$\max \quad \mu_1 R_1 + \mu_2 R_2, \tag{2.21}$$

where the maximization is done over the available system resources, (e.g., power, time, or bandwidth), subject to some constraints on those resources. Here, R_i is the rate of source node i, and the constant parameter μ_i is the weight of that rate. Typically, the weights are normalized so that $\sum_i \mu_i = 1$. This maximization results in the optimal power and channel resource allocation at one point on the boundary of the achievable rate region. This point maximizes the achievable rate region in the direction $\frac{\mu_1}{\mu_2}$. Therefore, by changing the values of the weights, we can maximize the achievable rate regions in different directions and obtain the jointly optimal power and channel resource allocation at different points on the boundary of that region.

An alternative approach to obtain the jointly optimal power and channel resource allocation at each point on the boundary of the achievable rate region is to maximize one of the rates subject to a given target value of the other rate; e.g., for a case of two users, the problem can be written as

$$\begin{aligned} &\max && R_1 \\ &\text{subject to} && R_2 \geqslant R_{2,\text{tar}}. \end{aligned} \tag{2.22}$$

This approach maximizes the achievable rate region in the direction of R_1 axis, as

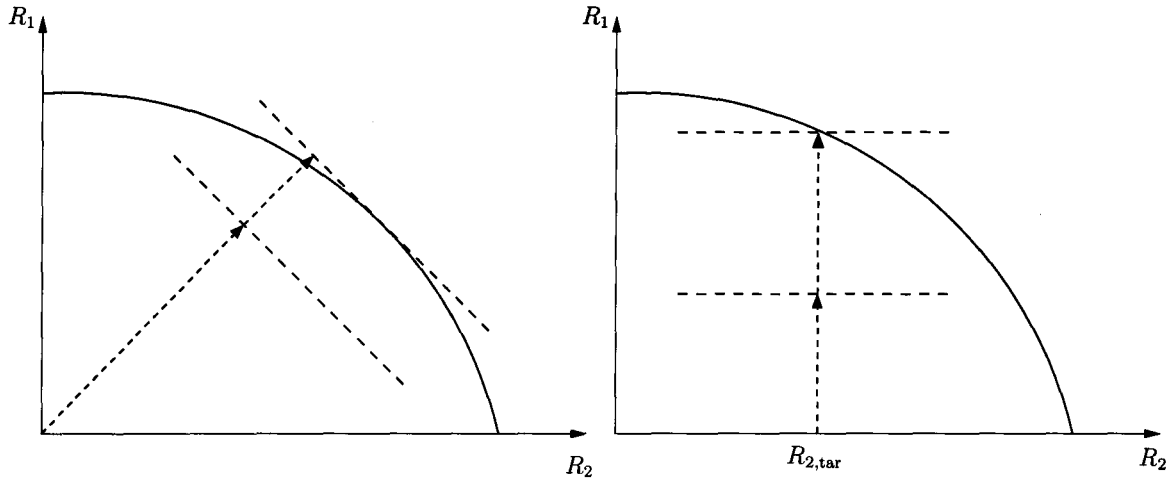

Figure 2.4: Two approaches to maximize the different points on the boundary of the achievable rate region.

shown in Fig. 2.4, and by changing the value of the target rate, different points on the boundary of the achievable rate region can be obtained, along with their jointly optimal power and channel resource allocations.

Each of the two approaches has its applications. For example, the first approach can be used when it is desirable to maximize the sum rate of the system regardless of the fairness of the distribution of the components of that sum between the users. In contrast, the second approach may be of particular interest in heterogeneous systems, in which some of the users have applications that require fixed data rate, (e.g., voice, video), while other users have applications that work using the best effort data rate, e.g., file transfer, text messaging. In this thesis, it will be shown that adopting the second approach facilitates the development of efficient algorithms for jointly optimal power and resource allocation. It will also be shown that, under certain conditions, the solution to the problem in (2.21) can be obtained by iteratively solving the problem in (2.22).

In both approaches the maximization is either done over power or jointly over

power and channel resource parameters. In cooperative systems, each source node transmits a signal that is composed of different components. For example, in a two-user cooperative system the signal of each source node may contain its own data and the data that is being relayed for the other source node. Furthermore, each source node may divide its own data into direct component which is transmitted directly to the destination and a cooperative component which is transmitted to the other user in order to be relayed to the destination. Therefore, a natural question arises: How should each source node allocate its power between these components? It should be clear that each power allocation corresponds to a different achievable rate vector. Also, changing the power allocation of one user affects the achievable rate of the other user which further complicates the problem. The situation is somewhat simpler in orthogonal cooperative systems, in which radio resources are divided between different source nodes so that they transmit on orthogonal channels. Moreover, in half-duplex systems the source nodes divide the available radio resources between transmission and reception. Therefore, in orthogonal half-duplex systems resource allocation represents another important process in the maximization of the achievable rates of the source nodes.

In this thesis, the channel model of the wireless cooperative systems is assumed to be slow fading. That is, the coherence time of the channel is long relative to the delay requirements of the system. This assumption allows feedback of the gain of different channels without expending a significant amount of the channel resources. Furthermore, we consider rate maximization using a short term average or fixed power constraint.[1]

The goal of this thesis is to maximize the achievable rate regions of different

[1]The choice between short term average and fixed power constraint depends on whether the different components of the transmitted signal are sent on different time slots or at the same time slot.

cooperative schemes. This requires solving one of the problems in (2.21) and (2.22). The development of efficient algorithms to solve these problems can be facilitated by showing that the problem is convex or quasi-convex, or by transforming the problem into one of these classes. In Section 2.4, we briefly review the concepts of convexity and quasi-convexity, and why it is important to transform the optimization problem into a convex or quasi-convex problem.

2.4 Convex Functions and Quasi-convex functions

The general form of any optimization problem consists of an objective function that needs to be maximized or minimized and a number of constraints. Mathematically, it can be represented as

$$\min_{\mathbf{x}} \quad f_0(\mathbf{x}) \tag{2.23a}$$

$$\text{subject to} \quad f_i(\mathbf{x}) \leqslant a_i \qquad i = 1, 2, \ldots, m \tag{2.23b}$$

$$h_i(\mathbf{x}) = b_i \qquad i = 1, 2, \ldots, n, \tag{2.23c}$$

where the vector $\mathbf{x}$ is the optimization variable, $f_0(\mathbf{x})$ is the objective function, $f_i(\mathbf{x})$ for $i = 1, 2, \ldots, m$ are the inequality constraint functions, $h_i(\mathbf{x})$ for $i = 1, 2, \ldots, n$ are the equality constraint functions, and a_i and b_i are constants. The globally optimal value of $\mathbf{x}$ is usually denoted as $\mathbf{x}^*$. In order for $\mathbf{x}^*$ to be a global minimum, it has to satisfy that for any $\mathbf{x} \neq \mathbf{x}^*$, $f_0(\mathbf{x}) \geqslant f_0(\mathbf{x}^*)$.

The importance of having convex or quasi-convex problems lies in the fact that there are efficient algorithms that can solve problems of those classes reliably and in an efficient manner; e.g., interior point methods and the bisection method [5]. A fundamental property of convex optimization problems is that any locally optimal point is also (globally) optimal.

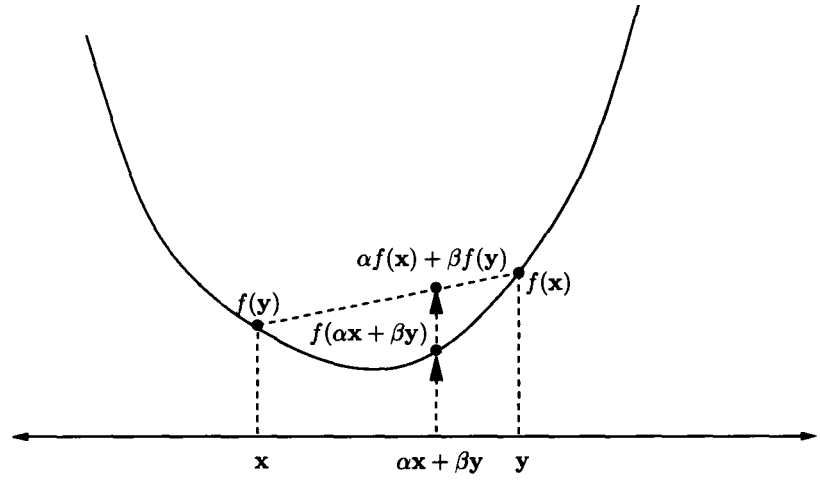

Figure 2.5: An example of a convex function.

In order for a function to be convex, it has to satisfy the following constraint

$$f(\alpha\mathbf{x} + \beta\mathbf{y}) \leqslant \alpha f(\mathbf{x}) + \beta f(\mathbf{y}), \tag{2.24}$$

for any $\mathbf{x}$ and $\mathbf{y}$, where $\alpha + \beta = 1$, $\alpha \geqslant 0$ and $\beta \geqslant 0$. A function $f(\mathbf{x})$ for which $-f(\mathbf{x})$ is convex is said to be concave. In general, convex problems are mathematically defined as in (2.23), with each $f_i(\mathbf{x})$ being convex and each $h_i(\mathbf{x})$ being linear.

Similar to the minimization problems, if we have a maximization problem written as

$$\max_{\mathbf{x}} \quad f_0(\mathbf{x}) \tag{2.25a}$$

$$\text{subject to} \quad f_i(\mathbf{x}) \leqslant a_i \qquad i = 1, 2, \ldots, m \tag{2.25b}$$

$$h_i(\mathbf{x}) = b_i \qquad i = 1, 2, \ldots, n, \tag{2.25c}$$

then in order for this problem to be a concave maximization problem, the objective function must concave, the inequality constraint functions must be convex, and the the equality constraint functions must be linear. Note also that maximizing $f_0(\mathbf{x})$ is equivalent to minimizing $-f_0(\mathbf{x})$.

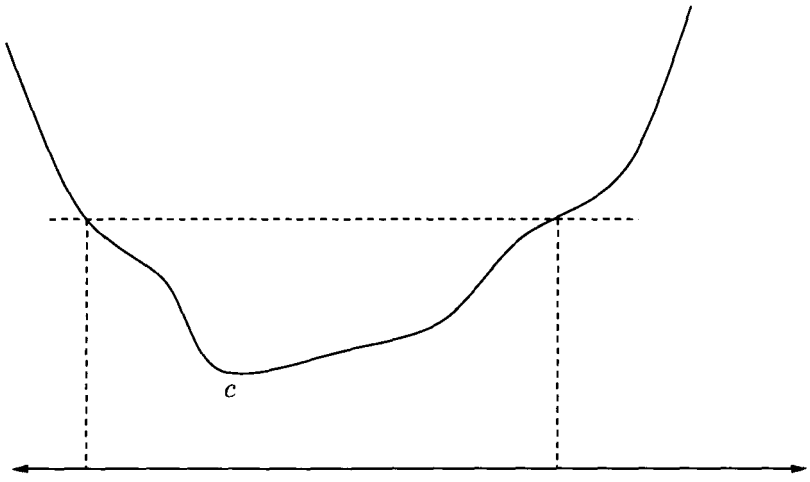

Figure 2.6: An example of a quasi-convex function.

Similar to convex problems, the class of quasi-convex problems is interesting, because there exist efficient algorithms to solve this class of problems [5]. The conditions required for a problem to be quasi-convex are related to those of the convex problem. An optimization problem of the form of (2.23) is said to be a quasi-convex problem if the objective function is quasi-convex, the inequality constraint functions are convex or quasi-convex, and the equality constraint functions are linear.

There are several ways to check whether a function $f(\mathbf{x})$ is quasi-convex or not. In this thesis, we use two criteria that are based on the sub-level sets[2] of the function and the second order differentiation of the function:

1. A function $f(\mathbf{x})$ is quasi-convex if and only if the sub-level sets of the function f are convex.

2. A twice differentiable function $f(\mathbf{x})$ is quasi-convex if for all $\mathbf{x}, \mathbf{y} \in \text{dom} f$

$$\mathbf{y}^T \nabla f(\mathbf{x}) = 0 \Rightarrow \mathbf{y}^T \nabla^2 f(\mathbf{x}) \mathbf{y} > 0. \tag{2.26}$$

[2]The α sub-level set of a function $f(\mathbf{x})$ is the set of all vectors $\mathbf{x}$ that satisfy that $f(\mathbf{x})$ is below a certain level α, i.e, $f(\mathbf{x}) \leqslant \alpha$. The super-level sets are defined in a similar way using $f(\mathbf{x}) \geqslant \alpha$.

If one wants to determine whether a function is quasi-concave, then the super-level sets should be used in the first criteria instead of the sub-level sets, while in the second criteria the condition would be

$$\mathbf{y}^T \nabla f(\mathbf{x}) = 0 \Rightarrow \mathbf{y}^T \nabla^2 f(\mathbf{x}) \mathbf{y} < 0. \tag{2.27}$$

For general optimization problems that have differentiable objectives, constraint functions and obey a certain regularity condition, Karush, and Kuhn and Tucker developed a set of necessary conditions for the optimal solution of the problem. These conditions are called KKT conditions [5]. If the problem is convex and certain constraint qualifications hold, then these conditions are also sufficient. In particular, if the problem is convex and satisfies Slater's condition that the feasible set has a non-empty relative interior, then the KKT conditions are necessary and sufficient. The KKT conditions can play an important role in solving the optimization problem. In a few cases, the KKT conditions can be solved analytically to obtain the optimal solution of the optimization problem. Moreover, many of the algorithms used to obtain the optimal solution of an optimization problem can be interpreted as iterative methods of solving the KKT conditions. In Chapter 4, the KKT conditions will be exploited to gain insight into the structure of the optimal power allocation and it will be shown that obtaining this structure will help to obtain closed-form solutions to the optimal power allocations, and in proving the quasi-convexity of the resource allocation problem.

Chapter 3

Optimized Power Allocation For Pairwise Cooperative Multiple Access

In this chapter, the class of pairwise decode-and-forward cooperative multiple access schemes in which channel state information is available at the transmitters is considered. The natural formulation of the power allocation problem for full-duplex cooperative schemes is not convex. It is shown herein that this non-convex formulation can be simplified and re-cast in a convex form. In fact, closed-form expressions for the optimal power allocation for each point on the boundary of an achievable rate region are obtained. In practice, a half-duplex cooperative scheme, in which the channel resource is partitioned in such a way that interference is avoided, may be preferred over a full-duplex scheme. The channel resource is often partitioned equally, but we develop an efficient algorithm for the joint allocation of power and the channel resource for a modified version of an existing half-duplex cooperative scheme. We demonstrate that this algorithm enables the resulting scheme to attain a

significantly larger fraction of the achievable rate region for the full-duplex case than the underlying scheme that employs a fixed resource allocation.

3.1 Introduction

In conventional multiple access schemes each node attempts to communicate its message directly to the destination node; e.g., the base station in a cellular wireless system. While such schemes can be implemented in a straightforward manner, alternative schemes in which nodes are allowed to cooperate have the potential to improve the quality of service that is offered to the transmitting nodes by enlarging the achievable rate region and by reducing the probability of outage; e.g., [4,38,66,67]. The basic principle of cooperative multiple access is for the nodes to mutually relay (components of) their messages to the destination node, and hence the design of such schemes involves the development of an appropriate composition of several relay channels [10, 22, 34]. In particular, power and other communication resources, such as time-frequency cells/dimensions, must be allocated to the direct transmission and cooperation tasks. The realization of the potential improvement in quality of service provided by cooperation is contingent on this allocation (among other things), and the development of efficient algorithms for optimal power and resource allocation for certain classes of cooperative multiple access schemes forms the core of this chapter.

In this chapter we will focus on cooperative multiple access schemes in which the transmitting nodes cooperate in pairs and have access to full channel state information. The transmitting nodes will cooperate by (completely) decoding the cooperative messages transmitted by their partners, and hence the cooperation strategy can be broadly classified as being of the decode-and-forward type. We will consider an independent block fading model for the channels between the nodes, and will assume that

the coherence time is long. This enables us to neglect the communication resources assigned to the feeding back of channel state information to the transmitters, and also suggests that an appropriate system design objective would be to enlarge the achievable rate region for the given channel realization.

We will begin our development with the derivation (in Sections 3.2 and 3.3) of a closed-form expressions for optimal power allocations for cooperative schemes that are allowed to operate in full-duplex mode; i.e., schemes that allow each node to simultaneously transmit and receive in the same time-frequency cell. Although the demands on the communication hardware required to facilitate full-duplex operation, such as sufficient electrical isolation between the transmission and reception modules and perfect echo cancellation, are unlikely to be satisfied in wireless systems with reasonable cost, the full-duplex case represents an idealized scenario against which more practical systems can be measured. It also provides a simplified exposition of the principles of our approach. The performance required from the communication hardware can be substantially relaxed by requiring each node to communicate in a half-duplex fashion; e.g., [4, 38, 66, 67]. However, half-duplex operation requires the allocation of both power and the channel resource. In Section 3.5 an efficient jointly optimal power and resource allocation algorithm for a (modified) block-based version of the half-duplex scheme in [67, Section III] will be developed. (The scheme in [67, Section III] employs a fixed, and equal, resource allocation). It will be demonstrated that the ability of the proposed scheme to partition the channel resource according to the rate requirements of each node enables it to achieve a larger fraction of the achievable rate region of the full-duplex case than the underlying scheme.

An impediment to the development of reliable, efficient power allocation algorithms for full-duplex cooperative multiple access has been that the direct formulation of the power allocation problem is not convex unless the transmission scheme is

constrained to avoid interference. However, by examining the structure of this problem, it is shown that the non-convex direct formulation can be transformed into a convex one. In particular, it is shown in Section 3.2 that for a given rate requirement for one of the nodes, the power allocation problem for the full-duplex case can be transformed into a convex problem that has a closed-form solution. In addition to the computational efficiencies that this closed form provides, the ability to directly control the rate of one of the nodes can be convenient in the case of heterogeneous traffic at the cooperative nodes, especially if one node has a constant rate requirement and the other is dominated by "best effort" traffic. The derivation of our closed-form expressions involved the independent discovery of some of the observations in [30,31] regarding the properties of the optimal solution to the sum-rate optimization problem. In particular, using different techniques from those in [30,31], we independently showed [46] that for each node, one of the components of the optimal power allocation is zero (although which one depends on the scenario), and that the optimization of the remaining powers can be formulated as a convex optimization problem. In [30,31], these observations were used to derive a power allocation algorithm with an ergodic achievable rate objective and long-term average power constraints, whereas our focus is on a setting in which the channel coherence time is long. A distinguishing feature of our approach is that the convex optimization problem for the remaining powers admits a closed-form solution.

The development of reliable, efficient, power allocation algorithms for half-duplex cooperative multiple access schemes with fixed resource allocation is simpler than that for the full-duplex case, because interference is explicitly avoided and the problem becomes convex. However, the joint allocation of power and the channel resource remains non-convex. In Section 3.5 a half-duplex scheme based on that in [67, Section III] is considered, and it is shown that for a given rate requirement for one of the

nodes the maximal achievable rate of the other node is a quasi-concave function of the resource allocation parameter. Therefore, an efficient algorithm for the optimal resource allocation using a standard quasi-convex search can be constructed. At each stage of the search, a convex optimization problem with just two variables is solved. The complexity reduction obtained by exploiting the underlying quasi-convexity suggests that it may be possible to develop an on-line implementation of the jointly optimal power and resource allocation algorithm without resorting to approximation.

3.2 Full-Duplex Model

A block diagram of the model for full-duplex pairwise cooperative multiple access is provided in Fig. 3.1; see [66,81]. A superposition (first order) block Markov coding scheme with backward decoding was proposed for this system in [66] (based on an earlier scheme in [11]), and we will adopt that scheme herein. We will now briefly describe that system; a more detailed description is provided in the Appendix of [66]. Let $w_{i0}(n)$ denote the n^{th} message to be sent directly from node i to the destination node (node 0), and let $w_{ij}(n)$ denote the nth message to be sent from node i to the destination node with the cooperation of node j. At the n^{th} (block) channel use, node i transmits the codeword

$$X_i = X_{i0} + X_{ij} + U_i, \tag{3.1}$$

where $X_{i0}(w_{i0}(n), w_{ij}(n-1), w_{ji}(n-1))$ carries the information sent by node i directly to the destination node, $X_{ij}(w_{ij}(n), w_{ij}(n-1), w_{ji}(n-1))$ carries the information that is sent by node i to the destination node via node j,[1] and $U_i(w_{ij}(n-1), w_{ji}(n-1))$ carries the cooperative information. (Note that all three components of X_i depend on the cooperative messages sent in the previous block.). Let P_{i0}, P_{ij} and P_{Ui} denote

[1]The destination node also receives X_{ij} directly.

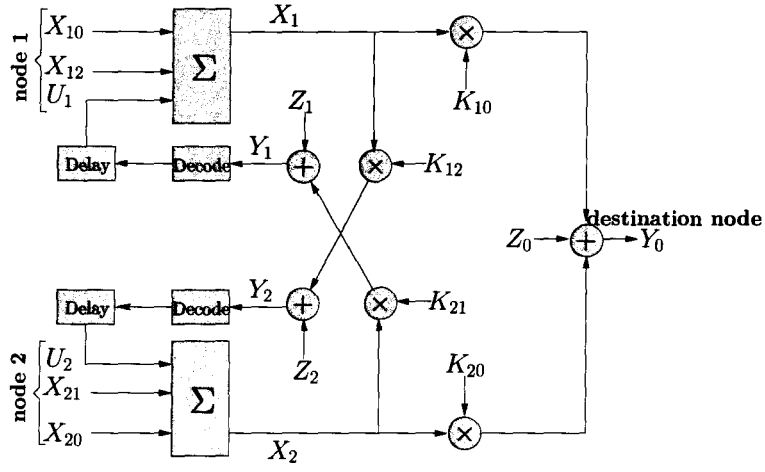

Figure 3.1: Full-duplex pairwise cooperative multiple access.

the power allocated to each component on the right hand side of (3.1), and define $P_i = P_{i0} + Pij + P_{Ui}$.

Assuming, as in [66], that perfect isolation and echo cancellation are achieved and that each transmitter knows the phase of the channels into which it transmits and has the means to cancel this phase, the received signal at each node can be written as

$$Y_0 = K_{10}X_1 + K_{20}X_2 + Z_0, \tag{3.2a}$$

$$Y_1 = K_{21}X_2 + Z_1, \qquad Y_2 = K_{12}X_1 + Z_2, \tag{3.2b}$$

respectively, where K_{ij} is the magnitude of the channel gain between node i and node j, and Z_i represents the additive zero-mean white circular complex Gaussian noise with variance σ_i^2 at node i. We define the (power) gain-to-noise ratio of each channel to be $\gamma_{ij} = K_{ij}^2/\sigma_j^2$. The transmitting nodes engage the channel in this way for N (block) channel uses, and the destination node employs backward decoding once all N blocks have arrived [66]. (The cooperating nodes employ forward decoding.)

The data rate of node i in the above model is $R_i = R_{i0} + R_{ij}$, where R_{i0} is

the rate of the message transmitted directly to the destination node, w_{i0}, and R_{ij} is the rate of the message transmitted with the cooperation of node j, w_{ij}. Under the assumption that all the channel parameters γ_{ij} are known at both transmitting nodes, an achievable rate region for a given channel realization is the closure of the convex hull of the rate pairs (R_1, R_2) that satisfy the following constraints [66][2]

$$R_{i0} \leqslant \log\left(1 + \gamma_{i0} P_{i0}\right), \tag{3.3a}$$

$$R_{10} + R_{20} \leqslant \log\left(1 + \gamma_{10} P_{10} + \gamma_{20} P_{20}\right), \tag{3.3b}$$

$$R_i \leqslant R_{i0} + \log\left(1 + \frac{\gamma_{ij} P_{ij}}{1 + \gamma_{ij} P_{i0}}\right), \tag{3.3c}$$

$$R_1 + R_2 \leqslant \log\left(1 + \gamma_{10} P_1 + \gamma_{20} P_2 + 2\sqrt{\gamma_{10}\gamma_{20} P_{U1} P_{U2}}\right). \tag{3.3d}$$

Here, (3.3a) and (3.3b) bound the conventional multiple access region (with no cooperation), and (3.3c) and (3.3d) capture the impact of cooperation. A natural design objective would be to operate the system in Fig. 3.1 at rates that approach the boundary of the region specified in (3.3), subject to constraints on the power transmitted from each node. The power allocation required to do so can be found by maximizing a convex combination of R_1 and R_2 subject to (3.3) and a bound on the transmitted powers,[3] or by maximizing R_i for a given value of R_j, subject to (3.3) and the bound on the transmitted powers. Unfortunately, the direct formulation of both these problems is not convex in the transmitted powers, due to the interference components in (3.3c). The lack of convexity renders the development of a reliable efficient algorithm for the solution of the direct formulation fraught with difficulty. However, in Section 3.3 it will be shown that by adopting the latter of the two frameworks above, the direct formulation can be transformed into a convex optimization problem that

[2]All logarithms are to base 2, and all rates are in bits per two dimensions.

[3]That problem that can be viewed as a special case of the problem in [30, 31], which involves power allocation over a distribution of channel realizations with an ergodic achievable rate objective and long-term average power constraints.

in most scenarios can be analytically solved to obtain closed-form expressions for the optimal power allocation. The overall strategy for obtaining this closed-form solution involves three main steps:

Step 1: For a given (feasible[4]) value of R_2, denoted $R_{2,\text{tar}}$, find a closed-form expression for the powers that maximize R_1 subject to (3.3) and the bound on the transmitted powers; i.e., solve

$$\max_{P_{i0},P_{ij},P_{Ui}} R_1 \tag{3.4a}$$

$$\text{subject to} \quad 0 \leqslant P_{i0} + P_{ij} + P_{Ui} \leqslant \bar{P}_i, \tag{3.4b}$$

$$\text{and equation (3.3) with } R_2 = R_{2,\text{tar}}. \tag{3.4c}$$

Then repeat for all feasible values of R_2.

Step 2: For a given (feasible) value of R_1, denoted $R_{1,\text{tar}}$, find a closed-form expression for the powers that maximize R_2 subject to (3.3) and the bound on the transmitted powers. Then repeat for all feasible values of R_1. The formulation of the optimization problem that appears in this step is the (algebraically) symmetric image of that in (3.4), in the sense that the powers and the rates of nodes 1 and 2 simply exchange roles.

Step 3: The achievable rate region of the system proposed in [66] is the convex hull of the rate regions obtained in Steps 1 and 2 . When a desired rate pair on the boundary of this convex hull is achieved by the solution to Step 1 or Step 2, an optimal power allocation is obtained directly. When this is not the case, a standard time-sharing strategy is applied.

[4]The set of feasible values for R_2 is $[0, R_{2,\max}]$, where a closed-form expression for $R_{2,\max}$ can be obtained by solving the problem in Step 2 for $R_{1,\text{tar}} = 0$. Analogously, a closed-form expression for $R_{1,\max}$ can be obtained by solving (3.4) for $R_{2,\text{tar}} = 0$.

In a conventional multiple access scheme, all points on the boundary of the capacity region can be obtained by time sharing (if necessary) between rate pairs that can be achieved by successive decoding of the messages from each node [9], and this significantly simplifies the system. A related result holds for the cooperative multiple access scheme, and significantly simplifies the power allocation problem. In particular, it is shown in Appendix A that in each of Steps 1 and 2 it is sufficient to consider two simplified problems in which the direct messages from each node are decoded sequentially — one in which the direct message from node 1 is decoded first (and is cancelled before the remaining messages are decoded), and one in which the direct message of node 2 is decoded first. Furthermore, solving Step 1 with the direct message of node 1 decoded first results in the same set of constraints on the rates (i.e., the same simplification of (3.3)) as solving Step 2 with the direct message of node 1 decoded first. Also, solving Step 1 with the direct message of node 2 decoded first results in the same set of constraints on the rates as solving Step 2 with the direct message of node 2 decoded first. Therefore, in Step 1 it is sufficient to consider only the case in which the direct message of node 1 is decoded first, and in Step 2 it is sufficient to consider only the case in which the direct message of node 2 is decoded first. Moreover, these two problems are (algebraically) symmetric images of each other. Therefore, the closed-form solution only for the problem in Step 1 in which the direct message of node 1 is decoded first will be explicitly stated.

A key observation in the derivation of our closed-form expressions for the optimal power allocation is that the monotonicity of the logarithm implies that for positive constants a and c, and non-negative constants b and d, the function $\log\left(\frac{a+bx}{c+dx}\right)$, which appears in the process of solving (3.4), is monotonic in $x \in [0, P]$. Hence, the optimal

solution to

$$\max_{x} \quad \log\left(\tfrac{a+bx}{c+dx}\right) \tag{3.5a}$$

$$\text{subject to} \quad 0 \leqslant x \leqslant P \tag{3.5b}$$

is

$$x^* = \begin{cases} P & \text{if } b - ad/c > 0, \\ 0 & \text{if } b - ad/c < 0. \end{cases} \tag{3.6}$$

(When $b - ad/c = 0$ all $x \in [0, P]$ are optimal.) Since problems of the form in (3.5) appear in two of the underlying components of (3.4), and since (3.6) has two important cases, four cases need to be considered in order to solve Step 1. (These four cases also arise in [30, 31], although in a different way.) In each case, we exploit the fact that since we are attempting to maximize R_1, the upper bound in (3.4b) on the transmitted power for node 1 will be active at optimality. In order to simplify the exposition, the closed-form expressions for the optimal power allocations are collected in Table 3.1, and to simplify the derivation of these expressions, each of the four cases will be considered in a separate subsection of Section 3.3, below. Before moving to those derivations, we point out that in each of the four cases in Table 3.1, for each node (at least) one of the components of the optimal power allocation is zero. That observation is a key step in the derivation of these expressions, because once it is made the remaining design problem is convex. (These observations were made independently of [30, 31], in which they arise from an analysis of the problem of optimizing the sum rate.) The particular powers that are zero imply that in Case 1 both nodes use cooperative transmission only; in Case 2 node 1 uses direct transmission only and node 2 uses only cooperative transmission; and in Case 3 node 1 uses cooperative transmission only, and node 2 uses only direct transmission.

Table 3.1: Power allocations for points on the boundary of the achievable rate region for the full-duplex cooperative system, in Cases 1–3 and in Step 1 of Case 4. Given a feasible rate for Node 2, $R_{2,\text{tar}}$, we define $\Phi_{2j} = (2^{R_{2,\text{tar}}}-1)/\gamma_{2j}$, and $\tilde{\Phi}_{20,4} = \max\{\Phi_{20}, (\gamma_{10}/\gamma_{12}-1)/\gamma_{20}\}$.

Case	Scenario	A, B[§]	B[¶]	P_{10}^*	P_{12}^*	P_{U1}^*	P_{20}^*	P_{21}^*	P_{U2}^*
1	$\gamma_{10} \leqslant \gamma_{12}$, $\gamma_{20} \leqslant \gamma_{21}$	(3.17)	> 0	0	$\bar{P}_1 - P_{U1}^*$	(3.18a)	0	Φ_{21}	$\bar{P}_2 - \Phi_{21}$
			$\leqslant 0$	0	$\bar{P}_1$	0	0	$\tilde{P}_2' - P_{U2}^*$	$[0, \tilde{P}_2' - \Phi_{21}]$
2	$\gamma_{10} > \gamma_{12}$, $\gamma_{20} \leqslant \gamma_{21}$	(3.22)	> 0	$\bar{P}_1 - P_{U1}^*$	0	(3.18a)	0	Φ_{21}	$\bar{P}_2 - \Phi_{21}$
			$\leqslant 0$	$\bar{P}_1$	0	0	0	$\breve{P}_2' - P_{U2}^*$	$[0, \breve{P}_2' - \Phi_{21}]$
3	$\gamma_{10} \leqslant \gamma_{12}$, $\gamma_{20} > \gamma_{21}$	(3.17)	> 0	0	$\bar{P}_1 - P_{U1}^*$	(3.18a)	Φ_{20}	0	$\bar{P}_2 - \Phi_{20}$
			$\leqslant 0$	0	$\bar{P}_1$	0	$\tilde{P}_2' - P_{U2}^*$	0	$[0, \tilde{P}_2' - \Phi_{20}]$
4[†]	$\gamma_{10} > \gamma_{12}$, $\gamma_{20} > \gamma_{21}$	(3.17)	> 0	0	$\bar{P}_1 - P_{U1}^*$	(3.18a)	$\tilde{\Phi}_{20,4}$	0	$\bar{P}_2 - \tilde{\Phi}_{20,4}$

[§] A and B are parameters in the expression in (3.18a).

[¶] If $B \leqslant 0$ there is a set of power allocations for node 2, rather than a unique allocation. The term $\tilde{P}_2'$ is an arbitrary power in $[\tilde{P}_2, \bar{P}_2]$, where $\tilde{P}_2$ is defined in (3.19), and $\breve{P}_2' \in [\breve{P}_2, \bar{P}_2]$, where $\breve{P}_2$ is defined in (3.23). Those allocations for which $\tilde{P}_2' = \tilde{P}_2$ (or $\breve{P}_2' = \breve{P}_2$) use the minimum power required to achieve the boundary. (Note that $\tilde{P}_2 \geqslant \Phi_{21}$ and $\breve{P}_2 \geqslant \Phi_{21}$.)

[†] In Case 4, the achievable rate region is the convex hull of this region, the analogous region generated in Step 2, and the conventional multiple access region; see Section 3.3.4.

3.3 Derivation of Expressions in Table 3.1

3.3.1 Case 1: $\gamma_{10} \leqslant \gamma_{12}$ and $\gamma_{20} \leqslant \gamma_{21}$

In this case the cooperation channel for both nodes has a higher gain-to-noise ratio than the direct channel. Following the discussion in Section 3.2, we will assume that node 1's direct message will be decoded first, and hence the constraint on $R_{2,\text{tar}}$ in (3.3c) can be written as

$$R_{2,\text{tar}} \leqslant \log\left(1+\gamma_{20}P_{20}\right) + \log\left(1+\frac{\gamma_{21}P_{21}}{1+\gamma_{21}P_{20}}\right). \tag{3.7}$$

Furthermore, since $P_i \leqslant \bar{P}_i$ the constraint on R_1 in (3.3d) can be written as

$$R_1 \leqslant \log\left(1+\gamma_{10}\bar{P}_1+\gamma_{20}\bar{P}_2+2\sqrt{\gamma_{10}\gamma_{20}P_{U1}P_{U2}}\right) - R_{2,\text{tar}}. \tag{3.8}$$

The first step in the solution of (3.4) is to determine the powers of node 2 such that (3.7) is satisfied and the bound on the right hand side of (3.8) is maximized. To do so, we need to maximize $P_{U2} = \bar{P}_2 - (P_{20}+P_{21})$, which is the portion of the power node 2 uses to send the cooperative codeword. This can be done by minimizing the power required to satisfy (3.7). The power used to satisfy (3.7) is the sum of the powers allocated to the direct and indirect codewords, namely $S_2 = P_{20} + P_{21}$. To determine P_{20} and P_{21} such that S_2 is minimized, (3.7) is rewritten as

$$\begin{aligned} R_{2,\text{tar}} &\leqslant \log\left(1+\gamma_{20}P_{20}\right) + \log\left(\frac{1+\gamma_{21}S_2}{1+\gamma_{21}P_{20}}\right) \\ &= \log\left(\frac{1+\gamma_{20}P_{20}}{1+\gamma_{21}P_{20}}\right) + \log\left(1+\gamma_{21}S_2\right). \end{aligned} \tag{3.9}$$

From (3.9) it can be seen that in order to minimize S_2 such that (3.9) holds, we need to make the second term in (3.9) as small as possible. This can be achieved by making

the first term large. (Recall that $S_2 = P_{20} + P_{21}$.) That is, we seek to

$$\begin{aligned} \max_{P_{20}} \quad & \log\left(\frac{1+\gamma_{20}P_{20}}{1+\gamma_{21}P_{20}}\right) \\ \text{subject to} \quad & 0 \leqslant P_{20} \leqslant S_2. \end{aligned}$$

This problem has the form of (3.5), and since $\gamma_{21} \geqslant \gamma_{20}$, the solution is $P_{20}^* = 0$, and hence $P_{21} = \bar{P}_2 - P_{U2}$. For that power allocation, equation (3.7) can be written as

$$R_{2,\text{tar}} \leqslant \log\left(1+\gamma_{21}P_{21}\right), \tag{3.10}$$

and hence the minimum power required for $R_{2,\text{tar}}$ to be achievable is $S_2^* = P_{21}^* = (2^{R_{2,\text{tar}}} - 1)/\gamma_{21}$. As in Table 3.1, we define $\Phi_{21} = (2^{R_{2,\text{tar}}} - 1)/\gamma_{21}$. The remaining power available for the cooperative codeword is $P_{U2}^* = \bar{P}_2 - \Phi_{21}$.

Now consider the optimization of the remaining powers $\{P_{10}, P_{12}, P_{U1}\}$ so that R_1 is maximized (subject to $R_{2,\text{tar}}$ being achievable). The rate of node 1 has two constraints

$$R_1 \leqslant \log\left(1+\gamma_{10}P_{10}\right) + \log\left(1+\frac{\gamma_{12}P_{12}}{1+\gamma_{12}P_{10}}\right), \tag{3.11}$$

$$R_1 \leqslant \log\left(1+\gamma_{10}\bar{P}_1 + \gamma_{20}\bar{P}_2 + 2\sqrt{\gamma_{10}\gamma_{20}P_{U1}P_{U2}^*}\right) - R_{2,\text{tar}}. \tag{3.12}$$

To simplify (3.11), let $S_1 = P_{10} + P_{12} = \bar{P}_1 - P_{U1}$. This enables rewriting (3.11) as

$$R_1 \leqslant \log\left(1+\gamma_{10}P_{10}\right) + \log\left(\frac{1+\gamma_{12}S_1}{1+\gamma_{12}P_{10}}\right) \tag{3.13}$$

$$= \log\left(\frac{1+\gamma_{10}P_{10}}{1+\gamma_{12}P_{10}}\right) + \log\left(1+\gamma_{12}S_1\right). \tag{3.14}$$

For a given value of P_{U1}, S_1 is fixed and equation (3.14) can be maximized by solving

$$\begin{aligned} \max_{P_{10}} \quad & \log\left(\tfrac{1+\gamma_{10}P_{10}}{1+\gamma_{12}P_{10}}\right) \\ \text{subject to} \quad & 0 \leqslant P_{10} \leqslant S_1. \end{aligned}$$

This problem takes the form in (3.5), and since $\gamma_{12} \geq \gamma_{10}$, the solution is $P_{10}^* = 0$ and $P_{12} = \bar{P}_1 - P_{U1}$. The remaining two constraints on R_1 are (3.12) and $R_1 \leqslant \log\left(1 + \gamma_{12}(\bar{P}_1 - P_{U1})\right)$, and the remaining design variable is P_{U1}. Therefore, the problem in (3.4) has been reduced to

$$\max_{P_{U1}} \quad \min\left\{\beta_1(P_{U1}), \beta_2(P_{U1})\right\} \tag{3.15a}$$

$$\text{subject to} \qquad 0 \leqslant P_{U1} \leqslant \bar{P}_1, \tag{3.15b}$$

where

$$\beta_1(P_{U1}) = \log\left(1 + \gamma_{12}(\bar{P}_1 - P_{U1})\right), \tag{3.16a}$$

$$\beta_2(P_{U1}) = \log\left(1 + \gamma_{10}\bar{P}_1 + \gamma_{20}\bar{P}_2 + 2\sqrt{\gamma_{10}\gamma_{20}P_{U1}P_{U2}^*}\right) - R_{2,\text{tar}}. \tag{3.16b}$$

In order to solve (3.15) analytically, observe that the argument of the logarithm in $\beta_1(P_{U1})$ is linearly decreasing in P_{U1} while the argument of the logarithm in $\beta_2(P_{U1})$ is concave increasing. Therefore, the solution of (3.15) is the value of P_{U1} for which the two upper bounds on R_1 intersect (i.e, $\beta_1(P_{U1}) = \beta_2(P_{U1})$), so long that value of P_{U1} satisfies $0 \leqslant P_{U1} \leqslant \bar{P}_1$. (A similar observation was made in [21] in the context of relay channels.) Equating $\beta_1(P_{U1})$ and $\beta_2(P_{U1})$ results in a quadratic equation in P_{U1}, and to express the solution of that quadratic equation we define

$$A = \frac{\gamma_{12}}{2\sqrt{\gamma_{10}\gamma_{20}}}\, 2^{R_{2,\text{tar}}}, \tag{3.17a}$$

$$B = \left[2^{R_{2,\text{tar}}}\left(1 + \gamma_{12}\bar{P}_1\right) - \left(1 + \gamma_{10}\bar{P}_1 + \gamma_{20}\bar{P}_2\right)\right]/(2\sqrt{\gamma_{10}\gamma_{20}}). \tag{3.17b}$$

If $B > 0$, then the optimal power allocation for node 1 is[5]

$$P_{U1}^* = \frac{2AB + P_{U2}^* - \sqrt{(2AB + P_{U2}^*)^2 - 4A^2B^2}}{2A^2}, \tag{3.18a}$$

$$P_{10}^* = 0, \qquad P_{12}^* = \bar{P}_1 - P_{U1}^*, \tag{3.18b}$$

[5]It can be analytically shown that $0 \leqslant P_{U1}^* \leqslant \bar{P}_1$. Furthermore, the condition that $B > 0$ guarantees that the argument of the square root in (3.18a) is positive.

where $P_{U2}^* = \bar{P}_2 - \Phi_{21}$.

In some scenarios, the gain-to-noise ratios of the channels may be such that $B \leqslant 0$ for small values of $R_{2,\text{tar}}$. In that case, it can be shown that $\beta_1(P_{U1}) \leqslant \beta_2(P_{U1})$ for all admissible values of P_{U1}, and hence the problem in (3.15) simplifies to the maximization of $\beta_1(P_{U1})$, for which the optimal power allocation is $P_{U1}^* = 0$, and hence $P_{12}^* = \bar{P}_1$. The fact that $\beta_1(P_{U1}) \leqslant \beta_2(P_{U1})$ for all admissible P_{U1} means that for the given $R_{2,\text{tar}}$, node 2 does not have to use all its allowed power in order for node 1 to achieve its maximum achievable rate (while node 2 achieves its target rate). In fact, the minimum (total) power that node 2 must use is the power that would make B in (3.17b) zero; i.e.,

$$\tilde{P}_2 = \left(2^{R_{2,\text{tar}}}(1 + \gamma_{12}\bar{P}_1) - (1 + \gamma_{10}\bar{P}_1)\right)/\gamma_{20}. \tag{3.19}$$

Since $\gamma_{10} \leqslant \gamma_{12}$ and $\gamma_{20} \leqslant \gamma_{21}$, we have that $\tilde{P}_2 \geqslant \Phi_{21}$. If $\tilde{P}_2 > \Phi_{21}$, the additional power $\tilde{P}_2 - \Phi_{21}$ can be partitioned arbitrarily between X_{21} or U_2; see Table 3.1.[6]

An alternative perspective on scenarios in which $B \leqslant 0$ is provided by the observation that if $[0, R_{2,\text{B}}]$ denotes the interval, if any, of values of $R_{2,\text{tar}}$ that result in $B \leqslant 0$, then for all $R_{2,\text{tar}} \in [0, R_{2,\text{B}}]$ the optimal value of R_1 is equal to its maximum possible value. That is, for these cases the provision of a non-zero rate of up to $R_{2,\text{B}}$ to node 2 does not reduce the achievable rate for node 1. Such scenarios arise naturally in conventional multiple access systems. This property is illustrated in the achievable rate regions in Fig. 3.3 for the cases in which $E(K_{12}) = 0.63$ and $E(K_{12}) = 0.71$. The boundaries of these regions are constant for small values of $R_{2,\text{tar}}$.

As discussed in Step 1, the target rate $R_{2,\text{tar}}$ is achievable if (and only if) it lies in $[0, R_{2,\text{max}}]$, where $R_{2,\text{max}}$ can be found from the solution to Step 2 with target rate

[6]Since $P_{U1} = 0$, there is no coherent combining of U_1 and U_2 at the destination node, but U_2 can still play an active role in the backward decoder at the destination node; cf. [66, Appendix]. That said, setting $P_{21} = \tilde{P}_2$ and $P_{U2} = 0$ has the potential to simplify the encoder at node 2 and the decoder at the destination node.

$R_{1,\text{tar}} = 0$. Using a similar derivation to that above, we can show that under the conditions of Case 1, the solution to Step 2 with $R_{1\text{tar}} = 0$ has $P_{10}^* = 0$, $P_{12}^* = 0$ and $P_{U1}^* = \bar{P}_1$, and that the constraints on R_2 reduce to

$$R_2 \leqslant \log\left(1 + \gamma_{21} P_{21}\right), \tag{3.20a}$$

$$R_2 \leqslant \log\left(1 + \gamma_{10} P_1 + \gamma_{20} P_2 + 2\sqrt{\gamma_{10}\gamma_{20}\bar{P}_1(\bar{P}_2 - P_{21})}\right). \tag{3.20b}$$

Therefore, the problem of finding $R_{2,\max}$ has been reduced to finding the value of $P_{21} \in [0, \bar{P}_2]$ that maximizes the minimum of the two constraints in (3.20). A problem of this type arose in (3.15), and hence by applying techniques similar to those that followed (3.15) one can obtain a closed-form solution for the optimal value of P_{21}, and hence a closed-form expression for $R_{2,\max}$. Actually, this expression for $R_{2,\max}$ applies in any situation in which $\gamma_{21} \geqslant \gamma_{20}$. That is, it also applies to Case 2, below. For Cases 3 and 4, below, in which $\gamma_{21} < \gamma_{20}$, one can use similar arguments to show that $R_{2,\max}$ is the same as that for the conventional multiple access region, namely $\log(1 + \gamma_{20}\bar{P}_2)$.

3.3.2 Case 2: $\gamma_{10} > \gamma_{12}$ and $\gamma_{20} \leqslant \gamma_{21}$

In this case, the direct channel for node 1 has a higher gain-to-noise ratio than its cooperation channel, but for node 2 the opposite is true. Using a similar argument to Case 1, the minimum value of $P_{20} + P_{21}$ required for $R_{2,\text{tar}}$ to be achievable occurs when $P_{20} = 0$. Thus, an optimal power distribution for the second node is $P_{21}^* = \Phi_{21} = (2^{R_{2,\text{tar}}} - 1)/\gamma_{21}$, $P_{20}^* = 0$, $P_{U2}^* = \bar{P}_2 - P_{21}^*$. Therefore, the constraint in (3.3c) for node 1 reduces to that in (3.11). However, in this case it can be shown that the choices $P_{12}^* = 0$ and $P_{10}^* = \bar{P}_1 - P_{U1}^*$ maximize the constraint in (3.11). The two constraints on R_1 will be (3.3d) and $R_1 \leqslant \log\left(1 + \gamma_{10}(\bar{P}_1 - P_{U1})\right)$. That is, for Case 2

we have reduced the problem in (3.4) to

$$\max_{P_{U1}} \quad \min\{\beta_3(P_{U1}), \beta_2(P_{U1})\} \tag{3.21a}$$

$$\text{subject to} \qquad 0 \leqslant P_{U1} \leqslant \bar{P}_1, \tag{3.21b}$$

where $\beta_3(P_{U1}) = \log\big(1+\gamma_{10}(\bar{P}_1 - P_{U1})\big)$ and $\beta_2(P_{U1})$ was defined in (3.16b). By analogy to Case 1, the solution to this problem is the intersection point between the two terms inside the minimum function, so long as that value lies in $[0, \bar{P}_1]$. Let us define

$$A = \sqrt{\frac{\gamma_{10}}{4\gamma_{20}}}\, 2^{R_{2,\text{tar}}}, \tag{3.22a}$$

$$B = \big(2^{R_{2,\text{tar}}}(1+\gamma_{10}\bar{P}_1) - (1+\gamma_{10}\bar{P}_1+\gamma_{20}\bar{P}_2)\big)/(2\sqrt{\gamma_{10}\gamma_{20}}). \tag{3.22b}$$

If $B > 0$, the optimal value of P_{U1} has the same form as (3.18a). If $B \leqslant 0$, it can be shown that $\beta_3(P_{U1}) \leqslant \beta_2(P_{U1})$ for all admissible values of P_{U1}, and hence that $P^*_{U1} = 0$. As in Case 1, if $B \leqslant 0$ then node 2 can reduce its total transmission power, in this case to

$$\breve{P}_2 = \big(2^{R_{2,\text{tar}}} - 1\big)(1+\gamma_{10}\bar{P}_1)/\gamma_{20}, \tag{3.23}$$

and there is a range of optimal values for the pair (P_{21}, P_{U2}); see Table 3.1.

3.3.3 Case 3: $\gamma_{10} \leqslant \gamma_{12}$ and $\gamma_{20} > \gamma_{21}$

In this case, the cooperation channel of node 1 has a higher gain-to-noise ratio than the direct channel, while this property is reversed for node 2. This case is (algebraically) symmetric to Case 2, which means that it is optimal to set $P^*_{10} = 0$, $P^*_{21} = 0$, $P^*_{20} = \Phi_{20} = (2^{R_{2,\text{tar}}} - 1)/\gamma_{20}$ and $P^*_{U2} = \bar{P}_2 - P^*_{20}$. The problem in (3.4) can then be written in the same form as (3.15), except that $R_{2,\text{tar}} = \log(1+\gamma_{20}P^*_{20})$. Therefore, if we define A and B as in (3.17), then if $B > 0$ the optimal power allocation for node 1

will have the same form as (3.18). If $B \leqslant 0$, then $P_{U1}^* = 0$, and node 2 can reduce its total power to $\tilde{P}_2$.

3.3.4 Case 4: $\gamma_{10} > \gamma_{12}$ and $\gamma_{20} > \gamma_{21}$

In this case, for each node the cooperation channel is "weaker" than the direct channel. Therefore, we expect rather modest gains, if any, from cooperation. These expectations materialize in our solution. To solve the problem in Step 1, namely (3.4), under the assumption that node 1's direct message will be decoded first, we observe that the constraint set (3.3) can be written as

$$R_{2,\text{tar}} \leqslant \log\left(1+\gamma_{20}P_{20}\right) + \log\left(1+\frac{\gamma_{21}P_{21}}{1+\gamma_{21}P_{20}}\right), \tag{3.24a}$$

$$R_1 \leqslant \log\left(1+\frac{\gamma_{10}P_{10}}{1+\gamma_{20}P_{20}}\right) + \log\left(1+\frac{\gamma_{12}P_{12}}{1+\gamma_{12}P_{10}}\right), \tag{3.24b}$$

$$R_1 \leqslant \log\left(1+\gamma_{10}\bar{P}_1+\gamma_{20}\bar{P}_2+2\sqrt{\gamma_{10}\gamma_{20}P_{U1}P_{U2}}\right) - R_{2,\text{tar}}, \tag{3.24c}$$

where we have used the power constraint $P_i \leqslant \bar{P}_i$. To simplify (3.24b), let $S_1 = P_{10} + P_{12} = \bar{P}_1 - P_{U1}$. This enables us to write (3.24b) as

$$\begin{aligned} R_1 &\leqslant \log\left(\frac{(1+\gamma_{20}P_{20})+\gamma_{10}P_{10}}{1+\gamma_{20}P_{20}}\right) + \log\left(\frac{1+\gamma_{12}S_1}{1+\gamma_{12}P_{10}}\right) \\ &= \log\left(\frac{(1+\gamma_{20}P_{20})+\gamma_{10}P_{10}}{1+\gamma_{12}P_{10}}\right) + \log\left(\frac{1+\gamma_{12}S_1}{1+\gamma_{20}P_{20}}\right). \end{aligned} \tag{3.25}$$

For a given value of P_{U1}, S_1 is fixed and equation (3.25) can be maximized by solving

$$\begin{aligned} \max_{P_{10}} \quad & \log\left(\tfrac{(1+\gamma_{20}P_{20})+\gamma_{10}P_{10}}{1+\gamma_{12}P_{10}}\right) \\ \text{subject to} \quad & 0 \leqslant P_{10} \leqslant S_1. \end{aligned}$$

This problem takes the form of (3.5), and hence the solution is

$$P_{10}^* = \begin{cases} 0 & \text{if } P_{20} > (\frac{\gamma_{10}}{\gamma_{12}} - 1)/\gamma_{20}, \\ S_1 & \text{if } P_{20} < (\frac{\gamma_{10}}{\gamma_{12}} - 1)/\gamma_{20}. \end{cases} \tag{3.26}$$

Consider the first case in (3.26), namely $P_{20} > (\frac{\gamma_{10}}{\gamma_{12}} - 1)/\gamma_{20}$. In that case, the constraint set in (3.24) can be written as

$$R_{2,\text{tar}} \leqslant \log\left(1+\gamma_{20}P_{20}\right) + \log\left(1+\frac{\gamma_{21}P_{21}}{1+\gamma_{21}P_{20}}\right), \tag{3.27a}$$

$$R_1 \leqslant \log\left(1+\gamma_{12}P_{12}\right), \tag{3.27b}$$

$$R_1 \leqslant \log\left(1+\gamma_{10}\bar{P}_1+\gamma_{20}\bar{P}_2+2\sqrt{\gamma_{10}\gamma_{20}P_{U1}P_{U2}}\right) - R_{2,\text{tar}}. \tag{3.27c}$$

Our next step in the solution of (3.4) is to determine the powers of node 2 such that (3.27a) is satisfied and the bound on the right hand side of (3.27c) is maximized. To do so we need to maximize $P_{U2} = \bar{P}_2 - (P_{20}+P_{21})$. This can be done by minimizing the power required to satisfy (3.27a). The power used to satisfy (3.27a) is $S_2 = P_{20}+P_{21}$, and to determine P_{20} and P_{21} such that S_2 is minimized, rewrite (3.27a) as

$$\begin{aligned} R_{2,\text{tar}} &\leqslant \log\left(1+\gamma_{20}P_{20}\right) + \log\left(\frac{1+\gamma_{21}S_2}{1+\gamma_{21}P_{20}}\right) \\ &= \log\left(\frac{1+\gamma_{20}P_{20}}{1+\gamma_{21}P_{20}}\right) + \log\left(1+\gamma_{21}S_2\right). \end{aligned} \tag{3.28}$$

From (3.28) it can be seen that in order to minimize S_2 such that (3.28) holds, the second term in (3.28) needs to be as small as possible. This can be achieved by making the first term large; i.e.,

$$\begin{aligned} \max_{P_{20}} \quad & \log\left(\tfrac{1+\gamma_{20}P_{20}}{1+\gamma_{21}P_{20}}\right) \\ \text{subject to} \quad & 0 \leqslant P_{20} \leqslant S_2. \end{aligned}$$

This problem has the form of (3.5), and since $\gamma_{20} \geqslant \gamma_{21}$, the solution is $P_{21}^* = 0$ and hence $P_{20} = S_2 = \bar{P}_2 - P_{U2}$. For those power allocations, equation (3.27a) can be written as

$$R_{2,\text{tar}} \leqslant \log\left(1+\gamma_{20}P_{20}\right). \tag{3.29}$$

The minimum value of P_{20} required for (3.29) to be satisfied is $\Phi_{20} = (2^{R_{2,\text{tar}}} - 1)/\gamma_{20}$, and hence an optimal value for P_{20} under the conditions of the first case of (3.26) is $P_{20}^* = \max\{\Phi_{20}, (\frac{\gamma_{10}}{\gamma_{12}} - 1)/\gamma_{20}\}$. The remaining power available for node 2's cooperative codeword is $P_{U2}^* = \bar{P}_2 - P_{20}^*$.

Now consider the optimization of the remaining powers (P_{10}, P_{12}, P_{U1}) so that R_1 is maximized. Since the focus is on the first case in (3.26), $P_{12}^* = \bar{P}_1 - P_{U1}$, and hence the problem of maximizing R_1 can be written as

$$\max_{P_{U1}} \quad \min\{\beta_1(P_{U1}), \beta_2(P_{U1})\} \tag{3.30a}$$

$$\text{subject to} \qquad 0 \leqslant P_{U1} \leqslant \bar{P}_1, \tag{3.30b}$$

where $\beta_1(P_{U1})$ and $\beta_2(P_{U1})$ were defined in (3.16). Therefore, as we have seen in Case 1, the solution of (3.30) is the value of P_{U1} for which the two upper bounds on R_1 intersect, so long as this value lies in $[0, \bar{P}_1]$. If we define A and B as in (3.17), then if $B > 0$ the optimal power allocations for node 1 in the first case of (3.26) are given by the expressions in (3.18); see Table 3.1. If $B \leqslant 0$, then $\beta_1(P_{U1}) \leqslant \beta_2(P_{U1})$ for all admissible values of P_{U1}, and in order to maximize $\min\{\beta_1(P_{U1}), \beta_2(P_{U1})\}$, we would choose $P_{U1}^* = 0$ and hence $P_{12}^* = \bar{P}_1$. With that choice, the achievable rate R_1 for a given target rate $R_{2,\text{tar}}$ is $R_1 = \log\left(1 + \gamma_{12}\bar{P}_1\right)$. However, a feature of the scenario in Case 4 is that for values of $R_{2,\text{tar}}$ that result in a negative value of B, the conventional multiple access scheme provides a larger value for R_1 than that derived above; see Appendix B for the derivation. Therefore, in the first case of (3.26), if $R_{2,\text{tar}}$ is such that $B \leqslant 0$, then the optimal solution is to perform conventional multiple access.

In the second case of (3.26), namely $P_{20} < (\frac{\gamma_{10}}{\gamma_{12}} - 1)/\gamma_{20}$, the constraint set in

(3.24) can be written as

$$R_{2,\text{tar}} \leqslant \log\left(1+\gamma_{20}P_{20}\right) + \log\left(1+\frac{\gamma_{21}P_{21}}{1+\gamma_{21}P_{20}}\right), \tag{3.31a}$$

$$R_1 \leqslant \log\left(1+\frac{\gamma_{10}P_{10}}{1+\gamma_{20}P_{20}}\right), \tag{3.31b}$$

$$R_1 \leqslant \log\left(1+\gamma_{10}\bar{P}_1+\gamma_{20}\bar{P}_2+2\sqrt{\gamma_{10}\gamma_{20}P_{U1}P_{U2}}\right) - R_{2,\text{tar}}. \tag{3.31c}$$

It can be shown that letting $P_{20} = S_2$ and $P_{21} = 0$ increases (3.31c), but at the same time it increases the interference term in (3.31b). This suggests that the optimal values of P_{20} and P_{21} might both be non-zero, and hence the power allocation problem appears to become significantly more complex to solve. However, it is shown in Appendix C that it is sufficient to study the first case of (3.26), namely $P_{20} > (\frac{\gamma_{10}}{\gamma_{12}} - 1)/\gamma_{20}$, and the symmetric case that arises when solving Step 2. In particular, it is shown in Appendix C that the convex hull of the regions obtained by solving Step 1 for $P_{20} > (\frac{\gamma_{10}}{\gamma_{12}} - 1)/\gamma_{20}$ and Step 2 for $P_{10} > (\frac{\gamma_{20}}{\gamma_{21}} - 1)/\gamma_{10}$, and the conventional multiple access region contains all other regions that would result from solving Step 1 for $P_{20} < (\frac{\gamma_{10}}{\gamma_{12}} - 1)/\gamma_{20}$ and solving Step 2 for $P_{10} < (\frac{\gamma_{20}}{\gamma_{21}} - 1)/\gamma_{10}$.

In Cases 1–3 above, the proposed closed-form solution to (3.4) generates the achievable rate region directly. However, as stated in the previous paragraph, in the present case (Case 4) the most convenient description of the achievable rate region is via the convex hull of the rates generated by solving (3.4) in a special subcase, those generated by the solution of the (algebraically) symmetric image of that problem, and the conventional multiple access region. Fig. 3.2 shows the construction of the optimal rate region. The dotted curve is the union of the region generated by the power allocation in Table 3.1 and the conventional multiple access region. The dashed curve is the union of the region generated by the corresponding solution for

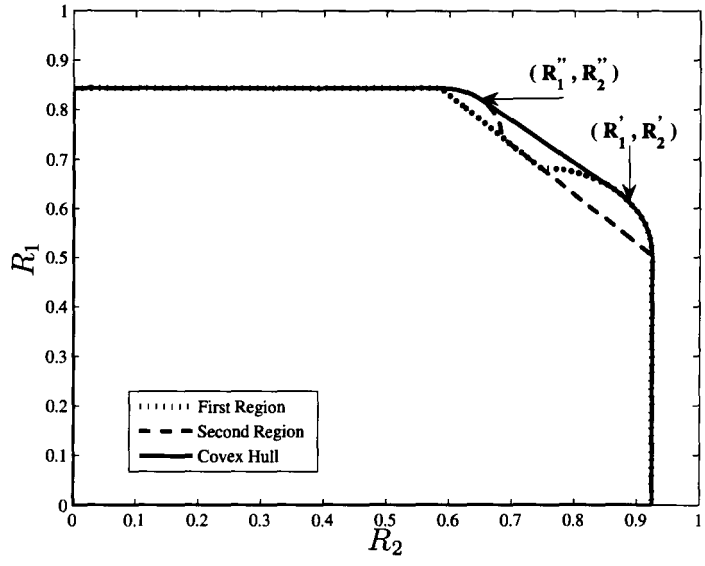

Figure 3.2: Convex hull of the two achievable rate regions in Case 4. $P_1 = P_2 = 2.0, \sigma_0^2 = \sigma_1^2 = \sigma_2^2 = 1, E(K_{12}) = E(K_{21}) = 0.55, E(K_{10}) = 0.63, E(K_{20}) = 0.67$.

Step 2 and the conventional multiple access region. The solid curve is the convex hull of the two component regions and hence is the optimized achievable rate region. The inner pentagon in Fig. 3.2 is the conventional (non-cooperative) multiple access region, and hence the cooperative gain in Case 4 is clear. (Recall that in Case 4 the direct channels are stronger than the cooperation channels, and hence the cooperative gain is expected to be modest.) Points on the interval (R_1', R_2') to (R_1'', R_2'') in Fig. 3.2 are not achieved by the solution of the problem for Step 1 nor that for Step 2, but can be achieved using standard time sharing techniques in which the system operates at the point (R_1', R_2') for a fraction ρ of the block length, and at the point (R_1'', R_2'') for the remainder of the block. Although we do not have a closed-form expression for the points (R_1', R_2') and (R_1'', R_2'') at this time, they can be determined using the procedure below.

The procedure for obtaining the points (R_1', R_2') and (R_1'', R_2'') is based on the following observations:

- The line connecting the two points is tangent to Regions 1 (with a dotted line) and 2 (with a dashed line) at points (R_1', R_2') and (R_1'', R_2''), respectively.

- If the equation of the line is $\mu R_1 + \bar{\mu} R_2 = m$, where $\bar{\mu} = 1 - \mu$ and m is a constant, then the pair (R_1', R_2') maximizes the weighted sum $\mu R_1 + \bar{\mu} R_2$ for Region 1 and the maximum value for this weighted sum is m, and the pair (R_1'', R_2'') maximizes the weighted sum $\mu R_1 + \bar{\mu} R_2$ for Region 2 and the maximum value for this weighted sum is also m.

- Therefore, the problem of finding the points (R_1', R_2') and (R_1'', R_2'') can be transformed into finding the value of μ such that the maximum values of the weighted sum $\mu R_1 + \bar{\mu} R_2$ for Regions 1 and 2 are equal.

- If we can obtain that value of μ then we can obtain the two points (R_1', R_2') and (R_1'', R_2'') by maximizing $\mu R_1 + \bar{\mu} R_2$ for Regions 1 and 2, respectively.

It can be shown that for a fixed value of μ the problem of maximizing $\mu R_1 + \bar{\mu} R_2$ is concave in P_{U1} and P_{U2} [30,31]. This problem can be written as

$$
\begin{aligned}
g_1(\mu) = \max_{P_{U1}, P_{U2}} \quad & \mu R_1 + \bar{\mu} R_2 \\
\text{subject to} \quad & R_1 \leqslant \log\left(1 + \gamma_{12}(P_1 - P_{U1})\right), \\
& R_2 \leqslant \log\left(1 + \gamma_{20}(P_2 - P_{U2})\right), \\
& R_1 + R_2 \leqslant \log\left(1 + \gamma_{10} P_1 + \gamma_{20} P_2 + 2\sqrt{\gamma_{10}\gamma_{20} P_{U1} P_{U2}}\right),
\end{aligned}
\tag{3.32}
$$

for the Region 1 and as

$$\begin{aligned} g_2(\mu) = \max_{P_{U1},P_{U2}} \quad & \mu R_1 + \bar{\mu} R_2, \\ \text{subject to} \quad & R_1 \leqslant \log\left(1+\gamma_{10}(P_1 - P_{U1})\right), \\ & R_2 \leqslant \log\left(1+\gamma_{21}(P_2 - P_{U2})\right), \\ & R_1+R_2 \leqslant \log\left(1+\gamma_{10}P_1+\gamma_{20}P_2+2\sqrt{\gamma_{10}\gamma_{20}P_{U1}P_{U2}}\right), \end{aligned} \tag{3.33}$$

for Region 2. The functions $g_1(\mu)$ and $g_2(\mu)$ can be shown to be convex in μ as follows. Consider the function $g_1(\mu)$, and assume $\mu_3 = \theta\mu_1 + \bar{\theta}\mu_2$, where μ_1, μ_2, and μ_3 are three distinct values for μ, and $\bar{\theta} = 1 - \theta$. It can be shown that

$$g_1(\mu_3) = \max_{P_{U1},P_{U2}} \theta(\mu_1 R_1 + \bar{\mu}_1 R_2) + \bar{\theta}(\mu_2 R_1 + \bar{\mu}_2 R_2) \tag{3.34a}$$

$$\leqslant \max_{P_{U1},P_{U2}} \theta(\mu_1 R_1 + \bar{\mu}_1 R_2) + \max_{P_{U1},P_{U2}} \bar{\theta}(\mu_2 R_1 + \bar{\mu}_2 R_2) \tag{3.34b}$$

$$\leqslant \theta g_1(\mu_1) + \bar{\theta} g_1(\mu_2), \tag{3.34c}$$

and hence $g_1(\mu)$ is a convex function of μ. Using a similar argument, $g_2(\mu)$ can be shown to be a convex function of μ. It can be seen from Fig 3.2 that $g_1(\mu)$ and $g_2(\mu)$ can intersect at only one point. Therefore, in order to obtain the value of μ at which $g_1(\mu)$ and $g_2(\mu)$ intersect, we consider the following problem

$$\begin{aligned} \min_{\mu} \quad & \max \ \{g_1(\mu), g_2(\mu)\} \\ \text{subject to} \quad & 0 \leqslant \mu \leqslant 1 \quad . \end{aligned} \tag{3.35a}$$

The solution to (3.35) gives the intersection point (the point at which $g_1(\mu) = g_2(\mu)$). Since the maximum of two convex functions is convex, the problem in (3.35) is a convex optimization problem. One simple way to solve this problem is to apply the bisection search technique over μ, and at each stage to exploit the convexity of the weighted sum rate problem in P_{U1} and P_{U2} in order to efficiently obtain the values of

$g_1(\mu)$ and $g_2(\mu)$ for the current value of μ for both regions. Once the value of μ that yields the intersection of $g_1(\mu)$ and $g_2(\mu)$ has been found along with the corresponding optimal power components for both regions, the points (R_1', R_2') and (R_1'', R_2'') can be obtained by direct substitution in the rate equations.

3.4 Simulation/Numerical results

In order to verify our derivations, the closed-form expressions are used to compute the average achievable rate regions in scenarios corresponding to those chosen for Fig. 2 of [66]. The resulting regions are plotted in Fig. 3.3 and, as expected, they match the corresponding regions in Fig. 2 of [66]. In the scenarios considered, the channels were independent block fading channels with long coherence times. The channel gains were Rayleigh distributed, the Gaussian noise variances were normalized to 1, and the transmission powers of the cooperating nodes were set to be equal $\bar{P}_1 = \bar{P}_2 = 2$. (Recall that each node has full channel state information.) As in Fig. 2 of [66], Fig. 3.3 is constructed for the case of a channel with symmetric statistics, in the sense that the direct channels between each node and the destination node is Rayleigh fading with the same mean value $E(K_{10}) = E(K_{20}) = 0.63$. Different curves are plotted for different values of the mean value of the inter-node channel $E(K_{12})$. (For each realization $K_{12} = K_{21}$.) The average achievable rate region was obtained by taking the direct sum of the achievable rate regions for each channel realization and then dividing by the number of realizations. Like Fig. 2 of [66], Fig. 3.3 demonstrates advantages of cooperative multiple-access, especially when the gain of the cooperative channels is (often) significantly larger than the gain of the direct channels.

In addition to the average achievable rate region, it is interesting to observe the

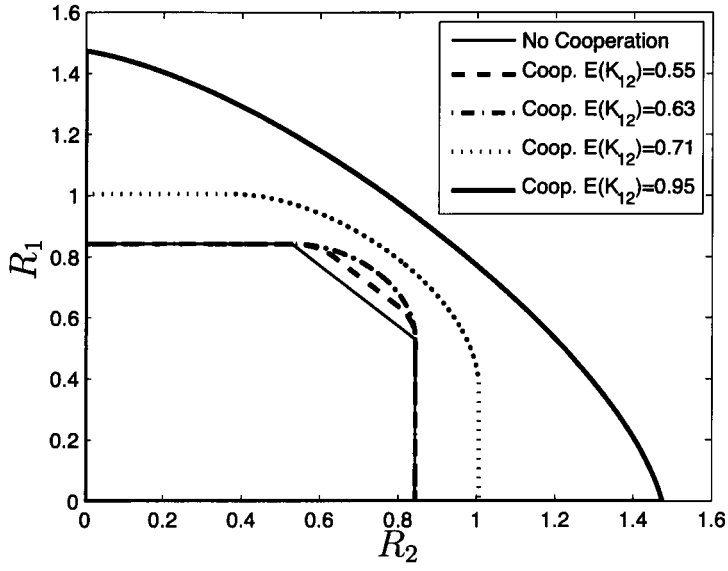

Figure 3.3: Achievable rate region in a case of statistically symmetric direct channels. $P_1 = P_2 = 2.0, \sigma_0^2 = \sigma_1^2 = \sigma_2^2 = 1, E(K_{10}) = E(K_{20}) = 0.63$.

optimal power allocations. Fig. 3.4 shows the allocation of the different power components for one channel realization in which $K_{10} = K_{20} = 0.4$ and $K_{12} = K_{21} = 0.7$. (These gains satisfy the conditions of Case 1 in our closed-form solution.) The figure plots the optimal power components that maximize the rate R_1 for each value of the rate R_2. We note from the figure that there is one power component for each node that is zero for all values of R_2; i.e., in this case $P_{10} = P_{20} = 0$. Also note that the curves for P_{12} and P_{21} intersect at the same value for R_2 as the curves for P_{U1} and P_{U2}. This intersection point represents the equal rate point at which $R_1 = R_2$. The figure also illustrates that as R_2 increases, node 2 allocates more power to P_{21} to increase the data rate sent to node 1. As R_2 increases, node 1 has to reduce its data rate, and this is reflected in the decreasing amount of power that is allocated to P_{12}.

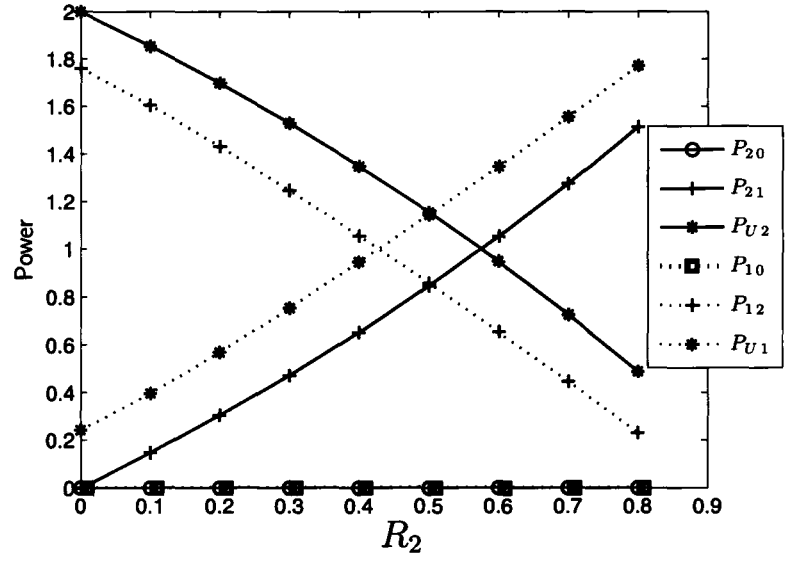

Figure 3.4: Power allocation for a channel realization that satisfies the conditions of Case 1.

3.5 Jointly Optimal Power and Resource Allocation for a Half-Duplex Scheme

The full-duplex cooperative multiple access scheme studied in the previous section places demands on the communication hardware that can be difficult to satisfy with a reasonable cost. Therefore, in this section we consider (a modified version of) an existing half-duplex cooperative scheme that partitions the channel resource in order to avoid interference at the receivers and hence can be implemented using conventional communication hardware. In practice, the channel resource is often partitioned equally, but in this section an efficient algorithm for the joint allocation of power and the channel resource for this scheme is developed, and it is demonstrated that this algorithm enables the resulting scheme to attain a significantly larger fraction of the achievable rate region for the full-duplex case than the underlying scheme.

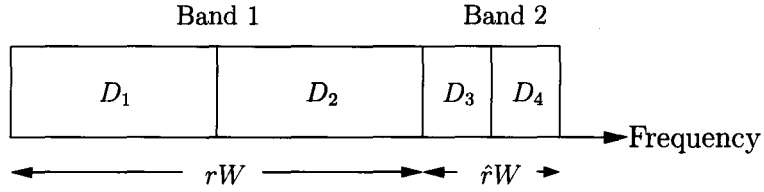

Figure 3.5: Partitioning of the total bandwidth W into two bands and four subchannels, where $\hat{r} = 1 - r$.

The half-duplex cooperation scheme that will be considered is a modified version of a block-based version of the scheme proposed in [67, Section III]. The modification is that the system bandwidth is partitioned into two bands of fractional bandwidth r and $\hat{r} = 1 - r$, $0 \leqslant r \leqslant 1$, respectively, rather than having r fixed to $r = 1/2$.[7] In the first band, node 2 acts as a relay for node 1 and does not attempt to transmit its own data, while in the second band, node 1 acts solely as a relay for node 2. The chosen relaying strategy is of the regenerative decode-and-forward (RDF) type, and exploits coherent combining at the destination node. (The chosen scheme does not require backward decoding.) Each band is partitioned into two orthogonal subchannels.[8] Those in the first band will be denoted D_1 and D_2 and those in the second band will be denoted D_3 and D_4. a repetition-based transmission strategy within each band will be adopted, and hence the subchannels D_1 and D_2 will each contain half of the bandwidth of the first band, and D_3 and D_4 will each contain half of the bandwidth of the second band. A typical bandwidth allocation for this system is given in Fig. 3.5.

The transmission strategy envisioned for this system is depicted in Fig. 3.6, where we have used $Q_i^{(k)}$ to denote the power allocated by node i to the k^{th} band, and

[7]It is possible to construct equivalent systems in which the communication resource that is partitioned is a time interval or the components of a (large) set of orthogonal spreading codes, rather than the system bandwidth, but the principles that underly our approach are the same in those cases. For ease of exposition we will focus on the case of bandwidth allocation.

[8]Again, for ease of exposition the focus will be on systems in which the subchannels are synthesized in frequency.

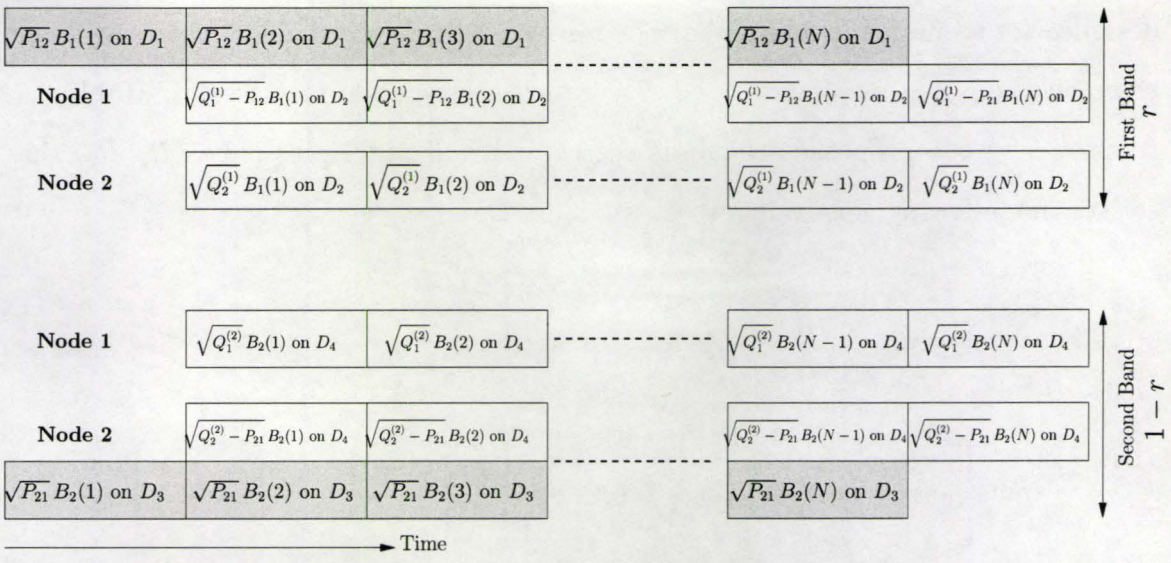

Figure 3.6: The modified half-duplex cooperation scheme. In the first band, node 2 acts as a regenerative relay for node 1, and in the second band these roles are reversed.

hence the total power transmitted by node i is $P_i = Q_i^{(1)} + Q_i^{(2)}$. Let us consider the operation of the first band, in which node 2 acts as solely a relay for node 1. In the n^{th} block channel use, $2 \leqslant n \leqslant N-1$, node 1 transmits a new codeword (or new segment of a larger codeword), $B_1(n)$, on subchannel D_1 with power P_{12}, and repeats its previous codeword, $B_1(n-1)$, on subchannel D_2 with power $Q_1^{(1)} - P_{12}$. In that same block, node 2 receives $B_1(n)$ on subchannel D_1, and regeneratively retransmits $B_1(n-1)$ on subchannel D_2 with power $Q_2^{(1)}$ and with the phase corrected so that it coherently combines at the destination node with the repeated transmission of $B_1(n-1)$ by node 1. The first block channel use contains only the first codeword (segment) from node 1, and the last block involves only repetition of the previous codeword, but the impact of these end effects can be neglected when N is large. In the second band, the roles are reversed, with powers as shown in Fig. 3.6.

The half-duplex cooperative multiple access scheme described above has been

designed for scenarios in which the cooperative channels are stronger than the direct channels; i.e., $\gamma_{12} \geqslant \gamma_{10}$ and $\gamma_{21} \geqslant \gamma_{20}$, which corresponds to Case 1 in Table 3.1. In that case, the proposed scheme is the convex hull of all rate pairs (R_1, R_2) that satisfy the following constraints (see Appendix D)

$$R_1 \leqslant \bar{R}_1 = \frac{r}{2} \min \left\{ \log\left(1 + \frac{\gamma_{12}P_{12}}{r/2}\right), \log\left(1 + \frac{\gamma_{10}P_{12} + \left(\sqrt{\gamma_{10}(Q_1^{(1)} - P_{12})} + \sqrt{\gamma_{20}Q_2^{(1)}}\right)^2}{r/2}\right) \right\}, \tag{3.36a}$$

$$R_2 \leqslant \bar{R}_2 = \frac{(1-r)}{2} \min \left\{ \log\left(1 + \frac{\gamma_{21}P_{21}}{(1-r)/2}\right), \log\left(1 + \frac{\gamma_{20}P_{21} + \left(\sqrt{\gamma_{20}(Q_2^{(2)} - P_{21})} + \sqrt{\gamma_{10}Q_1^{(2)}}\right)^2}{(1-r)/2}\right) \right\}. \tag{3.36b}$$

The first term on the right hand side of (3.36a) and the first term on the right hand side of (3.36b) ensure that the messages to the relaying nodes can be reliably decoded, while the second term on the right hand side of (3.36a) and the second term on the right hand side of (3.36b) arise from the combination of the repeated direct transmissions and the regeneratively relayed signals. In particular, in the econd term on the right hand side of (3.36a) the term $\gamma_{10}P_{12}$ is the SNR of the direct transmission of $B_1(n)$ to the destination node on subchannel D_1 in block n, and the term $\left(\sqrt{\gamma_{10}(Q_1^{(1)} - P_{12})} + \sqrt{\gamma_{20}Q_2^{(1)}}\right)^2$ is the SNR of the coherent combination of the repetition of $B_1(n)$ by node 1 on subchannel D_2 in block $n+1$ and the regenerative retransmission of $B_1(n)$ on subchannel D_2 in block $n+1$ by node 2. (The relay receives $B_1(n)$ on subchannel D_1 in block n.) The roles of nodes 1 and 2 are reversed

in the second band, leading to the second term on the right hand side of (3.36b).[9]

For a given value of the fractional bandwidth allocation, r, we can determine the achievable rate region by maximizing R_1 for each value of R_2 subject to (3.36) and the constraint that $P_i \leqslant \bar{P}_i$. Using techniques similar to those in Section 3.2, that problem can simplified to (see Appendix E for a derivation)

$$\max_{Q_1^{(1)},Q_2^{(1)}} \quad \frac{r}{2}\log\left(1+\frac{\gamma_{12}f_1(Q_1^{(1)},Q_2^{(1)})}{r/2}\right) \tag{3.37a}$$

$$\text{subject to} \quad \gamma_{20}^2\left(Q_2^{(1)}\right)^2 - B_0Q_2^{(1)} - 2\gamma_{10}\gamma_{20}Q_1^{(1)}Q_2^{(1)} + C_0Q_1^{(1)} + \gamma_{10}^2\left(Q_1^{(1)}\right)^2 + D_0 \leqslant 0, \tag{3.37b}$$

$$f_1\left(Q_1^{(1)},Q_2^{(1)}\right) - Q_1^{(1)} \leqslant 0, \tag{3.37c}$$

$$0 \leqslant Q_1^{(1)} \leqslant \bar{P}_1, \qquad 0 \leqslant Q_2^{(1)} \leqslant \bar{P}_2, \tag{3.37d}$$

where $f_1\left(Q_1^{(1)},Q_2^{(1)}\right)$ and the constants B_0, C_0 and D_0 are defined in Appendix E. It is shown in Appendix E that the problem in (3.37) is convex, and hence the optimal values for $Q_1^{(1)}$ and $Q_2^{(1)}$ can be efficiently obtained. Appendix E also contains the modifications that need to be made to (3.37) in the case where r is a timesharing parameter rather than a bandwidth sharing parameter.

The formulation in (3.37) gives the optimal power allocation for a given value of r. However, our goal is to find the value of r that enables the largest R_1; i.e., the largest optimal value in (3.37). It is clear that the optimal value of r depends on the target value of R_2; i.e, the different points on the boundary of the achievable rate region are not achieved with the same r. Therefore, in order to determine the achievable

[9]It is relatively straightforward to obtain an expression for the achievable rate region of the proposed scheme in the other cases in Table 3.1. In particular, if $\gamma_{ij} < \gamma_{i0}$, one would switch off the relaying activity of node j (i.e., set $Q_j^{(i)} = 0$), and the rate constraint on communication from node i to node j would be removed. That said, in such cases the proposed scheme operates like a repetition-based orthogonal multiple access scheme, and for certain target rates for one of the users, one may be able to achieve a larger rate for the other user by time sharing between the proposed scheme and a conventional multiple access scheme.

rate region, we will have to optimize over both the powers and the resource sharing parameter, r. Although the problem in (3.37) is not convex in r and the powers, the following result, which is proved in Appendix F, will enable the development of an efficient algorithm for the optimal value of r.

Proposition 3.1 *For a given rate $\bar{R}_2$, the maximum achievable rate $\bar{R}_1$ in* (3.37) *is a quasi-concave function of the resource sharing parameter r.*

Since $\bar{R}_1$ is quasi-concave in r, we can determine the optimal value of r using a standard search method for quasi-convex problems [5]. At each step in the search, a problem based on (3.37) with the current value for r is solved. Since the problem in (3.37) can be efficiently solved, and since the quasi-convex search can be efficiently implemented, the optimal design of r and the powers P_{12}, P_{21}, $Q_1^{(1)}$, $Q_1^{(2)}$, $Q_2^{(1)}$ and $Q_2^{(2)}$ can be efficiently obtained.

In (3.37) and in Proposition 3.1 the target rate approach was used to parameterize a certain point on the achievable rate region. However, using the result of Appendix E, it can be shown (see Appendix G) that the optimal solution to the weighted sum rate maximization problem can be obtained using an iterative algorithm in which the target rate problem is solved at each step.

To illustrate the performance of the modified half-duplex cooperation multiple access scheme, the average achievable rate regions for several multiple access schemes are plotted in Figs 3.7 and 3.8. We consider the case of no cooperation (i.e., conventional multiple access), an optimally power loaded block-based version of the half-duplex strategy in [67, Section III],[10] the proposed half-duplex strategy and the full-duplex strategy from Section 3.2. In each scenario, the noise variance and the

[10]Recall that the proposed scheme reduces to a block-based version of the scheme in [67, Section III] when r is set to $1/2$. Therefore, the optimal power loading for that scheme can be found by solving (3.37) with $r = 1/2$.

transmitted powers were normalized to one, and the channel gains were Rayleigh distributed. In Fig. 3.7, the direct channel gains are statistically symmetric with $E(K_{10}) = E(K_{20}) = 0.3$, and $K_{12} = K_{21}$ with $E(K_{12}) = 0.5$. In Fig. 3.8, the direct channel gains are statistically asymmetric with $E(K_{10}) = 0.4$, $E(K_{20}) = 0.3$, and $K_{12} = K_{21}$ with $E(K_{12}) = 0.7$. In both Figs 3.7 and 3.8, the proposed half-duplex strategy provides a significant expansion of the achievable rate region over that of the half-duplex strategy in [67] when the rates of the nodes are significantly different. This is a consequence of the efficient algorithm for finding the optimal resource sharing parameter. Since $r = 1/2$ is the optimal value of r when $R_1 = R_2$, boundaries of the achievable rate regions of the proposed strategy and that in [67] overlap at this point.

3.6 Conclusion

In this Chapter the power allocation problem in full-duplex cooperative multiple access schemes has been analyzed and the joint power and resource allocation problem in a class of half-duplex cooperative multiple access schemes has been solved. In the full-duplex case, the analysis revealed an underlying convex optimization problem that has a closed-form solution, while in the half-duplex case the quasi-convexity of the resource allocation problem was exposed and exploited to develop an efficient algorithm. In doing so, it has been demonstrated that a significantly larger fraction of the achievable rate region of the full-duplex case can be obtained with the proposed scheme. Moreover, the reduction that has been obtained in the complexity of finding the optimal power and resource allocation suggests that it may be possible to avoid approximations in the development of on-line algorithms.

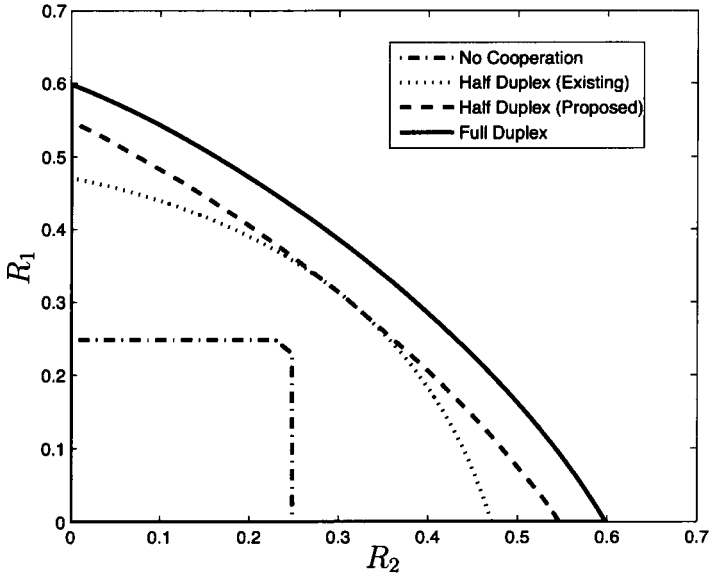

Figure 3.7: Achievable rate region for the no cooperation case, the existing cooperative strategy in [67], the proposed cooperative strategy and the full-duplex model in case of statistically symmetric direct channels. $P_1 = P_2 = 1.0, \sigma_0^2 = \sigma_1^2 = \sigma_2^2 = 1, E(K_{10}) = E(K_{20}) = 0.3, E(K_{12}) = E(K_{21}) = 0.5$.

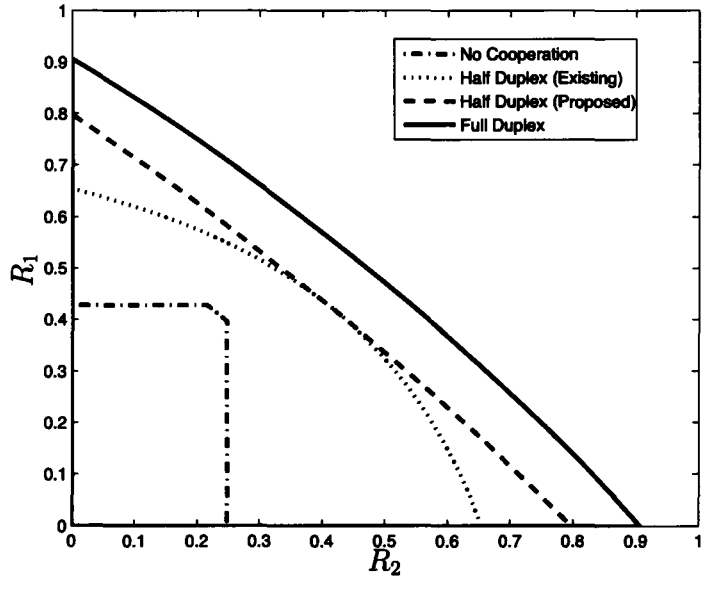

Figure 3.8: Achievable rate region for the no cooperation case, the existing cooperative strategy in [67], the proposed cooperative strategy and the full-duplex model in case of statistically asymmetric direct channels. $P_1 = P_2 = 1.0, \sigma_0^2 = \sigma_1^2 = \sigma_2^2 = 1, E(K_{10}) = 0.4, E(K_{20}) = 0.3, E(K_{12}) = E(K_{21}) = 0.7$.

Chapter 4

Joint Power and Resource Allocation for Two-User Orthogonal Amplify-and-Forward Cooperation

In this chapter the jointly optimal allocation of transmission power and channel resources for a two-user orthogonal amplify-and-forward (AF) cooperation scheme is considered. In particular, a simple efficient algorithm for determining the power and resource allocations required to operate at any point on the boundary of the achievable rate region is derived. The algorithm is based on two results derived herein: a closed-form solution for the optimal power allocation for a given channel resource allocation; and the fact that the channel resource allocation problem is quasi-convex. The structure of the optimal power allocation reveals that at optimality at most one user acts as a relay, and hence a fraction of the channel resource will be idle. A modified orthogonal AF cooperation scheme is proposed. The modified scheme uses the

channel resources more efficiently and hence provides a larger achievable rate region.

4.1 Introduction

The growing demand for reliable spectrally-efficient wireless communication has led to a resurgence of interest in systems in which nodes cooperate in the transmission of messages to a destination node; e.g., [66]. (See Fig. 4.1.) An achievable rate region for a full-duplex pairwise cooperative multiple access system was obtained in [66], based on earlier work in [81], and this achievable rate region was shown to be larger than the capacity region for conventional multiple access without cooperation between the source nodes. However, full-duplex cooperation requires sufficient electrical isolation between the transmitting and receiving circuits at each node in order to mitigate near-end cross-talk (e.g., [22,38,41,61]), and this is often difficult to achieve in practice. In order to avoid the need for stringent electrical isolation, the cooperation scheme can be constrained so that the source nodes do not simultaneously transmit and receive over the same channel, and such schemes are often said to be half-duplex; e.g., [4,38]. The subclass of half-duplex schemes with orthogonal components (e.g., [38]) further constrains the source nodes to use orthogonal subchannels.[1] This enables "per-user" decoding at the destination node, rather than joint decoding, and hence simplifies the receiver at the destination node. Motivated by this simplicity, we will focus on orthogonal (half-duplex) cooperation schemes in this chapter.

A feature of orthogonal pairwise cooperation schemes is that they can be decomposed into two parallel relay channels, each with orthogonal components [14,22,41].

[1]These subchannels can be synthesized by time division (e.g., [38]), or by frequency division; e.g., [41].

Therefore, the remaining design issues reduce to the choice of the relaying strategy, and the allocation of power and channel resources (radio resources) to the parallel relay channels. For the relaying strategy, a number of choices are available (e.g., [7, 10, 34, 36, 38, 53, 65]), and the focus in this chapter will be on the amplify-and-forward (AF) strategy, because it is the simplest in terms of the hardware requirements of the cooperating nodes. As such, the cooperative scheme that will be considered is a generalization of the orthogonal AF scheme in [38]. One of the contributions will be the development of a simple efficient algorithm for joint power and channel resource allocation for this scheme, for scenarios in which full channel state information (CSI) is available.[2]

As mentioned above, the design of an orthogonal AF cooperation scheme requires the appropriate allocation of powers and channel resources to the components of each of the underlying parallel relay channels. Unfortunately, the problem of joint power and resource allocation so as to enable operation on the boundary of the achievable rate region is not convex; a fact that might suggest that this is a rather difficult problem to solve. Some progress has been made by considering power allocation alone [1].[3] In particular, it was shown in [1] that for a given resource allocation, the problem of finding the power allocation that maximizes a weighted-sum of achievable rates can be written in a quasi-convex (e.g., [5]) form. In this chapter, the problem of jointly allocating the power and the channel resource will be considered. In particular, it will be shown that for a given target rate of one node, the maximum achievable rate of the other node can be written as a convex function of the transmission powers (see Section 4.3.1) and a quasi-convex function of the resource allocation parameter

[2]That is, the design is based on knowledge of the (effective) channel gain on each of the four links in Fig. 4.1.

[3]See [72] for some related work on a non-orthogonal AF cooperation scheme, [84] for some related work with an outage objective, and [47, 55] for some related work on half-duplex cooperation with decode-and-forward relaying. There has also been a considerable amount of work on power and resource allocation for a variety of relaying schemes with achievable rate or outage objectives; e.g., [3, 22, 39, 41, 56, 65, 83].

(see Section 4.4). Furthermore, using the Karush-Kuhn-Tucker (KKT) optimality conditions (e.g., [5]), a closed-form solution for the optimal power allocation for a given resource allocation will be derived (see Section 4.3.3). By combining this closed-form solution with the quasi-convexity of the maximum achievable rate in the resource allocation parameter, a simple efficient algorithm for the jointly optimal power and channel resource allocation will be obtained (see Section 4.4). In addition to the computational efficiencies that this approach provides, the ability to directly control the rate of one of the nodes can be convenient in the case of heterogeneous traffic at the cooperative nodes, especially if one node has a constant rate requirement and the other is dominated by "best effort" traffic.

The structure of the closed-form solution to the optimal power allocation problem for a fixed channel resource allocation (see Section 4.3.2) suggests that under the assumption that channel state information is available, the adopted cooperative communication scheme (which is based on that proposed in [38]) does not use all the available channel resources. (A related observation was made in [72] for a non-orthogonal half-duplex AF cooperation scheme.) Hence, the cooperative scheme itself incurs a reduction in the achievable rate region. In order to mitigate this rate reduction, in Section 4.5 a modified cooperative scheme is proposed. The modified scheme retains the orthogonal half-duplex property of the original scheme (and that in [38]), yet can achieve a significantly larger achievable rate region. Similar to original cooperative scheme, a closed-form solution to the problem of optimal power allocation (for fixed resource allocation) for this modified scheme is obtained, and it is shown that the problem of optimal channel resource allocation is quasi-convex (see Section 4.5). Therefore, the jointly optimal power and channel resource allocation for this modified scheme can also be obtained using a simple efficient algorithm.

Although the focus of this chapter will be on scenarios in which perfect channel

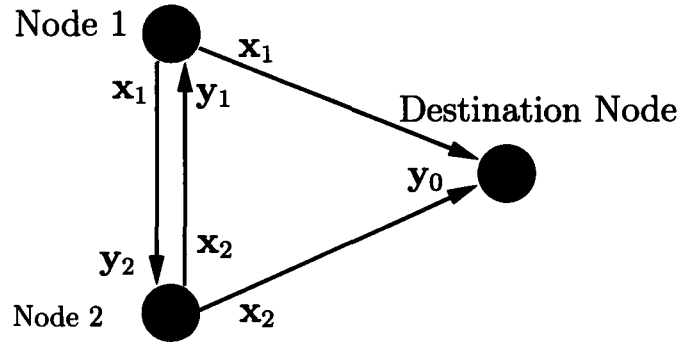

Figure 4.1: Transmitted and received signals of the cooperative channel.

$x_1(1) = \sqrt{P_{11}}B_{11}$	$x_1(2) = 0$	$x_1(3) = 0$	$x_1(4) = A_1 y_1(3)$
$x_2(1) = 0$	$x_2(2) = A_2 y_2(1)$	$x_2(3) = \sqrt{P_{22}}B_{21}$	$x_2(4) = 0$

r $\hat{r} = 1 - r$

Figure 4.2: A frame of the orthogonal half-duplex amplify-and-forward cooperation scheme under consideration.

state information (CSI) is available, in Section 4.6 an example of a simple modification of the proposed approach that encompasses scenarios with imperfect CSI is provided.

4.2 System Model and Direct Formulation

This chapter considers a system in which two users (Nodes 1 and 2) wish to cooperate in the transmission of messages to a destination node (Node 0); cf. Fig. 4.1. In order to enable simple implementation, an orthogonal half-duplex amplify-and-forward cooperation scheme will be adopted. In particular, the scheme illustrated in Fig. 4.2

will be adopted,[4] which is a mild generalization of the scheme proposed in [38].[5] Each frame of the scheme consists of four time blocks, with the first two blocks being of fractional length $r/2$ and the second two blocks having fractional length $\hat{r}/2$, where $\hat{r} = 1 - r$.[6] In the first block, Node 1 transmits its message while Node 2 listens. In the second block, Node 2 works as a relay for Node 1; it amplifies the signal received in the first block by a factor A_2 and re-transmits that signal to the master node. In the third and fourth blocks the roles of Nodes 1 and 2 are reversed, so that Node 1 works as a relay for Node 2. In Fig. 4.2, resource allocation is implemented in the time domain by allocating a fraction r of the frame for the message from Node 1, and a fraction $\hat{r} = 1 - r$ of the frame for the message of Node 2.

A block fading channel model is considered with a coherence time that is long enough to focus on the case in which full channel state information (CSI) can be acquired without expending a significant fraction of the available power and channel resources. (A scenario with uncertain CSI will be considered in Section 4.6.) If we define $\mathbf{y}_n(\ell)$ to be the signal block received by Node n during block ℓ, then the received signals of interest are $\mathbf{y}_1(\ell)$ for $\ell \bmod 4 = 3$, $\mathbf{y}_2(\ell)$ for $\ell \bmod 4 = 1$, and $\mathbf{y}_0(\ell)$ for all ℓ. If we define K_{mn} to be the complex channel gain between Nodes $m \in \{1, 2\}$ and $n \in \{0, 1, 2\}$, and $\mathbf{z}_n(\ell)$ to be the zero-mean additive white circular complex Gaussian noise vector with independent components of variance σ_n^2 at Node n, then the received

[4] In Fig. 4.2 the orthogonal subchannels are synthesized by time division. Although we will focus on that case, our work can be modified in a straightforward way to address the case of frequency division.

[5] In the scheme in [38] the resource allocation parameter is fixed at $r = 1/2$. In the proposed scheme, r is a design variable.

[6] The first and the second blocks have the same length because the adoption of the amplify-and-forward relaying means that the length of the signals to be transmitted in these two blocks is the same. For that reason the third and fourth blocks are also of the same length.

signal blocks can be written as[7]

$$\mathbf{y}_1(\ell) = \begin{cases} K_{21}\mathbf{x}_2(\ell) + \mathbf{z}_1(\ell) & \ell \bmod 4 = 3, \\ \mathbf{0} & \ell \bmod 4 \neq 3, \end{cases} \tag{4.1}$$

$$\mathbf{y}_2(\ell) = \begin{cases} K_{12}\mathbf{x}_1(\ell) + \mathbf{z}_2(\ell) & \ell \bmod 4 = 1, \\ \mathbf{0} & \ell \bmod 4 \neq 1, \end{cases} \tag{4.2}$$

$$\mathbf{y}_0(\ell) = \begin{cases} K_{10}\mathbf{x}_1(\ell) + \mathbf{z}_0(\ell) & \ell \bmod 4 = 1, \\ K_{20}A_2\mathbf{y}_2(\ell-1) + \mathbf{z}_0(\ell) & \ell \bmod 4 = 2, \\ K_{20}\mathbf{x}_2(\ell) + \mathbf{z}_0(\ell) & \ell \bmod 4 = 3, \\ K_{10}A_1\mathbf{y}_1(\ell-1) + \mathbf{z}_0(\ell) & \ell \bmod 4 = 0, \end{cases} \tag{4.3}$$

where A_1 and A_2 represent the amplification factors of Nodes 1 and 2, respectively, when they act as a relay. Let us define P_{ij} to be the power allocated by Node i to the transmission of the message from Node j. With that definition, the powers of the (non-zero) transmitted signals in the blocks in Fig. 4.2 are P_{11}, P_{21}, P_{22}, and P_{12}, respectively. Furthermore, the amplification factors A_1 and A_2 that ensure that all the available relaying power is used are [38]

$$A_1 = \sqrt{\frac{P_{12}}{|K_{21}|^2 P_{22} + \sigma_1^2}}, \qquad A_2 = \sqrt{\frac{P_{21}}{|K_{12}|^2 P_{11} + \sigma_2^2}}. \tag{4.4}$$

We will impose average transmission power constraints on each node, namely, the power components should satisfy the average power constraints $\frac{r}{2}P_{i1} + \frac{\hat{r}}{2}P_{i2} \leqslant \bar{P}_i$, where $\bar{P}_i$ is the maximum average power for Node i. For notational simplicity, define the effective channel gain to be $\gamma_{mn} = |K_{mn}|^2/\sigma_n^2$.

For a given allocation for the power components, $\mathcal{P} = (P_{11}, P_{12}, P_{21}, P_{22})$, and a given value for r, the achievable rate region of the system described above is the set of all rate pairs (R_1, R_2) that satisfy [38]

$$R_1 \leqslant \bar{R}_1(\mathcal{P}, r) = \frac{r}{2}\log\left(1 + \gamma_{10}P_{11} + \frac{\gamma_{20}\gamma_{12}P_{11}P_{21}}{1 + \gamma_{20}P_{21} + \gamma_{12}P_{11}}\right), \tag{4.5a}$$

[7]We use **0** to represent blocks in which the receiver is turned off.

$$R_2 \leqslant \bar{R}_2(\mathcal{P}, r) = \frac{\hat{r}}{2} \log\left(1 + \gamma_{20} P_{22} + \frac{\gamma_{10}\gamma_{21} P_{12} P_{22}}{1 + \gamma_{21} P_{22} + \gamma_{10} P_{12}}\right). \tag{4.5b}$$

Since we are considering scenarios in which full channel state information (CSI) is available (i.e., γ_{10}, γ_{20}, γ_{12}, and γ_{21} are known), one way in which the power and channel resource allocation required to approach a specified point on the boundary of the achievable rate region can be found is by maximizing a weighted sum of $\bar{R}_1$ and $\bar{R}_2$ subject to the bound on the transmitted powers; i.e.,

$$\max_{P_{ij}, r} \quad \mu \bar{R}_1(\mathcal{P}, r) + (1-\mu)\bar{R}_2(\mathcal{P}, r) \tag{4.6a}$$

$$\text{subject to} \quad \tfrac{r}{2} P_{11} + \tfrac{\hat{r}}{2} P_{12} \leqslant \bar{P}_1, \tag{4.6b}$$

$$\tfrac{r}{2} P_{21} + \tfrac{\hat{r}}{2} P_{22} \leqslant \bar{P}_2, \tag{4.6c}$$

$$P_{ij} \geqslant 0. \tag{4.6d}$$

An alternative approach to finding the required power and channel resource allocation is to maximize $\bar{R}_i$ for a given target value of $\bar{R}_j$, subject to the bound on the transmitted powers; i.e.,

$$\max_{P_{ij}, r} \quad \bar{R}_1(P_{ij}, r) \tag{4.7a}$$

$$\text{subject to} \quad \bar{R}_2(P_{ij}, r) \geqslant R_{2,\text{tar}}, \tag{4.7b}$$

$$\tfrac{r}{2} P_{11} + \tfrac{\hat{r}}{2} P_{12} \leqslant \bar{P}_1, \tag{4.7c}$$

$$\tfrac{r}{2} P_{21} + \tfrac{\hat{r}}{2} P_{22} \leqslant \bar{P}_2, \tag{4.7d}$$

$$P_{ij} \geqslant 0. \tag{4.7e}$$

Unfortunately, neither (4.6) nor (4.7) is jointly convex P_{ij} and r, and this makes the development of a reliable efficient allocation algorithm rather difficult. However, it will be shown below that by adopting the approach in (4.7), the direct formulation can be transformed into the composition of a convex optimization problem and a quasi-convex problem. Furthermore, a closed-form solution for the (inner) convex problem

(see Section 4.3) will be derived, and it will be shown that this enables the solution of (4.7) using a simple efficient search over the resource allocation parameter, r; see Section 4.4.

4.3 Optimal Power Allocation

In this section a closed-form expression for the optimal power allocation for a given channel resource allocation r is obtained. The derivation of this closed-form expression involves three main steps: the derivation of a convex problem that is equivalent to the problem in (4.7) with a fixed value for r; an analysis of KKT optimality conditions for that problem; and analytic solutions to a pair of scalar optimization problems. To simplify our development, let $R_{2,\max}(r)$ denote the maximum achievable value for R_2 for a given value of r; i.e., the value of $\bar{R}_2(\mathcal{P}, r)$ in (4.5b) with $\mathcal{P} = (0, 2\bar{P}_1, 0, 2\bar{P}_2)$.

4.3.1 A convex equivalent to (4.7) with a fixed value for r

For a given value for r, the problem in (4.7) involves optimization over P_{ij} only. If we define $\tilde{P}_{i1} = rP_{i1}$ and $\tilde{P}_{i2} = \hat{r}P_{i2}$, then for $r \in (0,1)$ and $R_{2,\text{tar}} \in (0, R_{2,\max}(r))$ we can rewrite (4.7) as[8]

$$\max_{\tilde{P}_{ij}} \quad \frac{r}{2}\log\left(1 + \frac{\gamma_{10}\tilde{P}_{11}}{r} + \frac{\gamma_{20}\gamma_{12}\tilde{P}_{11}\tilde{P}_{21}}{r(r+\gamma_{20}\tilde{P}_{21}+\gamma_{12}\tilde{P}_{11})}\right) \tag{4.8a}$$

$$\text{subject to} \quad \frac{\hat{r}}{2}\log\left(1 + \frac{\gamma_{20}\tilde{P}_{22}}{\hat{r}} + \frac{\gamma_{10}\gamma_{21}\tilde{P}_{12}\tilde{P}_{22}}{\hat{r}(\hat{r}+\gamma_{21}\tilde{P}_{22}+\gamma_{10}\tilde{P}_{12})}\right) \geqslant R_{2,\text{tar}}, \tag{4.8b}$$

$$\tilde{P}_{11} + \tilde{P}_{12} \leqslant 2\bar{P}_1, \tag{4.8c}$$

$$\tilde{P}_{21} + \tilde{P}_{22} \leqslant 2\bar{P}_2, \tag{4.8d}$$

$$\tilde{P}_{ij} \geqslant 0. \tag{4.8e}$$

[8]In (4.7), the resource allocation $r = 1$ is feasible only if $R_{2,\text{tar}} = 0$, and the allocation $r = 0$ is optimal only if $R_{2,\text{tar}} = R_{2,\max}(0)$. Also, if $R_{2,\text{tar}} = 0$, the optimal $\mathcal{P} = (2\bar{P}_1, 0, 2\bar{P}_2, 0)$ and if $R_{2,\text{tar}} = R_{2,\max}(r)$, the optimal $\mathcal{P} = (0, 2\bar{P}_1, 0, 2\bar{P}_2)$.

The formulation in (4.8) has the advantage that the power constraints in (4.8c) and (4.8d) are linear in $\tilde{P}_{ij}$, whereas the corresponding constraints in (4.7) are bilinear in P_{ij} and r.

For a given positive value of r and non-negative constant values of a, b, c and d, the function $\log(1+\frac{ax}{r}+\frac{bcxy}{r(r+bx+cy)})$ is not concave in x and y, and hence (4.8) is not a convex problem. However, it can be shown (see Appendix H) that the function $h(x,y)=\sqrt{\frac{ax}{r}+\frac{bcxy}{r(r+bx+cy)}}$ is concave in x and y (on the non-negative orthant). By taking the exponent of both sides, the constraint in (4.8b) can be rewritten as

$$\sqrt{\frac{\gamma_{20}\tilde{P}_{22}}{\hat{r}}+\frac{\gamma_{10}\gamma_{21}\tilde{P}_{12}\tilde{P}_{22}}{\hat{r}(\hat{r}+\gamma_{21}\tilde{P}_{22}+\gamma_{10}\tilde{P}_{12})}} \geqslant \sqrt{2^{\frac{2R_{2,\text{tar}}}{\hat{r}}}-1}. \tag{4.9}$$

which yields a convex feasible set for $(\tilde{P}_{12},\tilde{P}_{22})$ by virtue of the concavity of $h(x,y)$. Furthermore, since the logarithm and the square root functions are monotonically increasing functions for positive arguments, maximizing the objective function in (4.8a) is equivalent to maximizing $h(\tilde{P}_{11},\tilde{P}_{21})$ with $a=\gamma_{10}$, $b=\gamma_{20}$ and $c=\gamma_{12}$. Therefore, the problem in (4.8) is equivalent to

$$\max_{\tilde{P}_{ij}} \quad \sqrt{\frac{\gamma_{10}\tilde{P}_{11}}{r}+\frac{\gamma_{20}\gamma_{12}\tilde{P}_{11}\tilde{P}_{21}}{r(r+\gamma_{20}\tilde{P}_{21}+\gamma_{12}\tilde{P}_{11})}} \tag{4.10a}$$

$$\text{subject to} \quad \sqrt{\frac{\gamma_{20}\tilde{P}_{22}}{\hat{r}}+\frac{\gamma_{10}\gamma_{21}\tilde{P}_{12}\tilde{P}_{22}}{\hat{r}(\hat{r}+\gamma_{21}\tilde{P}_{22}+\gamma_{10}\tilde{P}_{12})}} \geqslant \sqrt{2^{\frac{2R_{2,\text{tar}}}{\hat{r}}}-1}, \tag{4.10b}$$

$$\tilde{P}_{11}+\tilde{P}_{12} \leqslant 2\bar{P}_1, \tag{4.10c}$$

$$\tilde{P}_{21}+\tilde{P}_{22} \leqslant 2\bar{P}_2, \tag{4.10d}$$

$$\tilde{P}_{ij} \geqslant 0. \tag{4.10e}$$

The concavity of $h(x,y)$ implies that (4.10) is a convex optimization problem. Furthermore, for all $R_{2,\text{tar}} \in (0, R_{2,\max}(r))$ the problem in (4.10) satisfies Slater's condition (e.g., [5]), and hence the KKT optimality conditions are necessary and sufficient. As will be shown below, this observation is a key step in the derivation of the closed-form solution to (4.8).

4.3.2 Structure of the optimal solution

The KKT optimality conditions will be used for (4.10) to show that at optimality one (or both) of $\tilde{P}_{12}$ and $\tilde{P}_{21}$ is zero.[9] Therefore, at optimality, at least one of the nodes has its relay mode turned off. We begin by observing that for all feasible $R_{2,\text{tar}}$ the optimal power allocation satisfies power constraints in (4.10c) and (4.10d) with equality; i.e., $\tilde{P}_{i2}^* = 2\bar{P}_i - \tilde{P}_{i1}^*$, where the asterisk indicates the optimal value. Therefore, the problem in (4.10) can be rewritten as the following (convex) optimization problem in $\tilde{P}_{11}$ and $\tilde{P}_{21}$:

$$\min_{\tilde{P}_{11},\tilde{P}_{21}} \; f_0(\tilde{P}_{11},\tilde{P}_{21}) \qquad \text{subject to} \qquad f_i(\tilde{P}_{11},\tilde{P}_{21}) \leqslant 0 \quad i=1,\ldots,5, \tag{4.11}$$

where

$$\begin{aligned}
f_0(\tilde{P}_{11},\tilde{P}_{21}) &= -\left(\frac{\gamma_{10}\tilde{P}_{11}}{r} + \frac{\gamma_{20}\gamma_{12}\tilde{P}_{11}\tilde{P}_{21}}{r(r+\gamma_{20}\tilde{P}_{21}+\gamma_{12}\tilde{P}_{11})}\right)^{1/2},\\
f_1(\tilde{P}_{11},\tilde{P}_{21}) &= \left(2^{\frac{2R_{2,\text{tar}}}{\hat{r}}}-1\right)^{1/2}\\
&\quad - \left(\frac{\gamma_{20}(2\bar{P}_2-\tilde{P}_{21})}{\hat{r}} + \frac{\gamma_{10}\gamma_{21}(2\bar{P}_1-\tilde{P}_{11})(2\bar{P}_2-\tilde{P}_{21})}{\hat{r}(\hat{r}+\gamma_{21}(2\bar{P}_2-\tilde{P}_{21})+\gamma_{10}(2\bar{P}_1-\tilde{P}_{11}))}\right)^{1/2},\\
f_2(\tilde{P}_{11},\tilde{P}_{21}) &= -\tilde{P}_{11}, \qquad f_3(\tilde{P}_{11},\tilde{P}_{21}) = -\tilde{P}_{21},\\
f_4(\tilde{P}_{11},\tilde{P}_{21}) &= \tilde{P}_{11}-2\bar{P}_1, \qquad f_5(\tilde{P}_{11},\tilde{P}_{21}) = \tilde{P}_{21}-2\bar{P}_2.
\end{aligned}$$

The KKT optimality conditions for this problem are

$$f_i(\tilde{P}_{11}^*,\tilde{P}_{21}^*) \leqslant 0, \tag{4.12a}$$

$$\lambda_i^* \geqslant 0, \tag{4.12b}$$

$$\begin{pmatrix} \frac{\partial f_0(\tilde{P}_{11}^*,\tilde{P}_{21}^*)}{\partial \tilde{P}_{11}} + \lambda_1^* \frac{\partial f_1(\tilde{P}_{11}^*,\tilde{P}_{21}^*)}{\partial \tilde{P}_{11}} + \lambda_4^* - \lambda_2^* \\ \frac{\partial f_0(\tilde{P}_{11}^*,\tilde{P}_{21}^*)}{\partial \tilde{P}_{21}} + \lambda_1^* \frac{\partial f_1(\tilde{P}_{11}^*,\tilde{P}_{21}^*)}{\partial \tilde{P}_{21}} + \lambda_5^* - \lambda_3^* \end{pmatrix} = \begin{pmatrix} 0 \\ 0 \end{pmatrix}, \tag{4.12c}$$

[9] A related observation was made in [72] for a non-orthogonal half-duplex amplify-and-forward cooperation scheme, although that observation arose from an analysis of the sum-rate optimization problem.

$$\lambda_i^* f_i(\tilde{P}_{11}^*, \tilde{P}_{21}^*) = 0, \tag{4.12d}$$

where λ_i is the ith dual variable. In Appendix I it will be shown that in order for (4.12) to hold, either $\tilde{P}_{12}^* = 0$ or $\tilde{P}_{21}^* = 0$, or both, must be zero. An alternative, and possibly more intuitive, proof can be constructed via the following bounding argument.

Consider a value for $r \in (0,1)$ and a set of feasible values for $\tilde{P}_{1j} = rP_{1j}$ and $\tilde{P}_{2j} = \hat{r}P_{2j}$ that satisfy the power constraints in (4.8c) and (4.8d) with equality. Furthermore, assume that both nodes are relaying for each other; i.e., $\tilde{P}_{12} > 0$, and $\tilde{P}_{21} > 0$. In that case, the achievable rates are

$$\bar{R}_1(P_{ij}, r) = \frac{r}{2}\log\left(1 + \frac{\gamma_{10}\tilde{P}_{11}}{r} + \frac{\gamma_{20}\gamma_{12}\tilde{P}_{11}\tilde{P}_{21}}{r(r + \gamma_{20}\tilde{P}_{21} + \gamma_{12}\tilde{P}_{11})}\right), \tag{4.13a}$$

$$\bar{R}_2(P_{ij}, r) = \frac{\hat{r}}{2}\log\left(1 + \frac{\gamma_{20}\tilde{P}_{22}}{\hat{r}} + \frac{\gamma_{10}\gamma_{21}\tilde{P}_{12}\tilde{P}_{22}}{\hat{r}(\hat{r} + \gamma_{21}\tilde{P}_{22} + \gamma_{10}\tilde{P}_{12})}\right). \tag{4.13b}$$

The key to the argument is to fix the rate of one of the nodes and show that re-allocating the powers so that this rate is achieved by direct transmission increases the achievable rate of the other node.

First, let us consider the case in which $\gamma_{10}\tilde{P}_{12} \geqslant \gamma_{20}\tilde{P}_{21}$. (The other case will be considered at the end of the argument.) In this case let the rate of Node 1 be fixed. If we let $\Delta_1 = \frac{\tilde{\Delta}_1}{r}$ denote the extra power that would need to be added to P_{11} in order to achieve $\bar{R}_1(P_{ij}, r)$ by direct transmission, then we have $\bar{R}_1(P_{ij}, r) = \frac{r}{2}\log\left(1 + \frac{\gamma_{10}(\tilde{P}_{11}+\tilde{\Delta}_1)}{r}\right)$, from which we obtain

$$\gamma_{10}\tilde{\Delta}_1 = \frac{\gamma_{20}\gamma_{12}\tilde{P}_{11}\tilde{P}_{21}}{r + \gamma_{20}\tilde{P}_{21} + \gamma_{12}\tilde{P}_{11}}. \tag{4.14}$$

Now, let $\tilde{P}'_{ij}$ denote the (scaled) power allocation for this scenario. First, $\tilde{P}'_{11} = \tilde{P}_{11} + \tilde{\Delta}_1$, and in order for the power constraint to be satisfied, we must have $\tilde{P}'_{12} \leqslant \tilde{P}_{12} - \tilde{\Delta}_1$. Furthermore, since Node 1 can achieve its desired rate by direct transmission, Node 2

need not allocate power to relay messages for Node 1; i.e., Node 2 can set $\tilde{P}'_{21} = 0$ and hence can set $\tilde{P}'_{22} = 2\bar{P}_2$. If Node 1 uses all of its remaining power to relay for Node 2, i.e., if $\tilde{P}'_{12} = \tilde{P}_{12} - \tilde{\Delta}_1$, then the achievable rate for Node 2 is

$$\bar{R}_2(P'_{ij}, r) = \frac{\hat{r}}{2} \log \left(1 + \frac{\gamma_{20}\tilde{P}'_{22}}{\hat{r}} + \frac{\gamma_{10}\gamma_{21}\tilde{P}'_{12}\tilde{P}'_{22}}{\hat{r}(\hat{r} + \gamma_{21}\tilde{P}'_{22} + \gamma_{10}(\tilde{P}_{12} - \tilde{\Delta}_1))} \right). \tag{4.15}$$

Using the sequence of bounds in Appendix J, it can be shown that $\bar{R}_2(P'_{ij}, r) > \bar{R}_2(P_{ij}, r)$. Therefore, for the same value for the rate of Node 1 a higher rate for Node 2 is achievable if Node 1 operates via direct transmission rather than operating cooperatively. The above argument considered the case in which $\gamma_{10}\tilde{P}_{12} \geqslant \gamma_{20}\tilde{P}_{21}$. In the case that $\gamma_{10}P_{12} \leqslant \gamma_{20}P_{21}$, an analogous argument applies, but with the rate of Node 2 being fixed and achievable by direct transmission.

4.3.3 Closed-form solution to (4.8)

Since the problems in (4.8) and (4.10) are equivalent, the above KKT analysis has shown that the problem in (4.8) can be reduced to one of the following two one-dimensional problems:

$$\beta(r) = \max_{\tilde{P}_{21} \in [0, 2\bar{P}_2]} \quad \frac{r}{2} \log \left(1 + \frac{2\gamma_{10}\bar{P}_1}{r} + \frac{2\gamma_{20}\gamma_{12}\bar{P}_1\tilde{P}_{21}}{r(r + \gamma_{20}\tilde{P}_{21} + 2\gamma_{12}\bar{P}_1)} \right) \tag{4.16a}$$

$$\text{subject to} \quad \frac{\hat{r}}{2} \log \left(1 + \frac{\gamma_{20}(2\bar{P}_2 - \tilde{P}_{21})}{\hat{r}} \right) \geqslant R_{2,\text{tar}}, \tag{4.16b}$$

and

$$\alpha(r) = \max_{\tilde{P}_{11} \in [0, 2\bar{P}_1]} \quad \frac{r}{2} \log \left(1 + \frac{\gamma_{10}\tilde{P}_{11}}{r} \right) \tag{4.17a}$$

$$\text{subject to} \quad \frac{\hat{r}}{2} \log \left(1 + \frac{2\gamma_{20}\bar{P}_2}{\hat{r}} + \frac{2\gamma_{10}\gamma_{21}(2\bar{P}_1 - \tilde{P}_{11})\bar{P}_2}{\hat{r}(\hat{r} + 2\gamma_{21}\bar{P}_2 + \gamma_{10}(2\bar{P}_1 - \tilde{P}_{11}))} \right) \geqslant R_{2,\text{tar}}, \tag{4.17b}$$

where (4.16) arises in the case that $\tilde{P}^*_{12} = 0$, and (4.17) arises in the case that $\tilde{P}^*_{21} = 0$. Using the properties of the logarithm, the transformation that led to (4.9), and the

power constraints, it can be shown that the feasible set of each of these problems is a simple bounded interval. In both problems, the objective is monotonically increasing on that interval, and hence for all feasible $R_{2,\text{tar}}$, the optimal solutions to (4.16) and (4.17) occur when the constraints in (4.16b) and (4.17b), respectively, hold with equality. That is, the solutions to (4.16) and (4.17) are

$$\tilde{P}_{21}^{*} = \tilde{Q}_{\beta} = 2\bar{P}_2 - \frac{\hat{r}}{\gamma_{20}}\left(2^{\frac{2R_{2,\text{tar}}}{\hat{r}}} - 1\right), \tag{4.18}$$

$$\tilde{P}_{11}^{*} = \tilde{Q}_{\alpha} = 2\bar{P}_1 - \frac{(2\bar{P}_2\gamma_{21} + \hat{r})\left(\hat{r}(2^{\frac{2R_{2,\text{tar}}}{\hat{r}}} - 1) - 2\bar{P}_2\gamma_{20}\right)}{\gamma_{10}\left(2\bar{P}_2\gamma_{21} - \left(\hat{r}(2^{\frac{2R_{2,\text{tar}}}{\hat{r}}} - 1) - 2\bar{P}_2\gamma_{20}\right)\right)}, \tag{4.19}$$

respectively. The optimal solution to (4.8) is then the power allocation that corresponds to the larger of the values of $\beta(r)$ and $\alpha(r)$. However, since (4.16) corresponds to the case in which the target rate for Node 2 is met by direct transmission, then it will generate the larger value whenever $R_{2,\text{tar}}$ is less than $R_{2,\text{thresh}}(r) = \frac{\hat{r}}{2}\log\left(1 + \frac{2\gamma_{20}\bar{P}_2}{\hat{r}}\right)$. Therefore, if we let $\tilde{\mathcal{P}} = (\tilde{P}_{11}, \tilde{P}_{12}, \tilde{P}_{21}, \tilde{P}_{22})$ denote a (scaled) power allocation, then for each $r \in (0,1)$ and each $R_{2,\text{tar}} \in (0, R_{2,\max}(r))$ the optimal solution to (4.8) is

$$\tilde{\mathcal{P}}^{*} = \begin{cases} (2\bar{P}_1,\ 0,\ \tilde{Q}_{\beta},\ 2\bar{P}_2 - \tilde{Q}_{\beta}) & \text{if } R_{2,\text{tar}} \leq R_{2,\text{thresh}}(r), \\ (\tilde{Q}_{\alpha},\ 2\bar{P}_1 - \tilde{Q}_{\alpha},\ 0,\ 2\bar{P}_2) & \text{if } R_{2,\text{tar}} > R_{2,\text{thresh}}(r). \end{cases} \tag{4.20}$$

This expression clearly shows that at points on the boundary of the achievable rate region (for the given value of r), at most one node is acting as a relay; i.e., $\tilde{P}_{12} = 0$ or $\tilde{P}_{21} = 0$, or both.

4.4 Optimal power and resource allocation

The expression in (4.20) provides the optimal power allocation for a given value of r. However, different points on the boundary of the achievable rate region are

not necessarily achieved with the same r, and the goal of this section is to jointly optimize the power and resource allocations. Although the problem in (4.7) is not jointly convex in r and the powers, the following result will enable the development of a simple algorithm for finding the optimal value of r.

Proposition 4.1 *If the direct channels of both source nodes satisfy $\gamma_{i0}\bar{P}_i \geqslant \frac{1}{2}$, then for a given target rate for Node j, $R_{j,\text{tar}}$, the maximum achievable rate for Node i is a quasi-concave function of the channel resource allocation parameter r.*

Proof. For simplicity, consider the case in which $i = 1$ and $j = 2$. The first step is to show (see Appendix K) that the condition $\gamma_{10}\bar{P}_1 \geqslant 1/2$ is sufficient for the function $\beta(r)$ in (4.16) to be quasi-concave in the resource sharing parameter r. The function $\alpha(r)$ can be shown to be quasi-concave in r in a similar way. Therefore, the set of values of r for which $\beta(r)$ is greater than a given rate, say $R_{1,\text{test}}$, is a convex set. Let $\mathcal{S}_\beta = \{r|\beta(r) \geq R_{1,\text{test}}\}$ denote that set. Similarly, the condition $\gamma_{20}\bar{P}_2 \geqslant 1/2$ is sufficient for the set $\mathcal{S}_\alpha = \{r|\alpha(r) \geq R_{1,\text{test}}\}$ to be a convex set. Therefore, the set of values for r for which the solution of the original problem in (4.8) is greater than $R_{1,\text{test}}$ is the union of $\mathcal{S}_\beta$ and $\mathcal{S}_\alpha$. To complete the proof, it must be shown that the union of these sets is, itself, convex. When only one of the problems can achieve a rate of at least $R_{1,\text{test}}$, one of $\mathcal{S}_\beta$ and $\mathcal{S}_\alpha$ is empty, and hence the convexity of the union follows directly from the convexity of the non-empty set. For cases in which both $\mathcal{S}_\beta$ and $\mathcal{S}_\alpha$ are non-empty, the fact that r is a scalar means that it is sufficient to prove that the sets intersect. A proof that they do intersect is provided in Appendix L. Therefore, when $\gamma_{i0}\bar{P}_i \geqslant 1/2$, for a given target rate for Node 2, the set of values for r for which the maximum achievable value for the rate of Node 1 is greater than a given rate is a convex set. Hence, the maximum achievable rate for Node 1 is quasi-concave in r.

The result in Proposition 4.1 means that whenever the maximum achievable SNR of both direct channels is greater than -3 dB, as would typically be the case in practice, the optimal value for r can be determined using a standard efficient search method for quasi-convex problems; e.g. [5]. For the particular problem at hand, a simple approach that is closely related to bisection search is provided in Table 4.1. At each step in that approach, the closed-form expression in (4.20) is used to determine the optimal power allocation for each of the current values of r. Since the quasi-convex search can be efficiently implemented and since it converges rapidly, the jointly optimal value for r and the (scaled) powers $\tilde{P}_{ij}$ can be efficiently obtained. Furthermore, since the condition $\gamma_{i0}\bar{P}_i > \frac{1}{2}$ depends only on the direct channel gains, the noise variance at the master node and the power constraints, this condition is testable before the design process commences.

4.5 Modified Orthogonal AF Cooperation Scheme

The analysis of the KKT optimality conditions for the problem in (4.8) showed that for the cooperation scheme in Fig. 4.2, the optimal power allocation results in at least one of $\tilde{P}_{12}$ and $\tilde{P}_{21}$ being equal to zero; see Section 4.3.2. As a result, both nodes will be silent in at least one of the blocks in Fig. 4.2. This suggests that the cooperation scheme in Fig. 4.2 does not make efficient use of the channel resources. A question that then arises is whether there is an alternative orthogonal half-duplex amplify-and-forward cooperation scheme that retains the benefits of the original scheme, such as simplified transmitters and receivers, yet uses the channel resources more efficiently. In this section a modified version of the protocol in Fig. 4.2 that satisfies these requirements is proposed.

The proposed scheme is based on time sharing between the states shown in Fig. 4.3.

Table 4.1: A simple method for finding r^*

Given $R_{2,\text{tar}} \in (0, R_{2,\max}(0))$, for $r \in (0,1)$ define $\psi(r)$ denote the optimal value of (4.8) if $R_{2,\text{tar}} \in (0, R_{2,\max}(r))$ and zero otherwise. Set $\psi(0) = 0$ and $\psi(1) = 0$. Set $t_0 = 0$, $t_4 = 1$, and $t_2 = 1/2$. Using the closed-form expression for the optimal power allocation in (4.20) compute $\psi(t_2)$. Given a tolerance ϵ,

1. Set $t_1 = (t_0 + t_2)/2$ and $t_3 = (t_2 + t_4)/2$.
2. Using the closed-form expression in (4.20), compute $\psi(t_1)$ and $\psi(t_3)$.
3. Find $k^* = \arg\max_{k \in \{0,1,\ldots,4\}} \psi(t_k)$.
4. Replace t_0 by $t_{\max\{k^*-1,0\}}$, replace t_4 by $t_{\min\{k^*+1,4\}}$, and save $\psi(t_0)$ and $\psi(t_4)$. If $k^* \notin \{0,4\}$ set $t_2 = t_{k^*}$ and save $\psi(t_2)$, else set $t_2 = (t_0 + t_4)/2$ and use (4.20) to calculate $\psi(t_2)$.
5. If $t_4 - t_0 \geq \epsilon$ return to 1), else set $r^* = t_{k^*}$.

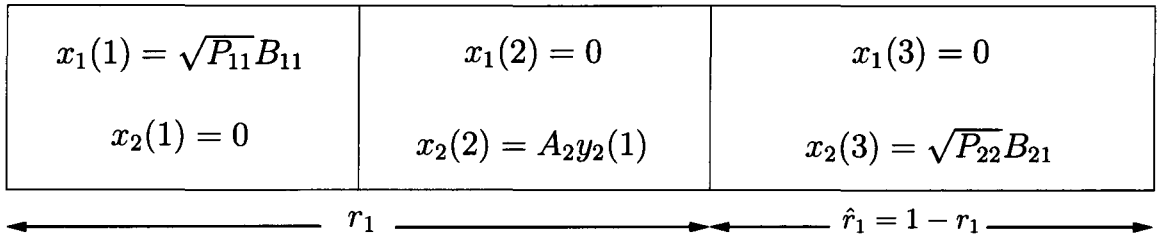

(a) State 1

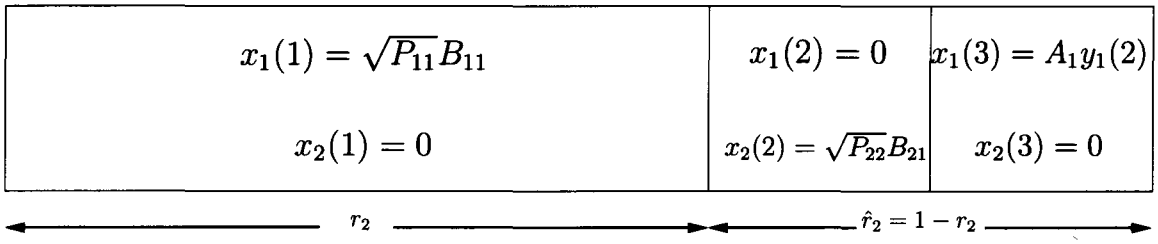

(b) State 2

Figure 4.3: One frame of each state of the proposed modified orthogonal amplify-and-forward cooperation scheme.

In the first state, the message of Node 1 is transmitted using AF relaying in a fraction r_1 of the frame, with Node 2 working as the relay and allocating a power P_{21} to the relaying of the message of Node 1. In contrast, Node 2 employs direct transmission to transmit its message to the master node in a fraction $\hat{r}_1 = 1 - r_1$ of the frame using power P_{22}. In the second state, Nodes 1 and 2 exchange roles. In the first state, the received signal blocks can be expressed as

$$\mathbf{y}_2(\ell) = \begin{cases} K_{12}\mathbf{x}_1(\ell) + \mathbf{z}_2(\ell) & \ell \bmod 3 = 1, \\ \mathbf{0} & \ell \bmod 3 \neq 1, \end{cases} \tag{4.21}$$

$$\mathbf{y}_0(\ell) = \begin{cases} K_{10}\mathbf{x}_1(\ell) + \mathbf{z}_0(\ell) & \ell \bmod 3 = 1, \\ K_{20}A_2\mathbf{y}_2(\ell - 1) + \mathbf{z}_0(\ell) & \ell \bmod 3 = 2, \\ K_{20}\mathbf{x}_2(\ell) + \mathbf{z}_0(\ell) & \ell \bmod 3 = 0, \end{cases} \tag{4.22}$$

where $A_2 = \sqrt{\frac{P_{21}}{|K_{12}|^2 P_{11}+\sigma_2^2}}$. In the second state, the received signal blocks are

$$\mathbf{y}_1(\ell) = \begin{cases} K_{21}\mathbf{x}_2(\ell) + \mathbf{z}_1(\ell) & \ell \bmod 3 = 2, \\ \mathbf{0} & \ell \bmod 3 \neq 2, \end{cases} \tag{4.23}$$

$$\mathbf{y}_0(\ell) = \begin{cases} K_{10}\mathbf{x}_1(\ell) + \mathbf{z}_0(\ell) & \ell \bmod 3 = 1, \\ K_{20}\mathbf{x}_2(\ell) + \mathbf{z}_0(\ell) & \ell \bmod 3 = 2, \\ K_{10}A_1\mathbf{y}_1(\ell-1) + \mathbf{z}_0(\ell) & \ell \bmod 3 = 0, \end{cases} \tag{4.24}$$

where $A_1 = \sqrt{\frac{P_{12}}{|K_{21}|^2 P_{22}+\sigma_1^2}}$.

Using techniques analogous to those used in Sections 4.3 and 4.4, a simple efficient algorithm can be obtained for the joint optimization of the transmission powers and channel resource allocation for each state of the proposed cooperation scheme. In particular, in the first state, for a given resource allocation parameter $r_1 \in (0,1)$ and a feasible $R_{2,\text{tar}}$, it can be shown that $\tilde{P}_{12}^* = 0$, and hence the optimal power allocation problem can be reduced to

$$\phi(r_1) = \max_{\tilde{P}_{21},\tilde{P}_{22}} \quad \frac{r_1}{2}\log\left(1 + \frac{\gamma_{10}(2\bar{P}_1)}{r_1} + \frac{\gamma_{20}\gamma_{12}(2\bar{P}_1)\tilde{P}_{21}}{r_1(r_1+\gamma_{20}\tilde{P}_{21}+\gamma_{12}(2\bar{P}_1))}\right) \tag{4.25a}$$

$$\text{subject to} \qquad \hat{r}_1\log\left(1+\frac{\gamma_{20}\tilde{P}_{22}}{2\hat{r}_1}\right) \geqslant R_{2,\text{tar}}, \tag{4.25b}$$

$$\tilde{P}_{21} + \tilde{P}_{22} \leqslant 2\bar{P}_2, \qquad \tilde{P}_{21} \geqslant 0, \quad \tilde{P}_{22} \geqslant 0. \tag{4.25c}$$

Using a similar argument to that in Section 4.3.3, the optimal solution to (4.25) can be shown to be $\tilde{P}_{21}^* = 2\bar{P}_2 - \breve{Q}_1$, where $\breve{Q}_1 = \frac{2\hat{r}_1}{\gamma_{20}}(2^{\frac{R_{2,\text{tar}}}{\hat{r}_1}} - 1)$, and hence the the optimal (scaled) power allocation is $\tilde{\mathcal{P}}_1^* = (2\bar{P}_1,\, 0,\, 2\bar{P}_2 - \breve{Q}_1,\, \breve{Q}_1)$. In the second state, for a given $r_2 \in (0,1)$ and a feasible $R_{2,\text{tar}}$, it can be shown that $\tilde{P}_{21}^* = 0$, and hence the optimal power allocation problem can be reduced to

$$\lambda(r_2) = \max_{\tilde{P}_{11},\tilde{P}_{12}} \qquad r_2\log\left(1+\frac{\gamma_{10}\tilde{P}_{11}}{2r_2}\right) \tag{4.26a}$$

$$\text{subject to} \quad \tfrac{\hat{r}_2}{2}\log\left(1+\tfrac{\gamma_{20}(2\bar{P}_2)}{\hat{r}_2}+\tfrac{\gamma_{10}\gamma_{21}\tilde{P}_{12}(2\bar{P}_2)}{\hat{r}_2(\hat{r}_2+\gamma_{21}(2\bar{P}_2)+\gamma_{10}\tilde{P}_{12})}\right)\geqslant R_{2,\text{tar}}. \tag{4.26b}$$

$$\tilde{P}_{11}+\tilde{P}_{12}\leqslant 2\bar{P}_1, \qquad \tilde{P}_{11}\geqslant 0, \quad \tilde{P}_{12}\geqslant 0. \tag{4.26c}$$

By adapting the argument in Section 4.3.3, the optimal solution to (4.26) can be shown to be $\tilde{P}_{11}^{*}=2\bar{P}_1-\breve{Q}_2$, where

$$\breve{Q}_2=\frac{(2\bar{P}_2\gamma_{21}+\hat{r}_2)\big(\hat{r}_2(2^{\frac{2R_{2,\text{tar}}}{\hat{r}_2}}-1)-2\bar{P}_2\gamma_{20}\big)}{\gamma_{10}\big(2\bar{P}_2\gamma_{21}-\big(\hat{r}_2(2^{\frac{2R_{2,\text{tar}}}{\hat{r}_2}}-1)-2\bar{P}_2\gamma_{20}\big)\big)}, \tag{4.27}$$

and hence the the optimal (scaled) power allocation is $\tilde{\mathcal{P}}_2=(2\bar{P}_1-\breve{Q}_2,\ \breve{Q}_2,\ 0,\ 2\bar{P}_2)$.

Furthermore, using a proof analogous to that in Appendix K, it can be shown that $\phi(r_1)$ and $\lambda(r_2)$ are quasi-convex in r_1 and r_2, respectively. Hence, the jointly optimal power and channel resource allocation for each point on the boundary of the achievable rate region for each of the two states can be efficiently obtained. The achievable rate region for the proposed cooperation scheme is the convex hull of those two regions. In the numerical results section below, this region will be shown to subsume the region achieved by the cooperation scheme in Fig. 4.2.

4.6 Numerical Results

The goal of this section is three fold. First, the achievable rate regions of the original cooperative scheme in Fig. 4.2 with jointly optimal power and channel resource allocation are compared to the achievable rate regions obtained by the same scheme with optimal power allocation but a fixed channel resource allocation. Second, the achievable rate region of the (jointly optimized) modified cooperation scheme in Section 4.5 is compared against that of the (jointly optimized) original scheme in Fig. 4.2. Finally, the performance of an approach to robust power and resource allocation that provides achievable rate guarantees in the presence of uncertain channel state information (CSI) is investigated. For each investigation, two cases are examined, namely,

the case of symmetric direct channels and the case of asymmetric direct channels. In the first case, the channels between each of the nodes and the master node have the same gain, while in the second case the channels between each of the users and the master node have different gains.

First the original cooperation scheme in Fig. 4.2 is considered in the case of symmetric direct channels. In Fig. 4.4, the achievable rate region that can be obtained by jointly optimizing both the power components and the time sharing parameter r using the efficient quasi-convex search method suggested in Section 4.4 is plotted with a solid line. In the same figure, the rate regions that can be achieved with a fixed resource allocation parameter; i.e., fixed r and optimized power allocation are plotted. (The rate region for equal power and resource allocation is plotted, as well.) Values for $r = 0.1k$, for $k = 1, 2, \ldots, 9$ are used. These regions are plotted with a dotted lines, except for the region for $r = 0.5$, which represents the case in which the channel resources are equally distributed between the two users and is plotted with a dashed line. Fig. 4.6 is analogous to Fig. 4.4, except that it considers a case of asymmetric direct channels. We note that in both Figs 4.4 and 4.6, the region bounded by the solid curve, which represents the achievable rate region when one jointly optimizes over both the transmission powers and r, subsumes the regions bounded by the dashed curve and all the dotted curves. In fact, the region bounded by the solid curve represents the convex hull of all the achievable rate regions for fixed resource allocation. Also, we point out that each of the dotted curves and the dashed curve touches the solid curve at only one point. This is the point at which this particular value of r is optimal.

The optimal value of the resource allocation parameter r and the optimized (scaled) power allocations $\tilde{P}_{11}$ and $\tilde{P}_{21}$ are plotted as a function of the target value $R_{2,\text{tar}}$ in Figs 4.5 and 4.7. In both these figures, we observe that the value of r decreases

as $R_{2,\text{tar}}$ increases. This is what one would expect, because for increasing values of $R_{2,\text{tar}}$ the fraction of the channel resource allocated to Node 2 (i.e., $\hat{r} = 1 - r$) should be increased. We also notice that when $R_{2,\text{tar}} = 0$ all the power and the channel resources will be allocated to the message of Node 1 and in this case the rate R_1 will achieve its maximum value. When $R_{2,\text{tar}}$ takes on its maximum value, $R_1 = 0$ and all the power and channel resources will be allocated to the message of Node 2. Fig. 4.5 also verifies the analysis of the KKT conditions in Section 4.3.2, which revealed that at optimality at least one of the nodes will turn off its relaying function. When $R_{2,\text{tar}}$ is small, we observe that $\tilde{P}_{11} = 2\bar{P}_1$ and hence $\tilde{P}_{12} = 0$. This means that Node 1 does not allocate any power for relaying, and hence that Node 2 must transmit directly to the master node. At high target rates for Node 2, $\tilde{P}_{21} = 0$, which means that Node 2 does not relay the message of Node 1. For a small range of target rates around $R_{2,\text{tar}} = 0.3$, both $\tilde{P}_{12} = 0$ and $\tilde{P}_{21} = 0$, and there is no cooperation between the two nodes. (Both nodes use direct transmission.) The increase in $R_{2,\text{tar}}$ in this region is obtained by decreasing the resource allocation parameter r (i.e., increasing $\hat{r}$), and the change in the slope of the dashed curve that represents r in Fig. 4.5 can be clearly seen in this region.

In Figs 4.8 and 4.9, the achievable rate region of the modified scheme proposed in Section 4.5 is compared against that of the original AF scheme in Fig. 4.2. Fig. 4.8 considers the case of symmetric channels, and Fig. 4.9 considers the asymmetric case. It is clear from these figures that the (jointly optimized) modified scheme provides a significantly larger achievable rate region than the (jointly optimized) original scheme. In Fig. 4.8, we note that the maximum achievable rate for Node 1 for the modified scheme is the same as that of the original scheme. This is because in this scenario, the effective gain of the inter-user channel ($\gamma_{12} = \gamma_{21}$) is large enough, relative to the effective gain of the direct channel, so that the maximum value of R_1 for the modified

scheme occurs in State 1, in which the message of Node 1 is relayed by Node 2 and all the transmission powers and channel resources are allocated to the message of Node 1. In contrast, in the scenario plotted in Fig. 4.9 the gain of the direct channel of Node 1 is large enough, relative to the effective gain of the inter-user channel, so that the maximum value of R_1 occurs in State 2, in which the message of Node 1 is transmitted directly and all the channel resources are allocated to the message of Node 1. As can be seen in Fig. 4.9, this means that the maximum achievable rate for Node 1 is larger than that provided by the original scheme in Fig. 4.2.

In the final experiment, a scenario in which the available CSI is uncertain, in the sense that the effective channel gains are only known to lie in the interval $\gamma_{ij} \in [\hat{\gamma}_{ij} - \delta_{ij}, \hat{\gamma}_{ij} + \delta_{ij}]$, is considered. This model is well matched to scenarios that involve the communication of quantized channel estimates of the channel gains via low-rate feedback. The goal of this experiment is to obtain the power and resource allocations that provide the largest rate region that is guaranteed to be achievable under all admissible uncertainties. This can be achieved by applying the existing approaches to the scenario in which all the effective channel gains assume their lowest admissible value; i.e., $\gamma_{ij} = \hat{\gamma}_{ij} - \delta_{ij}$. In Figs 4.10 and 4.11 the resulting robust achievable rate regions are compared to the achievable rate regions for the case of perfect CSI, for a scenario in which $\delta_{ij} = 1/32$. (This corresponds to a quantization scheme for γ_{ij} with four bits and a dynamic range of $[0, 1]$.) As expected, channel uncertainty reduces the size of the achievable rate region, but this example demonstrates that robust performance in the presence of channel uncertainties can be obtained in a relatively straightforward manner.

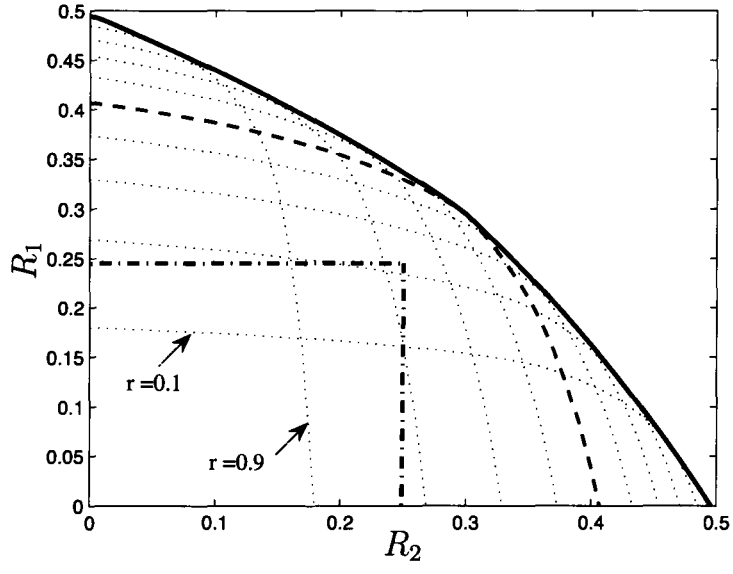

Figure 4.4: Achievable rate region in a case of symmetric direct channels. $\bar{P}_1 = \bar{P}_2 = 2.0, \sigma_0^2 = \sigma_1^2 = \sigma_2^2 = 1, |K_{12}| = |K_{21}| = 0.7, |K_{10}| = |K_{20}| = 0.4$. The solid curve represents the case of joint optimization over $\tilde{P}_{ij}$ and r, the dotted curves represent the case of fixing $r = 0.1k$, $k = 1, 2, \ldots, 9$ and optimizing only over $\tilde{P}_{ij}$. The dashed curve represents the case of optimization over $\tilde{P}_{ij}$ for $r = 0.5$. The dash-dot curve represents the case of equal power and resource allocation.

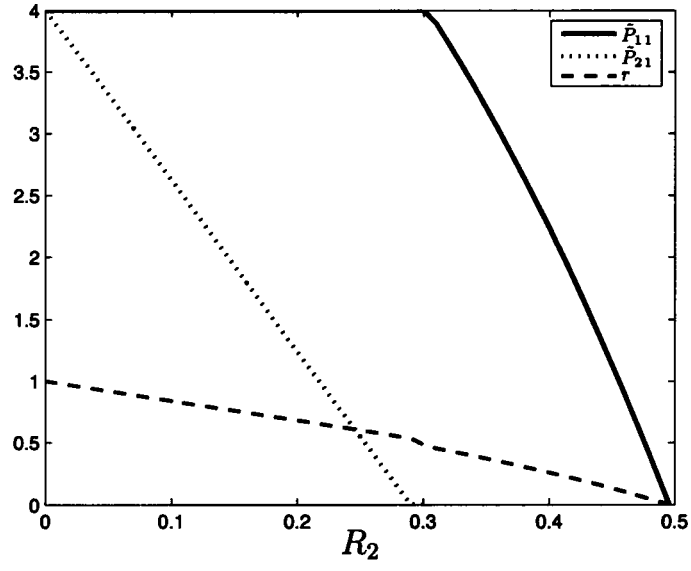

Figure 4.5: Jointly optimized power and resource allocations in the case of symmetric direct channels considered in Fig. 4.4.

4.7 Conclusion

In this chapter the problem of joint power and channel resource allocation for a two-user orthogonal amplify-and-forward cooperative scheme was addressed. A closed-form expression for the optimal power allocation problem for a given channel resource allocation was obtained, and the quasi-convexity of the power and channel resource allocation problem was exploited to obtain a simple efficient algorithm for the jointly optimal allocation. Analysis of some KKT optimality conditions showed that the original system under consideration does not use the channel resources efficiently. Therefore, a modified orthogonal AF cooperation scheme was proposed, and it was demonstrated that with optimal power and channel resource allocation this scheme can provide a larger achievable rate region than that provided by the original scheme.

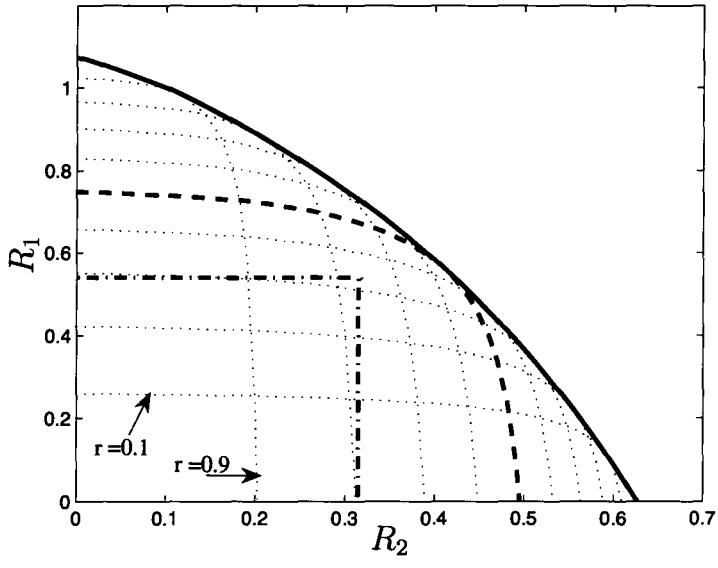

Figure 4.6: Achievable rate region in a case of asymmetric direct channels. $\bar{P}_1 = \bar{P}_2 = 2.0, \sigma_0^2 = \sigma_1^2 = \sigma_2^2 = 1, |K_{12}| = |K_{21}| = 0.7, |K_{10}| = 0.9, |K_{20}| = 0.3$. The solid curve represents the case of joint optimization over $\tilde{P}_{ij}$ and r, the dotted curves represent the case of fixing $r = 0.1k$, $k = 1, 2, \ldots, 9$ and optimizing only over $\tilde{P}_{ij}$. The dashed curve represents the case of optimization over $\tilde{P}_{ij}$ for $r = 0.5$. The dash-dot curve represents the case of equal power and resource allocation.

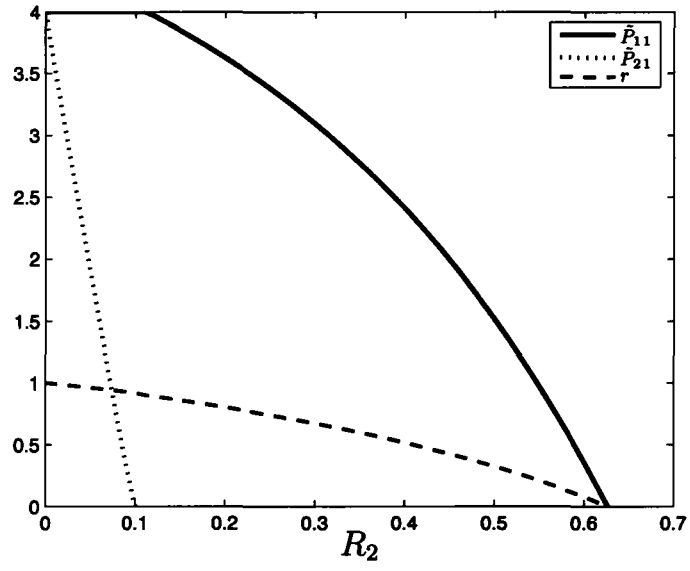

Figure 4.7: Jointly optimized power and resource allocations in the case of asymmetric direct channels considered in Fig. 4.6.

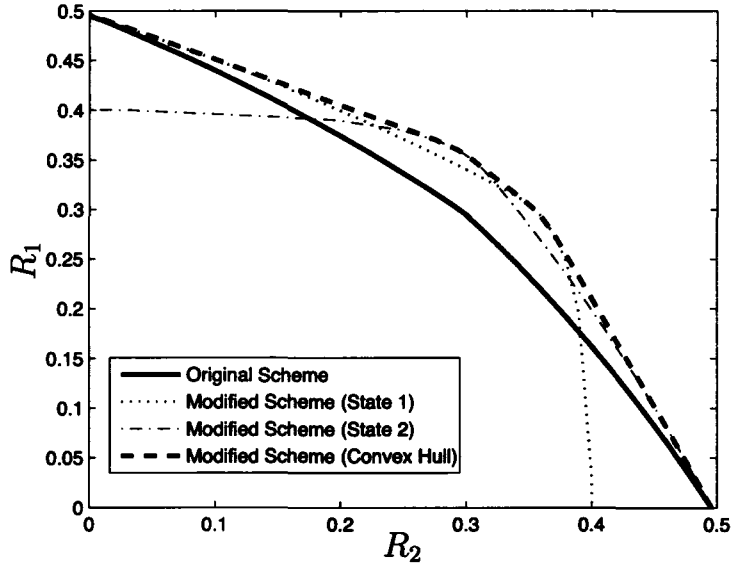

Figure 4.8: Achievable rate region of the modified orthogonal AF scheme in the case of symmetric direct channels considered in Fig. 4.4.

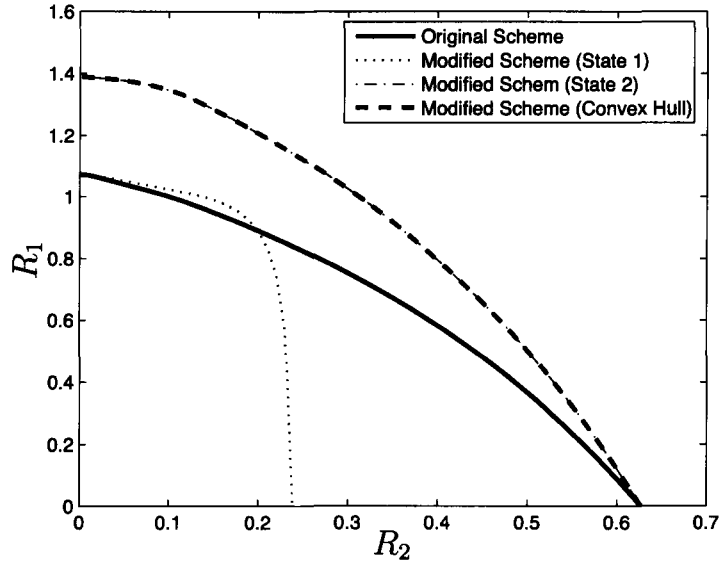

Figure 4.9: Achievable rate region of the modified orthogonal AF scheme in the case of asymmetric direct channels considered in Fig. 4.6.

Finally, a simple strategy that enables efficient optimization of a guaranteed achievable rate region in the presence of bounded uncertainties in the available channel state information was provided.

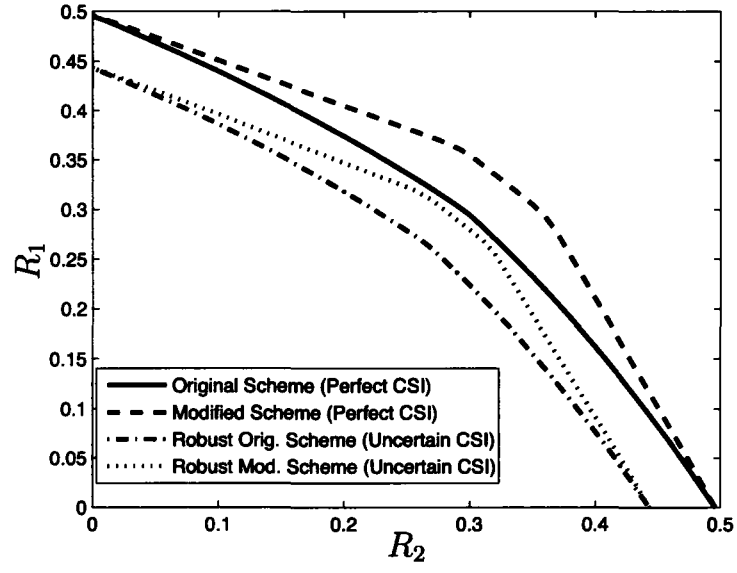

Figure 4.10: Achievable rate regions of the original and modified AF schemes with perfect and uncertain channel state information in the case of symmetric direct channels considered in Fig. 4.4.

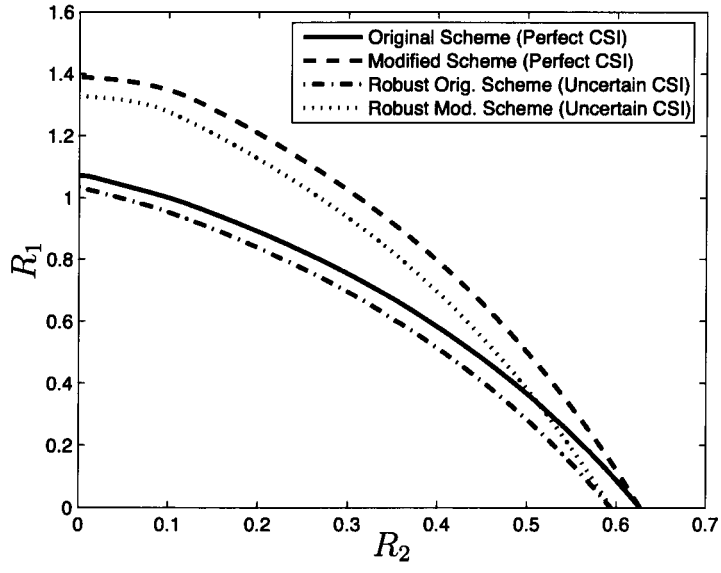

Figure 4.11: Achievable rate regions of the original and modified AF schemes with perfect and uncertain channel state information in the case of asymmetric direct channels considered in Fig. 4.6.

Chapter 5

Power and Resource Allocation for Orthogonal Multiple Access Relay Systems

In this chapter the problem of joint power and channel resource allocation for orthogonal multiple access relay (MAR) systems is considered in order to maximize the achievable rate region. Four relaying strategies are considered; namely, regenerative decode-and-forward (RDF), non-regenerative decode-and-forward (NDF), amplify-and-forward (AF), and compress-and-forward (CF). For RDF and NDF, it is shown that the problem can be formulated as a quasi-convex problem, while for AF and CF, it is shown that the problem can be made quasi-convex if the signal to noise ratios of the direct channels are at least -3 dB. Therefore, efficient algorithms can be used to obtain the jointly optimal power and channel resource allocation. Furthermore, it is shown that the convex subproblems in those algorithms admit a closed-form solution. The numerical results show that the joint allocation of power and the channel resource achieves significantly larger achievable rate regions than those achieved by

power allocation alone with fixed channel resource allocation. It is also demonstrated herein that assigning different relaying strategies to different users together with the joint allocation of power and the channel resources can further enlarge the achievable rate region.

5.1 Introduction

In multiple access relay (MAR) systems, several source nodes send independent messages to a destination node with the assistance of a relay node [34,35,60,62]; see also Fig. 5.1. These systems are of interest because they offer the potential for reliable communication at rates higher than those provided by conventional [9], and cooperative multiple access schemes [38, 66, 67] (in which source nodes essentially work as relays for each other.) For example, in [62] a comparison was made between the MAR system and the system that employs user cooperation, and the MAR system was shown to outperform the user cooperation system. Full-duplex MAR systems, in which the relay is able to transmit and receive simultaneously over the same channel, were studied in [34, 35, 60, 61], where inner and outer bounds for the capacity region were provided. However, full-duplex relays can be difficult to implement, due to the electrical isolation required between the transmitter and receiver circuits. As a result, half-duplex relays, which do not simultaneously transmit and receive on the same channel, are often preferred in practice. The receiver at the relay and destination nodes can be further simplified if the source nodes (and the relay) transmit their messages on orthogonal channels, as this enables 'per-user' decoding rather than joint decoding.

In this chapter, the design of orthogonal multiple access systems with a half-duplex relay will be considered. In particular, the problem of joint allocation of power and the

channel resource will be considered in order to maximize the achievable rate region. Four relaying strategies will be considered; namely, regenerative (RDF) and non-regenerative (NDF) decode-and-forward [38, 66], amplify-and-forward (AF) [38, 65], and compress-and-forward (CF) [10, 36]. The orthogonal half-duplex MAR system that will be considered is similar to that considered in [68]. However, the focus of that paper is on the maximization of the sum rate, and, more importantly, it is assumed therein that the source nodes will each be allocated an equal fraction of the channel resources (e.g., time or bandwidth).[1] In this chapter, we will provide an efficiently solvable formulation for finding the jointly optimal allocation of power and the channel resources that enables the system to operate at each point on the boundary of the achievable rate region.

Although the problem of power allocation for an equal allocation of the channel resource was shown to be convex in [68], the joint allocation of power and the channel resource is not convex, which renders the problem harder to solve. In this chapter it is shown that the joint allocation problem can be formulated in a quasi-convex form, and hence that the optimal solution can be obtained efficiently using standard quasi-convex algorithms; e.g., bisection-based methods [5]. Furthermore, for a given channel resource allocation, closed-form expressions for the optimal power allocation are obtained, which further reduces the complexity of the algorithm used to obtain the jointly optimal allocation.

The practical importance of solving the problem of the joint allocation of power and channel resources is that it typically provides a substantially larger achievable rate region than that provided by allocating only the power for equal (or fixed) channel resource allocation, as will be demonstrated in the numerical results. Those results

[1] This equal allocation of resources is only optimal in the sum rate sense when the source nodes experience equal effective channel gains towards the destination and equal effective channel gains towards the relay.

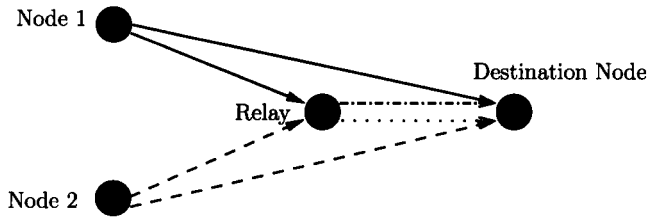

Figure 5.1: A simple multiple access relay channel with two source nodes.

will also demonstrate the superiority of the NDF and CF relaying strategies over the RDF and AF strategies, respectively; an observation that is consistent with an observation in [68] for the case of power allocation with equal resource allocation. The numerical results will also demonstrate that joint allocation of the relaying strategy together with the power and channel resources, rather assigning the same relaying strategy to all users, can further enlarge the achievable rate region.

5.2 System Model

An orthogonal multiple access relay (MAR) system is considered with N source nodes (Nodes $1, 2, \ldots N$), one destination node (Node 0), and one relay (Node R) that assists the source nodes in the transmission of their messages to the destination node.[2] Fig. 5.1 shows a simplified two-source MAR system. The focus here will be on a system in which the transmitting nodes use orthogonal sub-channels to transmit their signals, and the relay operates in half-duplex mode. This system model is similar to that used in [68]. The orthogonal sub-channels can be synthesized in time or in frequency, but given their equivalence it is sufficient to focus on the case in which they are synthesized in time. That is, the total frame length will be divided into N non-overlapping sub-frames of fractional length r_i, and the i^{th} sub-frame will be

[2]The generalization of this model to different destination nodes is direct.

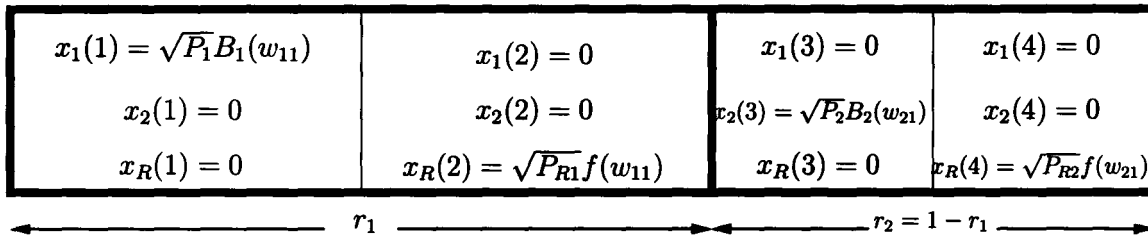

Figure 5.2: One frame of the considered orthogonal cooperation scheme for the case of 2 source nodes, and its constituent sub-frames.

allocated to the transmission (and relaying) of the message from source node i to the destination node. Fig. 5.2 shows the block diagram of the cooperation scheme and the transmitted signals during one frame of such an MAR system with two source nodes. As shown in Fig. 5.2, the first sub-frame is allocated to Node 1 and has a fractional length r_1, while the second sub-frame is allocated to Node 2 and has a fractional length $r_2 = 1 - r_1$. Each sub-frame is further partitioned into two equal-length blocks [68]. In the first block of sub-frame i of frame ℓ, Node i sends a new block of symbols $B_i(w_{i\ell})$ to both the relay and the destination node, where $w_{i\ell}$ is the component of the i^{th} user's message that is to be transmitted in the ℓ^{th} frame. In the second block of that sub-frame, the relay node transmits a function $f(\cdot)$ of the message it received from Node i in the first block. (The actual function depends on the relaying strategy.) We will let P_i represent the power used by Node i to transmit its message, and we will constrain it so that it satisfies the average power constraint $\frac{r_i}{2}P_i \leqslant \bar{P}_i$, where $\bar{P}_i$ is the maximum average power of Node i. We will let P_{Ri} represent the relay power allocated to the transmission of the message of Node i, and we will impose the average power constraint $\sum_{i=1}^{N} \frac{r_i}{2}P_{Ri} \leqslant \bar{P}_R$. (The function $f(\cdot)$ is normalized so that it has unit power.) In this chapter, we consider four relaying strategies:

- Regenerative decode-and-forward (RDF): The relay decodes the message $w_{i\ell}$, re-encodes it using the same code book as the source node, and transmits the codeword to the destination [38,66].

- Non-regenerative decode-and-forward (NDF): The relay decodes the message $w_{i\ell}$, re-encodes it using a different code book from that used by the source node, and transmits the codeword to the destination [2,41].

- Amplify-and-forward (AF): The relay amplifies the received signal and forwards it to the destination [38,65]. In this case, $f(w_{i\ell})$ is the signal received by the relay, normalized by its power.

- Compress-and-forward (CF): The relay transmits a compressed version of signal it receives [10,36].

Without loss of generality, the focus here will be on a two user system in order to simplify the exposition. However, as we will explain in Section 5.3.5, all the results of this chapter can be applied to systems with more than two source nodes. For the two source system, the received signals at the relay and the destination at block m, can be expressed as[3]

$$\mathbf{y}_R(m) = \begin{cases} K_{1R}\mathbf{x}_1(m) + \mathbf{z}_R(m) & m \bmod 4 = 1, \\ K_{2R}\mathbf{x}_2(m) + \mathbf{z}_R(m) & m \bmod 4 = 3, \\ \mathbf{0} & m \bmod 4 \in \{0,2\}, \end{cases} \tag{5.1}$$

$$\mathbf{y}_0(m) = \begin{cases} K_{10}\mathbf{x}_1(m) + \mathbf{z}_0(m) & m \bmod 4 = 1, \\ K_{R0}\mathbf{x}_R(m) + \mathbf{z}_0(m) & m \bmod 4 = 2, \\ K_{20}\mathbf{x}_2(m) + \mathbf{z}_0(m) & m \bmod 4 = 3, \\ K_{R0}\mathbf{x}_R(m) + \mathbf{z}_0(m) & m \bmod 4 = 0, \end{cases} \tag{5.2}$$

[3]We use $\mathbf{0}$ to represent blocks in which the receiver of the relay node is turned off.

where $\mathbf{y}_i$ and $\mathbf{x}_i$ vectors containing the block of received and transmitted signals of Node i, respectively, K_{ij}, $i \in \{1, 2, R\}$ and $j \in \{R, 0\}$, represents the channel gain between Nodes i and j, and $\mathbf{z}_j$ represents the additive zero-mean white circular complex Gaussian noise vector with independent components of variance σ_j^2 at Node j. For simplicity, we define the effective power gain $\gamma_{ij} = \frac{|K_{ij}|^2}{\sigma_j^2}$.

The focus of this chapter will be on a system in which full channel state information (CSI) is available at the source nodes, and the channel coherence time is long. The CSI is exploited to jointly allocate the powers P_{Ri} and the resource allocation parameters r_i, with the goal of enlarging the achievable rate region. Under the assumption of equal channel resource allocation (i.e., $r_i = r_s$, $\forall i, s$), expressions for the maximum achievable rate for a source node under each of the four relaying considered relaying strategies were provided in [68]. The extension of those expressions to the case of not necessarily equal resource allocation results in the following expressions for the maximum achievable rate of Node i as a function of P_i, the transmission power of Node i, P_{Ri}, the relay power allocated to Node i, and r_i, the fraction of the channel resource allocated to Node i:

- Regenerative decode-and-forward (RDF):

$$\bar{R}_{i,RDF} = \frac{r_i}{2} \min\{\log(1 + \gamma_{iR} P_i), \log(1 + \gamma_{i0} P_i + \gamma_{R0} P_{Ri})\}, \tag{5.3a}$$

- Non-regenerative decode-and-forward (NDF):

$$\bar{R}_{i,NDF} = \frac{r_i}{2} \min\{\log(1 + \gamma_{iR} P_i), \log(1 + \gamma_{i0} P_i) + \log(1 + \gamma_{R0} P_{Ri})\}, \tag{5.3b}$$

- Amplify-and-forward (AF):

$$\bar{R}_{i,AF} = \frac{r_i}{2} \log\left(1 + \gamma_{i0} P_i + \frac{\gamma_{iR}\gamma_{R0} P_i P_{Ri}}{(1 + \gamma_{iR} P_i + \gamma_{R0} P_{Ri})}\right), \tag{5.3c}$$

- Compress-and-forward (CF): Assuming that the relay uses Wyner-Ziv lossy compression [82], the maximum achievable rate is

$$\bar{R}_{i,CF} = \frac{r_i}{2} \log \left(1 + \gamma_{i0} P_i + \frac{\gamma_{iR}\gamma_{R0}(\gamma_{i0}P_i + 1)P_i P_{Ri}}{\gamma_{R0}(\gamma_{i0}P_i + 1)P_{Ri} + P_i(\gamma_{i0} + \gamma_{iR}) + 1} \right). \quad (5.3d)$$

It was shown in [68] that for fixed channel resource allocation, the rate expressions in (5.3) are concave functions in P_{Ri}.

The focus of the work in this chapter will be on systems in which the relay node relays the messages of all source nodes in the system using the same pre-assigned relaying strategy. However, as will be demonstrated in Section 5.4, the results obtained in this chapter naturally extend to the case of heterogeneous relaying strategies, and hence facilitate the development of algorithms for the jointly optimal allocation of the relaying strategy.

5.3 Joint Power and Channel Resource Allocation

It was shown in [68] that for fixed channel resource allocation, the problem of finding the power allocation that maximizes the sum rate is convex, and closed-form solutions for the optimal power allocation were obtained. However, the direct formulation of the problem of joint allocation of both the power and the channel resource so as to enable operation at an arbitrary point on the boundary of the achievable rate region is not convex, and hence is significantly harder to solve. Despite this complexity, the problem is of interest because it is expected to yield significantly larger achievable rate regions than those obtained with equal channel resource allocation. In the next four subsections the problem of finding the jointly optimal power and resource allocation will be studied for each relaying strategy. It will be shown that in each case the problem can be transformed into a quasi-convex problem, and hence an optimal solution can be obtained using simple and efficient algorithms; i.e., standard

quasi-convex search algorithms [5]. Furthermore, for a fixed resource allocation, a closed-form solution for the optimal power allocation is obtained. By exposing the quasi-convexity of the problem and by obtaining a closed-form solution to the power allocation problem, we are able to achieve significantly larger achievable rate regions without incurring substantial additional computational cost.

The jointly optimal power and channel resource allocation at each point on the boundary of the achievable rate region can be found by maximizing a weighted sum of the maximal rates $\bar{R}_1$ and $\bar{R}_2$ subject to the bound on the transmitted powers; i.e.,

$$\max_{P_i, P_{Ri}, r} \quad \mu\bar{R}_1 + (1-\mu)\bar{R}_2, \tag{5.4a}$$

$$\text{subject to} \quad \tfrac{r}{2}P_{R1} + \tfrac{\hat{r}}{2}P_{R2} \leqslant \bar{P}_R, \tag{5.4b}$$

$$\tfrac{r}{2}P_1 \leqslant \bar{P}_1, \quad \tfrac{\hat{r}}{2}P_2 \leqslant \bar{P}_2, \tag{5.4c}$$

$$P_{Ri} \geqslant 0, \quad P_i \geqslant 0, \tag{5.4d}$$

where $\bar{R}_i$ is the expression in (5.3) that corresponds to the given relaying strategy, $r = r_1$, $\hat{r} = r_2 = 1 - r$, and $\mu \in [0, 1]$ weights the relative importance of $\bar{R}_1$ over $\bar{R}_2$. Alternatively, the jointly optimal power and channel resource allocation at each point on the boundary of the achievable rate region can also be found by maximizing $\bar{R}_i$ for a given target value of $\bar{R}_j$, subject to the bound on the transmitted powers; e.g.,

$$\max_{P_i, P_{Ri}, r} \quad \bar{R}_1, \tag{5.5a}$$

$$\text{subject to} \quad \bar{R}_2 \geqslant R_{2,\text{tar}}, \tag{5.5b}$$

$$\tfrac{r}{2}P_{R1} + \tfrac{\hat{r}}{2}P_{R2} \leqslant \bar{P}_R, \tag{5.5c}$$

$$\tfrac{r}{2}P_1 \leqslant \bar{P}_1, \quad \tfrac{\hat{r}}{2}P_2 \leqslant \bar{P}_2, \tag{5.5d}$$

$$P_{Ri} \geqslant 0, \quad P_i \geqslant 0. \tag{5.5e}$$

Neither the formulation in (5.4) nor that in (5.5) is jointly convex in the transmitted

powers and the channel resource allocation parameter r, and hence it appears that it may be difficult to develop a reliable efficient algorithm for their solution. However, in the following sub-sections, it will be shown that by adopting the framework in (5.5), the direct formulation can be transformed into a composition of a convex problem (with a closed-form solution) and a quasi-convex optimization problem, and hence that it can be efficiently and reliably solved. Furthermore, using the concavity of the rate expressions in (5.3) in P_{Ri}, it can be shown (see Appendix G) that the optimal solution to the weighted sum rate maximization problem, in (5.4), can be obtained using an iterative algorithm in which the target rate problem, in (5.5), is solved at each step.

The first step in the analysis of (5.5) is to observe that since the source nodes transmit on channels that are orthogonal to each other and to that of the relay, then at optimality they should transmit at full power, i.e., the optimal values of P_1 and P_2 are $P_1^*(r) = 2\bar{P}_1/r$ and $P_2^*(r) = 2\bar{P}_2/\hat{r}$, respectively. In order to simplify the development, we will define $R_{2,\max}(r)$ to be the maximum achievable value for $\bar{R}_2$ for a given value of r and the given relaying strategy; i.e., the value of the appropriate expression in (5.3) with $P_{R2} = 2\bar{P}_R/\hat{r}$ and $P_2 = 2\bar{P}_2/\hat{r}$.

5.3.1 Regenerative Decode-and-Forward

For the regenerative decode-and-forward strategy, the problem in (5.5) can be written as

$$\max_{P_{Ri},r} \quad \tfrac{r}{2}\min\big\{\log(1+\gamma_{1R}P_1^*), \log(1+\gamma_{10}P_1^*+\gamma_{R0}P_{R1})\big\}, \tag{5.6a}$$

$$\text{subject to} \quad \tfrac{\hat{r}}{2}\min\big\{\log(1+\gamma_{2r}P_2^*), \log(1+\gamma_{20}P_2^*+\gamma_{R0}P_{R2})\big\} \geqslant R_{2,\text{tar}}, \tag{5.6b}$$

$$\tfrac{r}{2}P_{R1} + \tfrac{\hat{r}}{2}P_{R2} \leqslant \bar{P}_R, \tag{5.6c}$$

$$P_{Ri} \geqslant 0. \tag{5.6d}$$

Unfortunately, the set of values for r, P_{R1} and P_{R2} that satisfy the constraint in (5.6c) is bilinear, and hence the problem in (5.6) is not convex. However, if we define $\tilde{P}_{R1} = rP_{R1}$ and $\tilde{P}_{R2} = \hat{r}P_{R2}$, then the problem in (5.6) can be rewritten as

$$\max_{\tilde{P}_{Ri},r} \quad \tfrac{r}{2}\min\{\log(1+\tfrac{2\gamma_{1R}\tilde{P}_1}{r}), \log(1+\tfrac{2\gamma_{10}\tilde{P}_1+\gamma_{R0}\tilde{P}_{R1}}{r})\}, \tag{5.7a}$$

$$\text{subject to} \quad \tfrac{\hat{r}}{2}\min\{\log(1+\tfrac{2\gamma_{2r}\tilde{P}_2}{\hat{r}}), \log(1+\tfrac{2\gamma_{20}\tilde{P}_2+\gamma_{R0}\tilde{P}_{R2}}{\hat{r}})\} \geqslant R_{2,\text{tar}}, \tag{5.7b}$$

$$\tilde{P}_{R1} + \tilde{P}_{R2} = 2\bar{P}_R, \tag{5.7c}$$

$$\tilde{P}_{Ri} \geqslant 0. \tag{5.7d}$$

Formulating the problem as in (5.7) enables us to obtain the following result, the proof of which is provided in Appendix M

Proposition 5.1 *For a given feasible target rate $R_{2,\text{tar}} \in (0, R_{2,\max}(0))$, the maximum achievable rate $\bar{R}_{1,\max}$ in (5.7) is a quasi-concave function of the channel resource sharing parameter r.* □

In addition to the desirable property in Proposition 5.1, for any given channel resource allocation and for any feasible $R_{2,\text{tar}}$, a closed-form solution for the optimal power allocation can be found. In particular, for any given r, $\tilde{P}_{R1}$ must be maximized in order to maximize R_1. Therefore, the optimal value of $\tilde{P}_{R2}$ is the minimum value that satisfies the constraints in (5.7), and hence it can be written as

$$\tilde{P}^*_{R2}(r) = \begin{cases} 0 & \text{if } \gamma_{2R} \leqslant \gamma_{20}, \\ (\frac{A-2\gamma_{20}\bar{P}_2}{B})^+ & \text{if } \gamma_{2R} > \gamma_{20}, \end{cases} \tag{5.8}$$

where $A = \hat{r}(2^{\frac{2R_{2,\text{tar}}}{\hat{r}}} - 1)$, $B = \gamma_{R0}$, and $x^+ = \max(0, x)$. The optimal value of $\tilde{P}_{R1}$ is $\tilde{P}^*_{R1}(r) = \min\{2\bar{P}_R - \tilde{P}^*_{R2}(r), (\frac{2\bar{P}_1(\gamma_{1R}-\gamma_{10})}{\gamma_{R0}})^+\}$, where the second argument of the min function is the value of $\tilde{P}_{R1}$ that makes the two arguments of the min function in (5.7a) equal. In Section 5.3.5 the quasi-convexity result in Proposition 5.1 and

the closed-form expression for $\tilde{P}^*_{R2}(r)$ in (5.8) will be exploited to develop an efficient algorithm for the jointly optimal allocation of power and the channel resource.

5.3.2 Non-regenerative Decode-and-Forward

Using the definition of $\tilde{P}_{R1}$ and $\tilde{P}_{R2}$ from the RDF case, the problem of maximizing the achievable rate region for the NDF relaying strategy can be written as

$$\max_{\tilde{P}_{Ri},r} \quad \tfrac{r}{2}\min\Big\{\log(1+\tfrac{2\gamma_{1R}\bar{P}_1}{r}), \log(1+\tfrac{2\gamma_{10}\bar{P}_1}{r})+\log(1+\tfrac{\gamma_{R0}\tilde{P}_{R1}}{r})\Big\}, \tag{5.9a}$$

$$\text{subject to} \quad \tfrac{\hat{r}}{2}\min\Big\{\log(1+\tfrac{2\gamma_{2r}\bar{P}_2}{\hat{r}}), \log(1+\tfrac{2\gamma_{20}\bar{P}_2}{\hat{r}})+\log(1+\tfrac{\gamma_{R0}\tilde{P}_{R2}}{\hat{r}})\Big\} \geqslant R_{2,\text{tar}} \tag{5.9b}$$

$$\tilde{P}_{R1}+\tilde{P}_{R2} = 2\bar{P}_R, \tag{5.9c}$$

$$\tilde{P}_{Ri} \geqslant 0. \tag{5.9d}$$

Using the formulation in (5.9), the following result is obtained in Appendix N.

Proposition 5.2 *For a given feasible target rate $R_{2,\text{tar}} \in (0, R_{2,\max}(0))$, the maximum achievable rate $\bar{R}_{1,\max}$ in (5.9) is a quasi-concave function of r.* □

Similar to the RDF case, for a given r and a feasible $R_{2,\text{tar}}$, a closed-form expression for the optimal $\tilde{P}_{R2}$ can be obtained. This expression has the same form as that in (5.8), with the same definition for A, but with B defined as $B = \gamma_{R0} + 2\gamma_{20}\gamma_{R0}\bar{P}_2/\hat{r}$. The optimal value for $\tilde{P}_{R1}$ is $\tilde{P}^*_{R1}(r) = \min\big\{2\bar{P}_R - \tilde{P}^*_{R2}(r), \big(\frac{2\bar{P}_1(\gamma_{1R}-\gamma_{10})r}{\gamma_{R0}(r+2\bar{P}_1\gamma_{10})}\big)^+\big\}$, where the second argument of the min function is the value of $\tilde{P}_{R1}$ that makes the two arguments of the min function in (5.9a) equal.

5.3.3 Amplify-and-Forward

In the case of amplify-and-forward relaying, problem (5.5) can be written as

$$\max_{\tilde{P}_{Ri},r} \quad \tfrac{r}{2}\log\left(1+\tfrac{2\gamma_{10}\bar{P}_1}{r}+\tfrac{2\gamma_{1R}\gamma_{R0}\bar{P}_1\tilde{P}_{R1}}{r(r+2\gamma_{1R}\bar{P}_1+\gamma_{R0}\tilde{P}_{R1})}\right), \tag{5.10a}$$

$$\text{subject to} \quad \frac{\hat{r}}{2}\log\left(1+\frac{2\gamma_{20}\bar{P}_2}{\hat{r}}+\frac{2\gamma_{2R}\gamma_{R0}\bar{P}_2\tilde{P}_{R2}}{\hat{r}(\hat{r}+2\gamma_{2r}\bar{P}_2+\gamma_{R0}\tilde{P}_{R2})}\right)\geqslant R_{2,\text{tar}}, \tag{5.10b}$$

$$\tilde{P}_{R1}+\tilde{P}_{R2}=2\bar{P}_R, \tag{5.10c}$$

$$\tilde{P}_{Ri}\geqslant 0. \tag{5.10d}$$

Using this formulation, the following result is obtained in Appendix O.[4]

Proposition 5.3 *If the direct channels of both source nodes satisfy $\gamma_{i0}\bar{P}_i > \frac{1}{2}$, then for a given feasible target rate $R_{2,\text{tar}} \in (0, R_{2,\max}(0))$, the maximum achievable rate $\bar{R}_{1,\max}$ in (5.10) is a quasi-concave function of r.* □

Similar to the cases of RDF and NDF relaying, for a given r and a feasible $R_{2,\text{tar}}$, in order to obtain an optimal power allocation we must find the smallest $\tilde{P}_{R2}$ that satisfies the constraints in (5.10). If we define $C = A - 2\gamma_{20}\bar{P}_2$, a closed-form solution for $\tilde{P}_{R2}$ can be written as

$$\tilde{P}^*_{R2}(r)=\left(\frac{C(\hat{r}+2\gamma_{2R}\bar{P}_2)}{2\gamma_{2R}\gamma_{R0}\bar{P}_2-\gamma_{R0}C}\right)^+. \tag{5.11}$$

Hence, the optimal value of $\tilde{P}_{R1}$ is $\tilde{P}^*_{R1}(r) = 2\bar{P}_R - \tilde{P}^*_{R2}(r)$.

5.3.4 Compress-and-Forward

Finally, for the compress-and-forward relaying strategy, the problem in (5.5) can be written as

$$\max_{\tilde{P}_{Ri},r} \quad \frac{r}{2}\log\left(1+\frac{2\gamma_{10}\bar{P}_1}{r}+\frac{2\gamma_{1R}\gamma_{R0}\bar{P}_1(2\gamma_{10}\bar{P}_1+r)\tilde{P}_{R1}}{r(r^2+2(\gamma_{10}+\gamma_{1R})\bar{P}_1 r+\gamma_{R0}(2\gamma_{10}\bar{P}_1+r)\tilde{P}_{R1})}\right), \tag{5.12a}$$

$$\text{subject to} \quad \frac{\hat{r}}{2}\log\left(1+\frac{2\gamma_{20}\bar{P}_2}{\hat{r}}+\frac{2\gamma_{2R}\gamma_{R0}\bar{P}_2(2\gamma_{20}\bar{P}_2+\hat{r})\tilde{P}_{R2}}{\hat{r}(\hat{r}^2+2(\gamma_{20}+\gamma_{2R})\bar{P}_2\hat{r}+\gamma_{R0}(2\gamma_{20}\bar{P}_2+\hat{r})\tilde{P}_{R2})}\right)\geqslant R_{2,\text{tar}}, \tag{5.12b}$$

$$\tilde{P}_{R1}+\tilde{P}_{R2}=2\bar{P}_R, \tag{5.12c}$$

$$\tilde{P}_{Ri}\geqslant 0. \tag{5.12d}$$

[4]Note that $\gamma_{i0}\bar{P}_i$ is the maximum achievable destination SNR on the direct channel of source node i.

As stated in the following proposition (proved in Appendix P), the quasi-convex properties of the problem in (5.12) are similar to those of the amplify-and-forward case.

Proposition 5.4 *If the direct channels of both source nodes satisfy* $\gamma_{i0}\bar{P}_i > \frac{1}{2}$, *then for a given feasible target rate* $R_{2,\text{tar}} \in (0, R_{2,\max}(0))$, *the maximum achievable rate* $\bar{R}_{1,\max}$ *in* (5.12) *is a quasi-concave function of* r. □

If we define $D = \gamma_{R0}(2\gamma_{20}\bar{P}_2 + \hat{r})$, then the optimal solution for $\tilde{P}_{R2}$ for a given r and a feasible $R_{2,\text{tar}}$ can be written as

$$\tilde{P}^*_{R2}(r) = \left(\frac{C\hat{r}(\hat{r} + 2(\gamma_{20} + \gamma_{2R})\bar{P}_2)}{D(2\gamma_{2R}\bar{P}_2 - C)}\right)^+, \tag{5.13}$$

and the optimal $\tilde{P}_{R1}$ is $\tilde{P}^*_{R1}(r) = 2\bar{P}_R - \tilde{P}^*_{R2}(r)$.

5.3.5 Summary and Extensions

In the previous four subsections it has been shown that the problem of jointly allocating the power and the channel resource so as to enable operation at any point on the boundary of the achievable rate region is quasi-convex. In addition, it has been shown that for a given resource allocation, a closed-form solution for the optimal power allocation can be obtained. These results mean that the optimal value for r can be determined using a standard efficient search method for quasi-convex problems; e.g. [5].[5] For the particular problem at hand, a simple approach that is closely related to bisection search is provided in Table 5.1. At each step in that approach, the closed-form expressions for the optimal power allocation are used for each of the

[5]In the AF and CF cases these results are contingent on the maximum achievable SNR of both direct channels being greater than -3 dB, which would typically be the case in practice. Furthermore, since the condition $\gamma_{i0}\bar{P}_i > \frac{1}{2}$ depends only on the direct channel gains, the noise variance at the destination node, and the power constraints, this condition is testable before the design process commences.

current values of r. Since the quasi-convex search can be efficiently implemented and since it converges rapidly, the jointly optimal values for r and the (scaled) powers $\tilde{P}_{Ri}$ can be efficiently obtained.

In the above development the focus has been on the case of two source nodes. However, the core results extend directly to the case of $N > 2$ source nodes. Indeed, the joint power and resource allocation problem can be written in a form analogous to those in (5.7), (5.9), (5.10) and (5.12). To do so, we let $\bar{R}_i$ denote the appropriate maximal rate for Node i from (5.3), and we define $\tilde{P}_{Ri} = r_i P_{Ri}$, where P_{Ri} is the relay power allocated to the message of Node i. If we choose to maximize the achievable rate of Node j subject to target rate requirements for the other nodes, then the problem can be written as

$$\max_{\tilde{P}_{Ri}, r_i} \quad \bar{R}_j, \tag{5.14a}$$

$$\text{subject to} \quad \bar{R}_i \geqslant R_{i,\text{tar}} \qquad i = 1, 2, \ldots, N;\ i \neq j, \tag{5.14b}$$

$$\sum_{i=1}^{N} \tilde{P}_{Ri} \leqslant 2\bar{P}_R, \tag{5.14c}$$

$$\tilde{P}_{Ri} \geqslant 0, \tag{5.14d}$$

$$\sum_{i=1}^{N} r_i = 1. \tag{5.14e}$$

Using similar techniques to those in the previous subsections, it can be shown that this problem is quasi-convex in $(N-1)$ resource allocation parameters.[6] (The other parameter is not free as the resource allocation parameters must sum to one.) Furthermore, since for a given value of i, the expression $\bar{R}_i \geqslant R_{i,\text{tar}}$ depends only on $\tilde{P}_{Ri}$ and r_i, for a given set of target rates for Nodes $i \neq j$ and a given set of resource allocation parameters, a closed-form expression for the optimal $\tilde{P}_{Ri}$ can be obtained (for the chosen relaying strategy). These expressions have a structure that is analogous to

[6] In the AF and CF cases, this result is, again, contingent on the condition $\gamma_{i0}\bar{P}_i > 1/2$ holding for all i.

Table 5.1: A simple method for finding r^*

Given $R_{2,\text{tar}} \in (0, R_{2,\max}(0))$, for $r \in (0,1)$ define $\psi(r)$ denote the optimal value of (5.5) for a given r if $R_{2,\text{tar}} \in (0, R_{2,\max}(r))$ and zero otherwise. Set $\psi(0) = 0$ and $\psi(1) = 0$. Set $t_0 = 0$, $t_4 = 1$, and $t_2 = 1/2$. Using the closed-form expression for the optimal power allocations compute $\psi(t_2)$. Given a tolerance ϵ,

1. Set $t_1 = (t_0 + t_2)/2$ and $t_3 = (t_2 + t_4)/2$.
2. Using the closed-form expressions for the power allocations, compute $\psi(t_1)$ and $\psi(t_3)$.
3. Find $k^* = \arg\max_{k \in \{0,1,\ldots,4\}} \psi(t_k)$.
4. Replace t_0 by $t_{\max\{k^*-1,0\}}$, replace t_4 by $t_{\min\{k^*+1,4\}}$, and save $\psi(t_0)$ and $\psi(t_4)$. If $k^* \notin \{0,4\}$ set $t_2 = t_{k^*}$ and save $\psi(t_2)$, else set $t_2 = (t_0 + t_4)/2$ and use the closed-form expressions for the power allocations to calculate $\psi(t_2)$.
5. If $t_4 - t_0 \geq \epsilon$ return to 1), else set $r^* = t_{k^*}$.

---

the corresponding expression for the case of two source nodes that was derived in the sub-sections above. As we will demonstrate in Section 5.4, problems of the form in (5.14) can be efficiently solved using $(N-1)$–dimensional quasi-convex search methods, in which the closed-form solution for the optimal powers given a fixed resource allocation is used at each step.

In the development above, systems in which the relay node uses the same (pre-assigned) relaying strategy for each node have been considered. However, since the source nodes use orthogonal channels, the results extend directly to the case of different relaying strategies, and an example of such a heterogeneous multiple access relay system will be provided in the numerical results below.

5.4 Numerical Results

In this section, comparisons between the achievable rate regions obtained by different relaying strategies with the jointly optimal power and channel resource allocation derived in Section 5.3 are provided. Comparisons between the achievable rate regions obtained with jointly optimal power and channel resource allocation and those obtained using optimal power allocation alone, with equal channel resource allocation, $r = 0.5$, are also provided. the comparisons will be provided for two different channel models, whose parameters are given in Table 5.2. Finally, it will be shown that in some cases assigning different relaying strategies to different source nodes can result in a larger achievable rate region than assigning the same relaying strategy to all source nodes. In Fig. 5.3 the achievable rate regions for the four relaying strategies, RDF, NDF, CF, and AF are compared, in Scenario 1 in Table 5.2. In this scenario, the source-relay channel of Node 1 has higher effective gain than its direct channel,

Table 5.2: Parameters of the channel models used in the numerical results.

	$\lvert K_{10}\rvert$	$\lvert K_{1R}\rvert$	$\lvert K_{20}\rvert$	$\lvert K_{2R}\rvert$	$\lvert K_{R0}\rvert$	$\sigma_R^2 = \sigma_0^2$	$\bar{P}_1$	$\bar{P}_2$	$\bar{P}_R$
Scenario 1	0.3	1.2	0.8	0.6	0.4	1	2	2	4
Scenario 2	0.3	1.2	0.6	0.8	0.4	1	2	2	4

whereas for Node 2 the direct channel is better than the source-relay channel. Therefore, for small values of $\bar{R}_1$ one would expect the values of $\bar{R}_2$ that can be achieved by the CF and AF relaying strategies to be greater than those obtained by RDF and NDF, since the values of $\bar{R}_2$ that can be achieved by RDF and NDF will be limited by the source-relay link, which is weak for Node 2. Furthermore, for small values of $\bar{R}_2$, one would expect RDF and NDF to result in higher achievable values of $\bar{R}_1$ than CF and AF, since the source-relay link for Node 1 is strong and does not represent the bottleneck in this case. Both these expected characteristics are evident in Fig. 5.3. In Fig. 5.4 optimal the power allocation $\tilde{P}_{R1}$ for the four relaying strategies is provided, and Fig. 5.5 shows the optimal channel resource allocation. (Note that, as expected the optimal resource allocation is dependent on the choice of the relaying strategy.) It is interesting to observe that for the RDF strategy the relay power allocated to Node 2 is zero (i.e., $\tilde{P}_{R1} = 2\bar{P}_R$ for all feasible values of $R_{2,\text{tar}}$.) This solution is optimal because in Scenario 1 the achievable rate of Node 2 for the RDF strategy is limited by the source-relay link and there is no benefit to allocate any relay power to Node 2. For the same reason, the relay power allocated to Node 2 in the case of NDF relaying is also zero. However, in the case of NDF relaying, for small values of r, there is no need to use all the relay power to relay the messages of Node 1, i.e., $\tilde{P}_{R1} < 2\bar{P}_R$, and it is sufficient to use only the amount of power $\tilde{P}_{R1}$ that makes the

arguments of the min function in (5.9a) equal, i.e., $\tilde{P}_{R1} = \frac{2\bar{P}_1(\gamma_{1R}-\gamma_{10})r}{\gamma_{R0}(r+2\bar{P}_1\gamma_{10})}$. This can be seen in Fig. 5.4 as the (steeply) decreasing dotted curve that represents the optimal $\tilde{P}_{R1}$ for the case of NDF relaying. For values of $R_{2,\text{tar}}$ in this region, the average power that the relay needs to use is strictly less than its maximum average power. We also observe from Fig. 5.5 that the channel resource allocations for both RDF and NDF are the same. This situation arises because in both strategies the achievable rate of Node 2 is limited by the achievable rate of the source-relay link. This rate has the same expression for both strategies, and hence the same value of $\hat{r}$ will be allocated to Node 2. A further observation from Fig. 5.3 is that the achievable rate region for the CF relaying strategy is larger than that for AF and the achievable rate region for NDF is larger than that for RDF. This is consistent with the observation in [68], where the comparison was made in terms of the expression in (5.3) with $r = 1/2$.

To provide a quantitative comparison to the case of power allocation alone with equal resource allocation, in Fig. 5.6 the rate regions achieved by joint allocation and by power allocation alone for each relaying strategy are plotted. It is clear from the figure that the joint allocation results in significantly larger achievable rate regions.[7] As expected, each of the curves for $r = 0.5$ in Fig. 5.6 touches the corresponding curve for the jointly optimal power and channel resource allocation at one point. This point corresponds to the point at which the value $r = 0.5$ is (jointly) optimal.

In Figs 5.7–5.10, the performance of the considered scheme is examined in Scenario 2 of Table 5.2, in which the effective gain of the source-relay channel for Node 2 is larger than that in Scenario 1, and that of the source-destination channel is smaller. As can be seen from Fig. 5.7, increasing the gain of the source-relay channel of Node 2 expands the achievable rate of the RDF and NDF strategies, even though the gain of

[7]The horizontal segments of the regions with $r = 0.5$ in Fig. 5.6 arise from the allocation of all the relay power to Node 1. In these cases $R_{2,\text{tar}}$ can be achieved without the assistance of the relay, and hence all the relay power can be allocated to the message of Node 1.

the direct channel is reduced, whereas that change in the channel gains has resulted in the shrinkage of the achievable rate region for the CF and AF strategies. Therefore, we can see that the RDF and NDF strategies are more dependent on the quality of the source-relay channel than that of the source-destination channel,[8] while the reverse applies to the CF and AF strategies. Figs 5.8 and 5.9 show the allocation of the relay power and the channel resource parameter, respectively. It is interesting to note that for the RDF strategy, when $R_{2,\text{tar}}$ is greater than a certain value, the relay power allocated to Node 2 will be constant. The value of this constant is that which makes the two terms inside the min function in the left hand side of (5.7b) equal. This value can be calculated from the expression $\tilde{P}_{R2} = \frac{2(\gamma_{2R}-\gamma_{20})\bar{P}_2}{\gamma_{R0}}$. Fig. 5.10 provides comparisons between the achievable rate regions obtained by the jointly optimal allocation and those obtained by optimal power allocation alone with equal resource allocation. As in Fig. 5.6, it is again clear that the joint allocation results in significantly larger achievable rate regions.[9]

In Fig. 5.11 this comparison is extended to a three-user case. In order to obtain the jointly optimal power and channel resource allocations used to plot this figure, a two-dimensional quasi-convex search algorithm analogous to that in Table 5.1 is used to solve instances of the optimization problem in (5.14). As in the two-user case, a substantially larger rate region can be achieved by joint allocation of the power and the channel resource. It is worth mentioning that the $R_3 = 0$ slice through the jointly optimized region is the same as that obtained in the corresponding two-user case; cf. Fig. 5.7. This is because when $R_{3,\text{tar}} = 0$, the message from Node 3 will not be allocated any of the relay power, nor any of the channel resource. On the other hand,

[8]This observation holds so long as the first term in the argument of the min function in (5.3a) and (5.3b) is no more than the second term.

[9]In Fig. 5.10, the horizontal segments arise from all the relay power being allocated to Node 1, because the corresponding values of $R_{2,\text{tar}}$ can be achieved without the assistance of the relay.

the $R_3 = 0$ slice through the region with fixed (and equal) resource allocation will be smaller than the corresponding region in Fig. 5.7, because equal resource allocation in the three-user case corresponds to $r_i = 1/3$. This indicates that as the number of source nodes increases, so do the benefits of joint power and resource allocation.

In the above examples, the case in which the relay applies the same strategy to the messages of all source nodes has been considered. However, in Figs 5.12 and 5.13, it is shown that assigning different relaying strategies to the messages from different nodes may result in larger achievable rate regions. Fig. 5.12 shows that in Scenario 1, if the messages of Node 1 are relayed with the NDF strategy and the messages of Node 2 are relayed with the CF startegy, the resulting achievable rate region will be larger than that of the homogeneous NDF and CF strategies. If the relaying strategies are reversed, it can be seen that the achievable rate region will be smaller than that of both the homogeneous NDF and CF strategies. Since the NDF achievable rate region dominates the CF achievable rate region in Scenario 2 (see Fig. 5.7), it can be seen in Fig. 5.13 that both combinations NDF/CF and CF/NDF provide smaller achievable rate regions than the pure NDF region. Therefore, in Scenario 2 NDF relaying for both source nodes provides the largest achievable rate region. The examples in Figs 5.12 and 5.13 suggest that one ought to jointly optimize the power allocation, the resource allocation and the relaying strategy assigned for each node. Indeed, Figs 5.12 and 5.13 suggest that significant gains can be made by doing so. However, the direct formulation of that problem requires the joint allocation of power and the channel resource for each combination of relaying strategies, and hence the computational cost is exponential in the number of source nodes. Furthermore, as the achievable rate region of the overall system is the convex hull of the regions obtained by each combination of relaying strategies, time sharing between different combinations of relaying strategies may be required in order to maximize the achievable rate

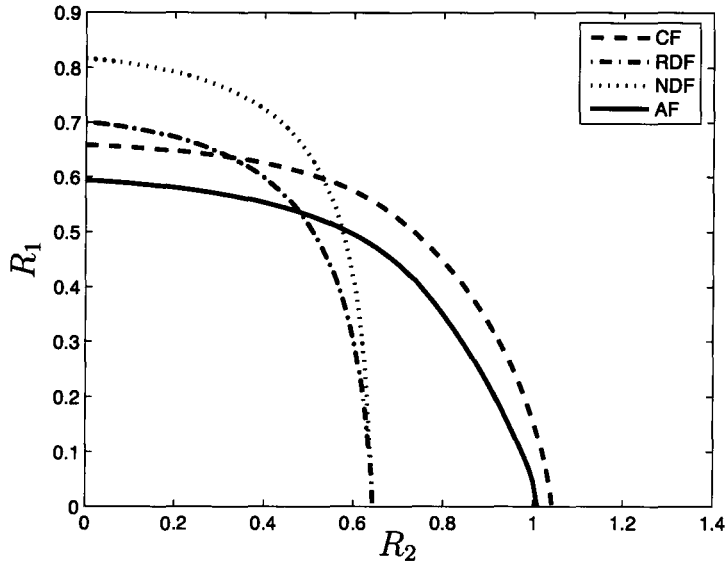

Figure 5.3: Achievable rate regions obtained via jointly optimal power and resource allocation in Scenario 1.

region. The approach in [54] to the design of relay networks based on orthogonal frequency division multiplexing (OFDM) offers some insight that may lead to more efficient algorithms for joint power, channel resource and strategy allocation, but the development of such algorithms lies beyond our current scope.

5.5 Conclusion

In this chapter it was shown that the problem of jointly optimal allocation of the power and channel resource in an orthogonal multiple access relay channel is quasi-convex, and hence that simple efficient algorithms can be used to obtain the optimal solution. In addition, a closed-form expression for the optimal power allocation for a given resource allocation was obtained, and this expression was exploited to significantly reduce the complexity of the algorithm. The numerical results obtained

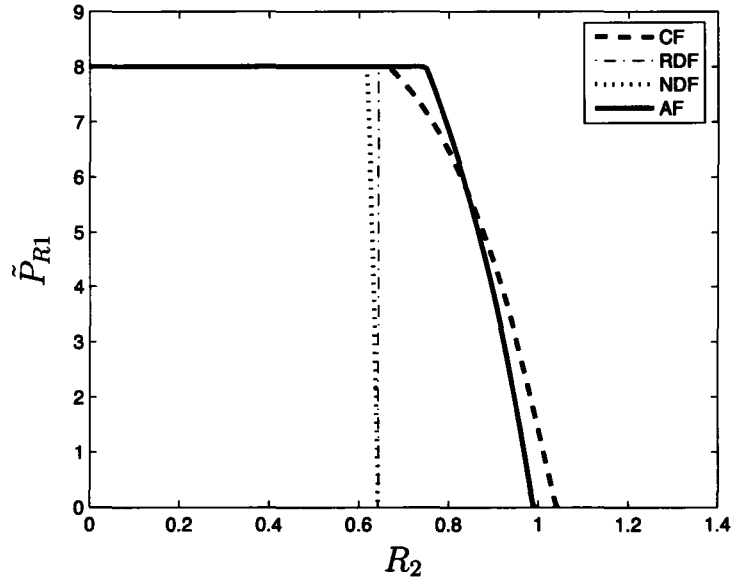

Figure 5.4: Powers allocated by jointly optimal algorithm in Scenario 1.

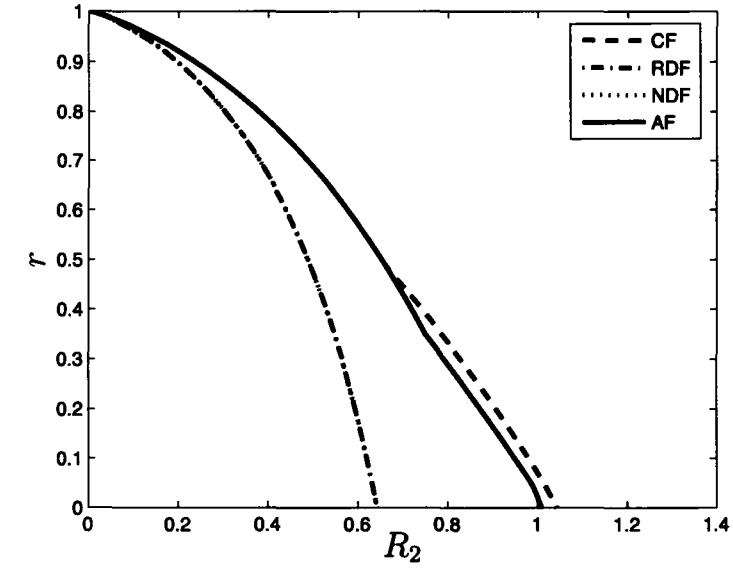

Figure 5.5: Resource allocation from the jointly optimal algorithm in Scenario 1.

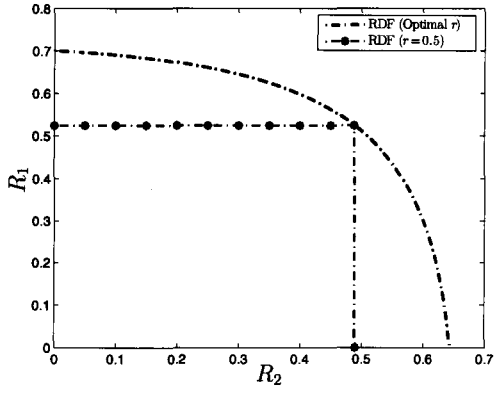

(a) RDF

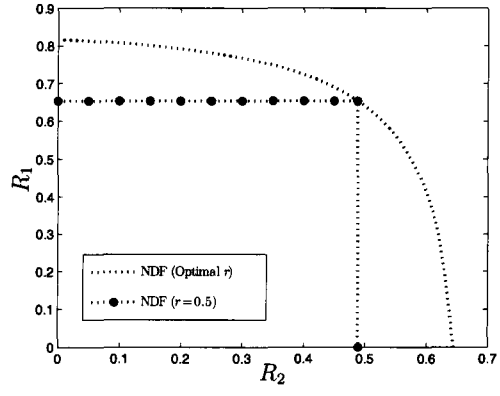

(b) NDF

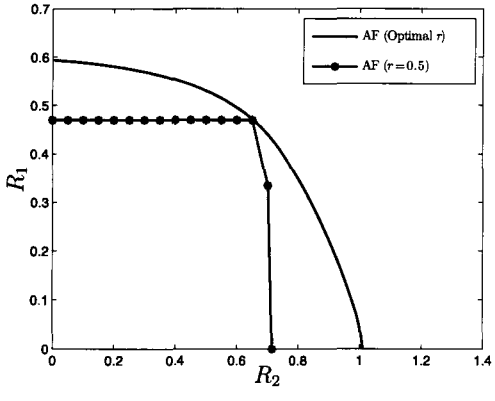

(c) AF

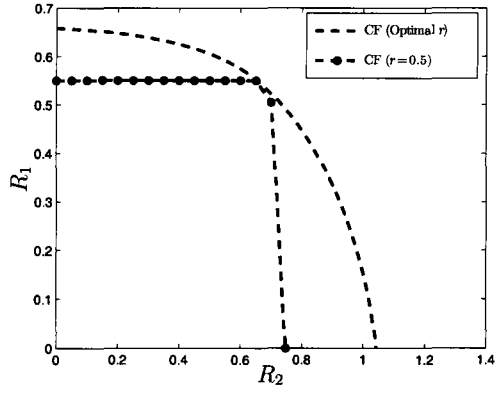

(d) CF

Figure 5.6: Comparisons between the achievable rate regions obtained by jointly optimal power and resource allocation and those obtained by power allocation only with equal resource allocation, for Scenario 1.

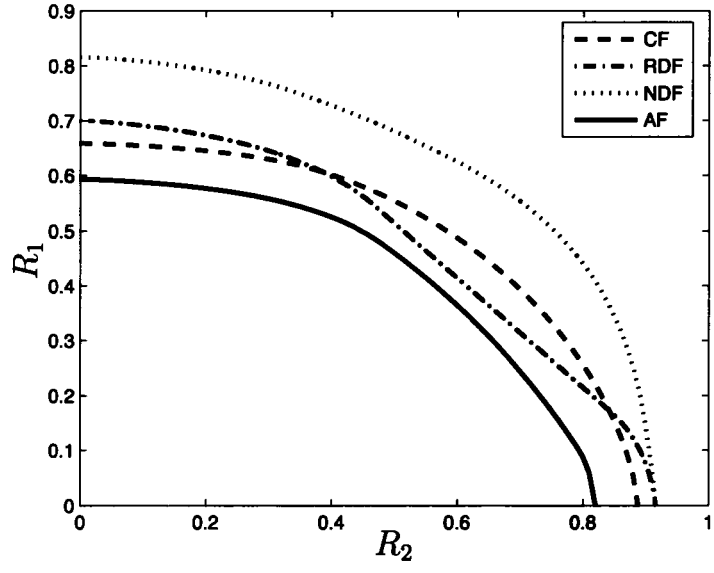

Figure 5.7: Achievable rate regions obtained via jointly optimal power and resource allocation in Scenario 2.

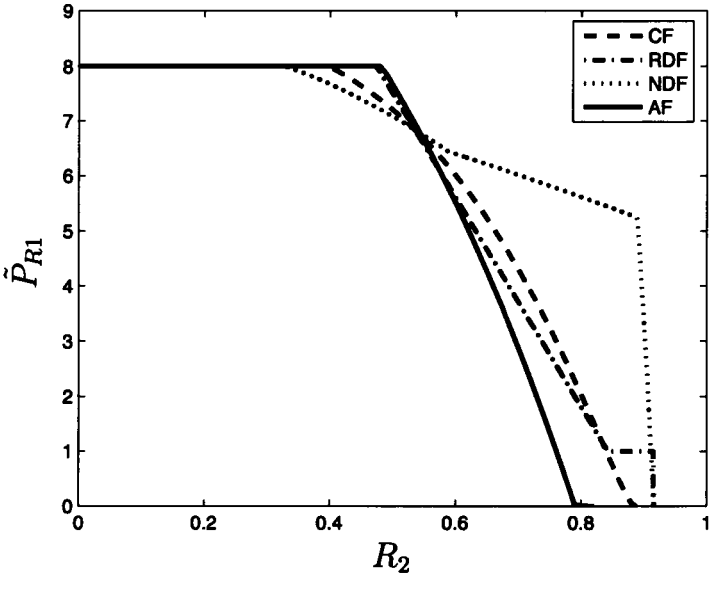

Figure 5.8: Powers allocated by jointly optimal algorithm in Scenario 2.

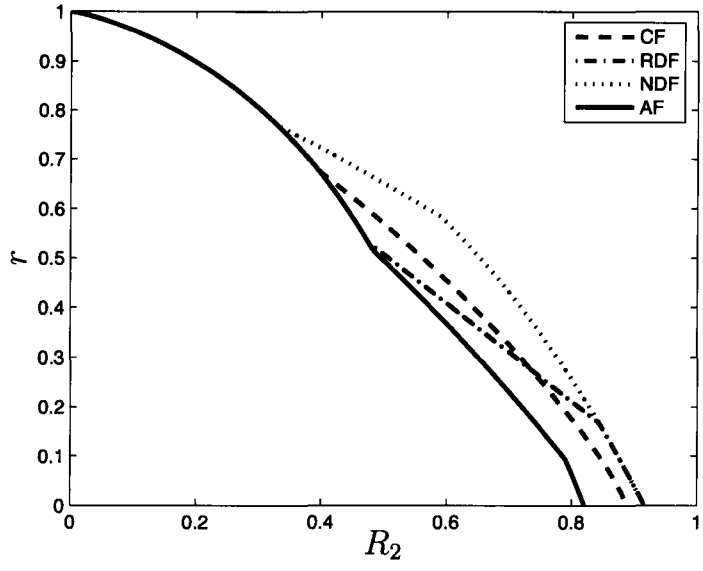

Figure 5.9: Resource allocation from the jointly optimal algorithm in Scenario 2.

using the proposed algorithm show that significant rate gains can be obtained over those schemes that apply only power allocation and equal channel resource allocation. Finally, an example of the joint allocation of the power, the channel resource, and the relaying strategy was provided, and it was shown that this has the potential to further enlarge the achievable rate region.

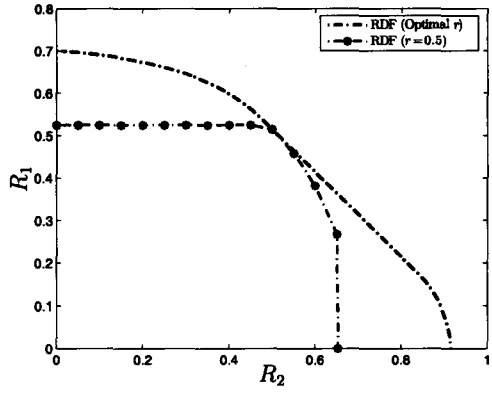

(a) RDF

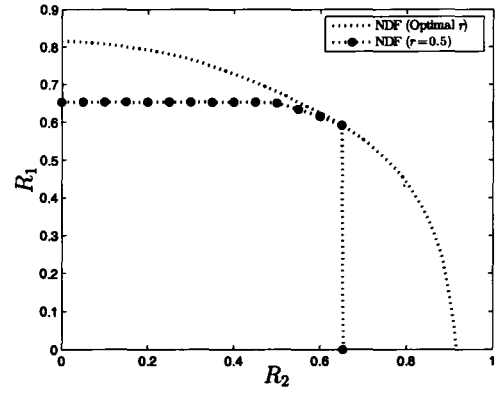

(b) NDF

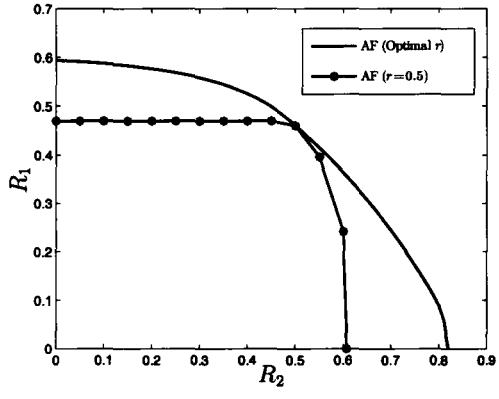

(c) AF

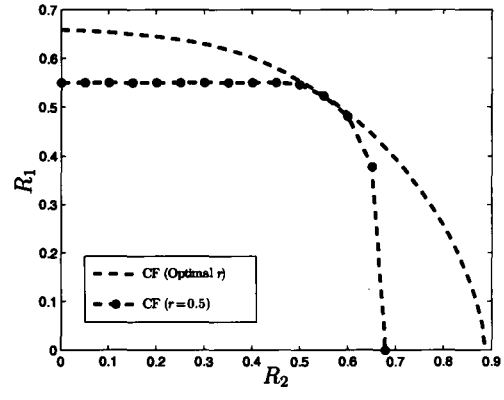

(d) CF

Figure 5.10: Comparisons between the achievable rate regions obtained by jointly optimal power and resource allocation and those obtained by power allocation only with equal resource allocation, for Scenario 2.

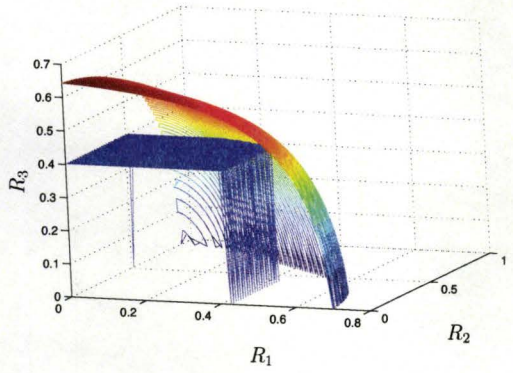

(a) RDF

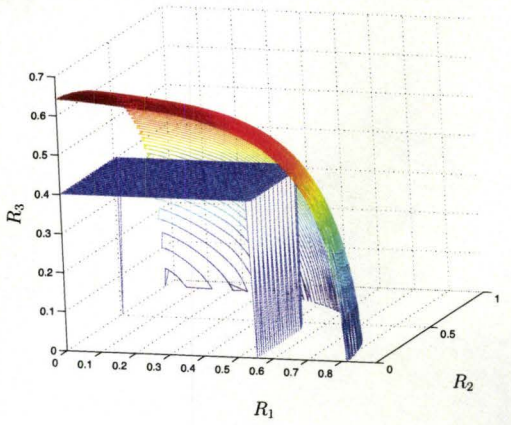

(b) NDF

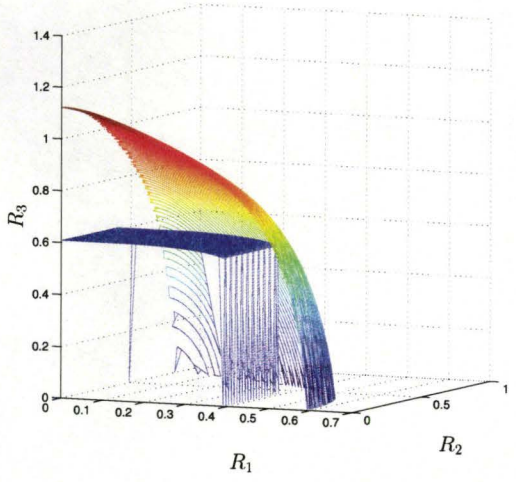

(c) AF

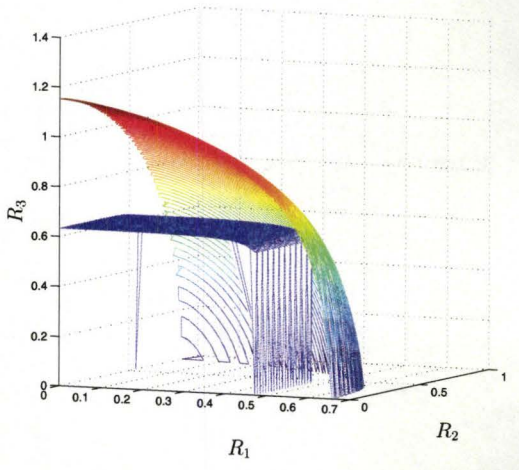

(d) CF

Figure 5.11: The achievable rate regions obtained by jointly optimal power and resource allocation and those obtained by power allocation alone with equal resource allocation for three-user system with $|K_{3R}| = 0.6$, $|K_{30}| = 0.9$, $\bar{P}_3 = 2$, and the remaining parameters from Scenario 2 in Table 5.2.

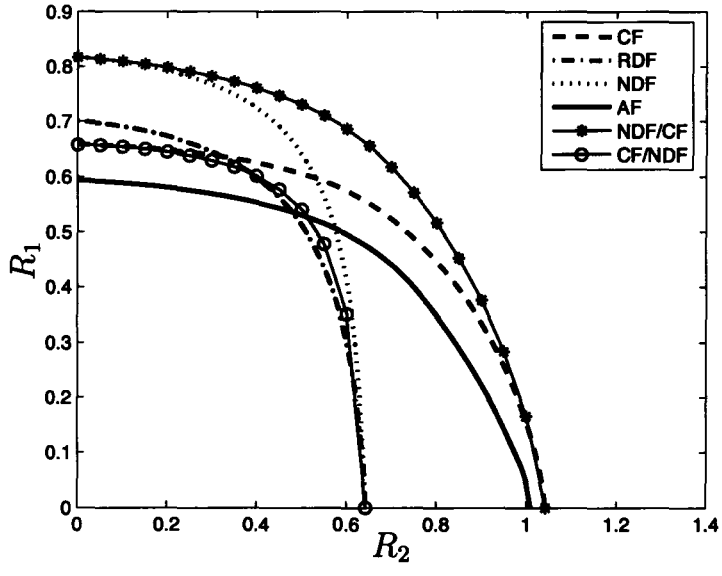

Figure 5.12: Comparison between the achievable rate regions when using the same relaying strategy for both users and when using different relaying strategies, for Scenario 1.

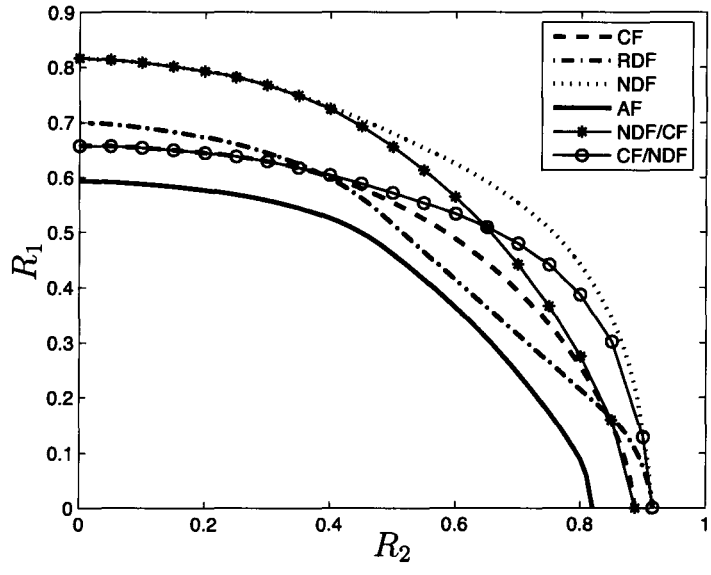

Figure 5.13: Comparison between the achievable rate regions when using the same relaying strategy for both users and when using different relaying strategies, for Scenario 2.

Chapter 6

Conclusion and Future Work

6.1 Conclusion

This thesis has considered problems of optimal power allocation and jointly optimal power and channel resource allocation for different cooperative communication schemes for which full channel state information is available. The channel model that was considered throughout the thesis is the slow fading channel model under which the coherence time of the channel is long enough to enable the feedback of the channel gains to the nodes without expending a significant fraction of the available power and channel resources. The availability of full channel state information enables the cooperating nodes to allocate their power and adapt their access to the channel resources in an optimal manner, and hence to optimally adjust their coding and decoding rates. The objective of the jointly optimal power and channel resource allocation is to maximize the achievable rate region. In other words, the objective is to obtain the joint allocation of the power and the channel resources that enables the cooperative system to operate at an arbitrary point on the boundary of the achievable rate region. Although this objective is achieved under the assumption that a well

designed long enough (capacity achieving) code is available, it provides a benchmark against which systems with capacity approaching codes can be compared.

The target rate approach that was proposed in the thesis provides a new perspective on the class of problems that consider maximizing the rate region, and enables the development of efficient algorithms for the jointly optimal power and channel resource allocation for different cooperative systems. Furthermore, in most of the cases that were considered, closed-form solutions for the optimal power allocation for a given channel resource allocation were provided. In particular, the main contributions of the thesis are as follows:

- In the first part of Chapter 3 the problem of power allocation in a full-duplex cooperative multiple access scheme that employs block Markov superposition encoding was analyzed. The goal was to obtain the optimal power allocation that enables the full-duplex cooperative system to achieve an arbitrary point on the boundary of the achievable rate region. The analysis revealed that the apparently non-convex problem can be transformed into a convex optimization problem that has a closed-form solution. That transformation was revealed by analyzing the structure of the solution at optimality. That structure revealed that at optimality two of the six power components that need to be allocated, one component for each user, must be zero, although which two depends on the channel state.

- In the second part of Chapter 3, a half-duplex cooperative multiple access scheme that employs the decode-and-forward relaying strategy was considered and the joint power and channel resource allocation problem for that scheme was solved. The analysis exposed the quasi-convexity of the resource allocation problem, and that property was exploited to develop an efficient algorithm

for the jointly optimal power and channel resource allocation. Moreover, for a given resource allocation, the power allocation problem was shown to be convex and the number of design variables was reduced from six to two. By applying this design approach, it was demonstrated that a substantial fraction of the achievable rate region of the full-duplex case can be obtained with the proposed half-duplex scheme. Furthermore, the reduction that was obtained in the complexity of finding the jointly optimal power and resource allocation suggests that it may be possible to avoid approximations in the development of on-line algorithms.

- In Chapter 4, the problem of joint power and channel resource allocation for a two-user orthogonal amplify-and-forward cooperative scheme was addressed. A closed-form expression for the optimal power allocation for a given channel resource allocation was obtained. Moreover, the power and channel resource allocation problem was shown to be quasi-convex under typical channel conditions. These results were exploited to develop a simple efficient algorithm for the jointly optimal allocation. Analysis of the KKT optimality conditions showed that the original system under consideration does not use the channel resources efficiently and that at optimality both source nodes will be idle during at least one quarter of the time slots. Therefore, a modified orthogonal AF cooperation scheme was proposed, and it was demonstrated that with optimal power and channel resource allocation the modified scheme can provide a significantly larger achievable rate region than that provided by the original scheme. Furthermore, a simple strategy that enables efficient optimization of a guaranteed achievable rate region in the presence of bounded uncertainties in the available channel state information was provided.

- Finally, in Chapter 5, an orthogonal half-duplex multiple access relay system was considered. In multiple access relay systems, the source nodes do not work as relays for each other. Instead, there exists an independent node that works only as a relay and serves all the source nodes. Four relaying strategies were employed; namely, regenerative decode-and-forward, non-regenerative-decode-and-forward, amplify-and-forward, and compress-and-forward. It was shown that the problem of jointly optimal allocation of the power and the channel resource in an orthogonal multiple access relay channel is quasi-convex under typical channel conditions, and hence that simple efficient algorithms can be used to obtain the optimal solution. In addition, a closed-form expression for the optimal power allocation for a given resource allocation was obtained and exploited to significantly reduce the complexity of the algorithm. The proposed efficient algorithm can be used for homogeneous cases, where the information of the source nodes are being relayed using the same relaying strategy, and also for heterogeneous cases, where different relaying strategies may be used for different users. The numerical results obtained using the proposed algorithm show that significant rate gains can be obtained over those schemes that apply only power allocation and equal channel resource allocation. Moreover, an example of the joint allocation of the power, the channel resource, and the relaying strategy, was provided and it was shown that this additional degree of freedom has the potential to significantly enlarge the achievable rate region.

6.2 Future Work

The area of cooperative wireless communication has been an area of intensive research over the last few years. Cooperative wireless communication systems have

demonstrated their potential to improve the quality of service provided for the users. There are several future research directions that will build on the current research in cooperative systems, including that presented in this thesis. One direction is to study cooperative systems under different and/or more pragmatic assumptions. Another direction is to study the different ways of integrating cooperative systems with the existing communication system and to study the behavior of cooperative systems when employed in conjunction with other communication schemes, e.g, systems with multiple antennas and/or multiple carriers. In the next two subsections, some specific problems related to these two directions are discussed.

6.2.1 Cooperative Systems with Pragmatic Assumptions

- Generalization to More Than Two Users

  In the thesis, cooperative multiple access schemes with two source nodes (users) were considered. The quasi-convexity of the joint power and channel resource allocation problems was proved for the case of two source nodes. Therefore, it would be interesting to generalize the schemes considered in this thesis to more than two users. In this case, it is not clear what the best cooperation protocol might be, or whether the expressions of the achievable rates will preserve the quasi-convexity or not. Furthermore, it is even not clear if the achievable rates will be convex in the power components for a given resource allocation or not. Nevertheless, the success reported herein for the two-user case suggests that this should be investigated.

- Design of Codes for Different Cooperative Configurations

  The optimal power and channel resource allocation algorithms proposed in this thesis were developed under an assumption of ideal coding. Therefore, the

development of efficiently encodable and decodable codes that can operate efficiently at rates close to those obtained by ideal codes is a critical step towards achieving the promised gains of the optimized cooperative systems. There has been some work on developing coded cooperation schemes using convolutional codes [70], turbo codes [29, 86] and rate-compatible punctured convolutional (RCPC) codes [23–26]. Furthermore, there has been some recent work that employs bilayer and multi-layer LDPC codes for the relay channels with single and multiple relays [57, 58]. However, these codes were developed for specific cooperative configurations, and hence codes for different configurations still need to be designed.

- Distributed Power and Resource Allocation Algorithms

  The channel model that was assumed in this thesis is a block fading channel model with a coherence time that is long enough to enable the nodes to acquire channel state information using a negligible fraction of the power and channel resources. However, if the channel experiences faster fading, then it will be difficult to employ the centralized power and channel resource allocation strategies proposed in the thesis. These strategies assume that the nodes have full instantaneous channel state information, and in the case of fast fading the communication of this CSI will require a significant fraction of the available power and channel resources. In this case, distributed power and channel resource allocation schemes that rely on partial CSI must be developed.

- Efficient Algorithms for Heterogeneous MARC

  In Chapter 5 joint power and channel resource allocation for the homogeneous and the heterogeneous MARC was considered. It was also shown that the heterogeneous MARC can achieve larger achievable rate regions if the relaying

strategy used for each user is optimally chosen. However, the optimal power, channel resource, and relaying strategy allocation is not an easy problem to solve. In the example of Chapter 5, an exhaustive search approach was used to determine the optimal strategy assignment, and the computational cost was exponential in the number of source nodes. Therefore, the development of an efficient and low complexity algorithms for optimal (or suboptimal) strategy assignment, together with jointly optimal power and channel resource allocation, is necessary to achieve the aforementioned gains in practice. In [54], an approach was developed for the design of relay networks based on orthogonal frequency division multiplexing (OFDM). This approach offers some insight that may lead to more efficient algorithms for joint power, channel resource and strategy assignment.

- Cooperation Among Correlated Sources

  Throughout the thesis it has been assumed that the source nodes have independent information to transmit to the destination. However, the problem of cooperative communication with correlated sources is an important and interesting problem to study. The importance of this problem comes from its high relevance to sensor networks, as the measurements taken at different sensors may have some correlation structure. To efficiently forward these measurements to a fusion center over noisy and fading links, distributed joint source-coding and cooperative diversity techniques should be developed. This is different from joint source-channel coding problems in the sense that both the source-coding and the cooperation take place at spatially dispersed nodes. New cooperation protocols that take the correlation structure into consideration are needed. Moreover, these protocols will be need to be robust in order to provide solutions to the

class of problems in which imperfect correlation information is provided.

- Cooperative Broadcast Channel

  While the algorithms developed in this thesis work well for cooperative multiple access channels with separate power constraints, one might consider adapting the algorithms for cooperative broadcast channels with a total power constraint. Although there has been some work in the literature that considers the duality between cooperative BC and cooperative MAC [12,28] and investigates bounds on the capacity regions of different cooperative broadcast schemes [40,42], the amount of that work is rather limited compared to the work that considers cooperative multiple access channels. Moreover, efficient algorithms for power and resource allocations to maximize the achievable rate regions need to be developed.

6.2.2 Integration of Cooperative Systems with Current Communication Schemes

- Cooperative MIMO Channels

  In this thesis, all the source nodes, relays and destination nodes were assumed to have a single antenna. However, multiple-input multiple-output (MIMO) technology increases the degrees of freedom of the communication system along with increased diversity. On the other hand, cooperative schemes also have the potential to increase the achievable rates and the diversity provided for the users. Moreover, for the same rate, cooperative schemes may increase the coverage area without the need to use more power. These powerful advantages in both technologies render it desirable to bridge between MIMO systems and cooperative communication schemes. Combining these two technologies is a

very wide research area to explore. Two interesting objectives for this research can be considered:

- Developing diversity-multiplexing optimal coding schemes for slow fading MIMO cooperative channels. The performance of slow fading MIMO channels is characterized using a tradeoff curve between the diversity order, which measures the reliability gain, and the multiplexing order, which measures the rate gain [73,87]. This tradeoff is used as a benchmark to compare different space-time coding schemes. Moreover, it defines the criteria for designing universal coding schemes for different classes of channels. Non-orthogonal cooperation schemes that achieve the diversity-multiplexing tradeoff have been developed for half-duplex single antenna cooperative systems, e.g., [4]. Furthermore, some schemes have been shown to be diversity-multiplexing optimal for MIMO channels, e.g., D-BLAST [74], and LAST [15, 16]. However, universal code design for optimal diversity-multiplexing tradeoff for MIMO cooperative channels is still an open area for further research. Recently, in [85] the diversity-multiplexing tradeoffs for several MIMO cooperative systems that employ the DF and CF strategies were examined. In some configurations, DF and CF strategies were shown to be diversity-multiplexing optimal.
- Exploring optimal transmission strategies for cooperative MIMO channels in different cases of transmitter channel state information. This research is expected to have a significant impact on the evolving communication standards that aim to provide high rates along with high reliability and broad coverage. A recent work that derives the optimal beamforming directions for a simple MIMO relay channel, with quantized feedback of the channel information to the transmitter, appears in [32]. This direction still

needs a substantial amount of research to obtain the optimal transmission strategies for different MIMO cooperative systems.

- MIMO-OFDM Cooperative Systems

  Orthogonal frequency division multiplexing (OFDM) is being extensively used in most emerging wideband communication systems. This proposed research aims to incorporate MIMO-OFDM modulation with cooperative schemes in order to combine their benefits. OFDM is often used in wideband transmission in order to efficiently communicate over frequency-selective fading channels, whereas MIMO and cooperative technologies have the powerful advantage of increasing the rate and the diversity provided. Therefore, combining the three technologies together would provide a dramatic improvement in the performance of current wireless technologies that use MIMO-OFDM, such as WiMAX IEEE 802.16. In fact, in addition to the gains in rate and diversity, combining cooperative schemes with WiMAX technology has the potential to provide substantial increase to the coverage of the WiMAX networks. Even shadowed users will be able to obtain high rates with high reliability.

Appendix A

Sufficiency of the corner points on the conventional multiple access region

Let us begin with a point on the line connecting the two corner points of the conventional multiple access region; i.e., the (R_{10}, R_{20}) region. Any point on that line can be achieved by time sharing between the two corners, [9]. That is,

$$R_{10} \leqslant \rho \log\left(1 + \frac{\gamma_{10}P_{10}}{1+\gamma_{20}P_{20}}\right) + \bar{\rho}\log\left(1+\gamma_{10}P_{10}\right), \tag{A.1}$$

$$R_{20} \leqslant \rho \log\left(1 + \gamma_{20}P_{20}\right) + \bar{\rho}\log\left(1 + \frac{\gamma_{20}P_{20}}{1+\gamma_{10}P_{10}}\right), \tag{A.2}$$

where $\rho \in [0,1]$ is a time sharing constant and $\bar{\rho} = 1 - \rho$. Since $R_1 = R_{10} + R_{12}$ and $R_2 = R_{20} + R_{21}$, we can write the constraints on R_1 and R_2 as

$$\begin{aligned} R_1 \leqslant & \rho \log\left(1 + \frac{\gamma_{10}P_{10}}{1+\gamma_{20}P_{20}}\right) + \bar{\rho}\log\left(1+\gamma_{10}P_{10}\right) \\ & + \log\left(1 + \frac{\gamma_{12}P_{12}}{1+\gamma_{12}P_{10}}\right), \end{aligned} \tag{A.3}$$

$$R_2 \leqslant \rho \log\left(1 + \gamma_{20}P_{20}\right) + \bar{\rho}\log\left(1 + \frac{\gamma_{20}P_{20}}{1+\gamma_{10}P_{10}}\right)$$

$$+\log\left(1+\frac{\gamma_{21}P_{21}}{1+\gamma_{21}P_{20}}\right), \tag{A.4}$$

$$R_1+R_2\leqslant\log\left(1+\gamma_{10}P_1+\gamma_{20}P_2+2\sqrt{\gamma_{10}\gamma_{20}P_{U1}P_{U2}}\right), \tag{A.5}$$

which can be written as

$$R_1\leqslant\rho R_1^*+\bar{\rho}R_1^{**}, \tag{A.6a}$$

$$R_2\leqslant\rho R_2^*+\bar{\rho}R_2^{**}, \tag{A.6b}$$

$$R_1+R_2\leqslant\log\left(A_0+2\sqrt{\gamma_{10}\gamma_{20}P_{U1}P_{U2}}\right), \tag{A.6c}$$

where

$$\begin{aligned}
R_1^* &= \log\left(1+\frac{\gamma_{10}P_{10}}{1+\gamma_{20}P_{20}}\right)+\log\left(1+\frac{\gamma_{12}P_{12}}{1+\gamma_{12}P_{10}}\right),\\
R_1^{**} &= \log\left(1+\gamma_{10}P_{10}\right)+\log\left(1+\frac{\gamma_{12}P_{12}}{1+\gamma_{12}P_{10}}\right),\\
R_2^* &= \log\left(1+\gamma_{20}P_{20}\right)+\log\left(1+\frac{\gamma_{21}P_{21}}{1+\gamma_{21}P_{20}}\right),\\
R_2^{**} &= \log\left(1+\frac{\gamma_{20}P_{20}}{1+\gamma_{10}P_{10}}\right)+\log\left(1+\frac{\gamma_{21}P_{21}}{1+\gamma_{21}P_{20}}\right),\\
A_0 &= 1+\gamma_{10}P_1+\gamma_{20}P_2.
\end{aligned}$$

Now, consider maximizing the region defined by the constraints in (A.6), subject to the power constraints in (3.4b). Any point on the boundary of the maximized region can be obtained by solving the following problem (maximize the weighted sum of rates)

$$\begin{aligned}
&\max_{\mathbf{p}} && \mu_1R_1+\mu_2R_2\\
&\text{subject to} && \text{(A.6a), (A.6b), (A.6c), (3.4b),}
\end{aligned}$$

where $\mathbf{p}$ is a vector containing all the power components. For simplicity, we will focus on the case in which $\mu_2\geq\mu_1$. The proof for the case in which $\mu_2<\mu_1$ is analogous.

If $\mu_2 \geq \mu_1$, then the above problem can be written as

$$\max_{\mathbf{p}} \quad \mu_1(R_1 + R_2) + (\mu_2 - \mu_1)R_2 \tag{A.7a}$$

$$\text{subject to} \quad \text{(A.6a), (A.6b), (A.6c), (3.4b).} \tag{A.7b}$$

The sum rate constraint in (A.6c) can be written as

$$R_1 + R_2 \leqslant \min\left\{\log\left(A_0 + 2\sqrt{\gamma_{10}\gamma_{20}P_{U1}P_{U2}}\right), \right.$$
$$\left. \rho R_1^* + \bar{\rho}R_1^{**} + \rho R_2^* + \bar{\rho}R_2^{**}\right\} \tag{A.8}$$

$$= \min\left\{f(\mathbf{p}), g(\mathbf{p})\right\}, \tag{A.9}$$

where

$$f(\mathbf{p}) = \log\left(A_0 + 2\sqrt{\gamma_{10}\gamma_{20}P_{U1}P_{U2}}\right),$$

$$g(\mathbf{p}) = \log\left(1 + \gamma_{10}P_{10} + \gamma_{20}P_{20}\right) + \log\left(1 + \frac{\gamma_{12}P_{12}}{1 + \gamma_{12}P_{10}}\right)$$
$$+ \log\left(1 + \frac{\gamma_{21}P_{21}}{1 + \gamma_{21}P_{20}}\right).$$

Now, (A.7) can be written as

$$\max_{\mathbf{p}} \quad \mu_1 \min\left\{f(\mathbf{p}), g(\mathbf{p})\right\} + (\mu_2 - \mu_1)R_2 \tag{A.10a}$$

$$\text{subject to} \quad \text{(A.6a), (A.6b), (A.6c), (3.4b).} \tag{A.10b}$$

Substituting for R_2 from (A.6b), the objective in (A.10a) can be rewritten as

$$\max_{\mathbf{p}} \quad \mu_1 \min\left\{f(\mathbf{p}), g(\mathbf{p})\right\} + (\mu_2 - \mu_1)(\rho R_2^* + \bar{\rho}R_2^{**}) \tag{A.11}$$

Furthermore, equation (A.11) can be bounded as

$$\max_{\mathbf{p}} \rho\left[\mu_1 \min\left\{f(\mathbf{p}), g(\mathbf{p})\right\} + (\mu_2 - \mu_1)R_2^*\right]$$
$$+ \bar{\rho}\left[\mu_1 \min\left\{f(\mathbf{p}), g(\mathbf{p})\right\} + (\mu_2 - \mu_1)R_2^{**}\right]$$

$$\leqslant \rho \max_{\mathbf{p}} [\mu_1 \min\{f(\mathbf{p}), g(\mathbf{p})\} + (\mu_2 - \mu_1) R_2^*]$$
$$+ \bar{\rho} \max_{\mathbf{p}} [\mu_1 \min\{f(\mathbf{p}), g(\mathbf{p})\} + (\mu_2 - \mu_1) R_2^{**}]. \quad \text{(A.12)}$$

The first term in the right hand side of (A.12) represents the maximization of the rate region assuming that the direct message of node 1 is decoded first, while the second term represents the maximization of the rate region assuming that the direct message of node 2 is decoded first. Therefore, it is clear from (A.12) that time sharing between the two regions corresponding to the two corner points of conventional multiple access region (i.e., the (R_{10}, R_{20}) region) contains all the regions corresponding to the points on the line connecting the two corners. Hence, it is sufficient to study only the two regions corresponding to the two corner points on the (R_{10}, R_{20}) region.

Appendix B

The first case of (3.26) with $B < 0$

In the first case of (3.26), if B is negative, then $\left(1+\gamma_{12}\bar{P}_1\right) < \frac{\left(1+\gamma_{10}\bar{P}_1+\gamma_{20}\bar{P}_2\right)}{2^{R_{2,\text{tar}}}}$. Taking the logarithm of both sides, we have that

$$\begin{aligned}\log\left(1+\gamma_{12}\bar{P}_1\right) &< \log\left(\frac{1+\gamma_{10}\bar{P}_1+\gamma_{20}\bar{P}_2}{2^{R_{2,\text{tar}}}}\right) \\ &= \log\left(1+\gamma_{10}\bar{P}_1+\gamma_{20}\bar{P}_2\right) - R_{2,\text{tar}}. \end{aligned} \tag{B.1}$$

Given the conditions on the channel gains for Case 4 to arise, we also have $\log\left(1+\gamma_{12}\bar{P}_1\right) < \log\left(1+\gamma_{10}\bar{P}_1\right)$. The conventional multiple access scheme provides an achievable R_1 that equals

$$\min\{\log\left(1+\gamma_{10}\bar{P}_1\right), \log\left(1+\gamma_{10}\bar{P}_1+\gamma_{20}\bar{P}_2\right) - R_{2,\text{tar}}\}. \tag{B.2}$$

Since both terms in the minimization in (B.2) are larger than $\log\left(1+\gamma_{12}\bar{P}_1\right)$, in this scenario the conventional multiple access scheme provides a higher achievable rate than that offered by a scheme that presumes cooperation.

Appendix C

Proof of sufficiency of the first case of (3.26) and its symmetric image

For simplicity, we let $f(P_{U1}, P_{U2}) = \log\left(1 + \gamma_{10}\bar{P}_1 + \gamma_{20}\bar{P}_2 + 2\sqrt{\gamma_{10}\gamma_{20}P_{U1}P_{U2}}\right)$. When $P_{20} < (\frac{\gamma_{10}}{\gamma_{12}} - 1)/\gamma_{20}$, the constraint set (3.24) can be written as

$$R_2 \leqslant \log\left(1 + \gamma_{20}P_{20}\right) + \log\left(1 + \frac{\gamma_{21}P_{21}}{1 + \gamma_{21}P_{20}}\right), \tag{C.1a}$$

$$R_1 \leqslant \log\left(1 + \frac{\gamma_{10}P_{10}}{1 + \gamma_{20}P_{20}}\right), \tag{C.1b}$$

$$R_1 + R_2 \leqslant f(P_{U1}, P_{U2}). \tag{C.1c}$$

The first term in the right hand side of (C.1a), and the term on the right hand side of (C.1b) represent the conventional multiple access region. Therefore, this constraint set can be rewritten as

$$R_2 \leqslant \log\left(1 + \gamma_{20}P_{20}\right) + \log\left(1 + \frac{\gamma_{21}P_{21}}{1 + \gamma_{21}P_{20}}\right), \tag{C.2a}$$

$$R_1 \leqslant \log\left(1 + \gamma_{10}P_{10}\right), \tag{C.2b}$$

$$R_1 + R_2 \leqslant \min\left\{f(P_{U1}, P_{U2}), \log\left(\frac{1 + \gamma_{10}P_{10} + \gamma_{20}P_{20}}{1 + \gamma_{21}P_{20}}\right)\right.$$

$$+\log\left(1+\gamma_{21}S_2\right)\}\,. \tag{C.2c}$$

Solving Step 1 with $P_{20} > (\frac{\gamma_{10}}{\gamma_{12}} - 1)/\gamma_{20}$, using (3.27) and (3.29), gives the following constraint set

$$R_2 \leqslant \log\left(1+\gamma_{20}P_{20}\right), \qquad R_1 \leqslant \log\left(1+\gamma_{12}P_{12}\right), \tag{C.3a}$$

$$R_1 + R_2 \leqslant f(P_{U1}, P_{U2}). \tag{C.3b}$$

Similarly, solving Step 2 with $P_{10} > (\frac{\gamma_{20}}{\gamma_{21}} - 1)/\gamma_{10}$ gives the following constraint set

$$R_2 \leqslant \log\left(1+\gamma_{21}P_{21}\right), \qquad R_1 \leqslant \log\left(1+\gamma_{10}P_{10}\right), \tag{C.4a}$$

$$R_1 + R_2 \leqslant f(P_{U1}, P_{U2}). \tag{C.4b}$$

Now consider the generic problem of maximizing a weighted sum of the rates R_1 and R_2, under the second case of (3.26), namely

$$\begin{aligned} \max_{\mathbf{p}} \quad & \mu_1 R_1 + \mu_2 R_2, \\ \text{subject to} \quad & \text{(C.2)}, \text{(3.4b)}, \; P_{20} < \left(\tfrac{\gamma_{10}}{\gamma_{12}} - 1\right)/\gamma_{20}, \end{aligned} \tag{C.5}$$

where $\mathbf{p}$ is the vector containing all the power components to be allocated. The region resulting from (C.5) is contained in the region that is achievable if the constraint $P_{20} < \left(\frac{\gamma_{10}}{\gamma_{12}} - 1\right)/\gamma_{20}$ is removed, namely

$$\begin{aligned} \max_{\mathbf{p}} \quad & \mu_1 R_1 + \mu_2 R_2, \\ \text{subject to} \quad & \text{(C.2)}, \text{(3.4b)}. \end{aligned} \tag{C.6}$$

The problem in (C.6) can be written as

$$\begin{aligned} \max_{\mathbf{p}} \quad & a(R_1 + R_2) + bR_1, \\ \text{subject to} \quad & \text{(C.2)}, \text{(3.4b)}, \end{aligned} \tag{C.7}$$

where $a = \mu_2$ and $b = \mu_1 - \mu_2$ are constants. The region resulting from the problem in (C.7) is contained in the following region

$$\max_{\tilde{\mathbf{p}}} \quad a \max_{P_{21}}(R_1 + R_2) + b \max_{P_{21}} R_1, \tag{C.8}$$

$$\text{subject to} \qquad (C.2), (3.4b), \tag{C.9}$$

where $\tilde{\mathbf{p}}$ contains all the power components to be allocated, except P_{21}. The objective in (C.9) can be expanded as

$$\max_{\tilde{\mathbf{p}}} \quad a \max_{P_{21}} \min\left\{f(P_{U1}, P_{U2}), \log\left(\frac{1+\gamma_{10}P_{10}+\gamma_{20}P_{20}}{1+\gamma_{21}P_{20}}\right) + \log(1+\gamma_{21}S_2)\right\} + b\,\log(1+\gamma_{10}P_{10}). \tag{C.10}$$

For a constant sum $S_2 = P_{20} + P_{21}$, maximizing over P_{21} takes the form of (3.5), and hence

$$P_{21}^* = \begin{cases} 0 & \text{if } P_{10} < (\frac{\gamma_{20}}{\gamma_{21}} - 1)/\gamma_{10}, \\ S_2 & \text{if } P_{10} > (\frac{\gamma_{20}}{\gamma_{21}} - 1)/\gamma_{10}. \end{cases} \tag{C.11}$$

For the first case of (C.11), namely $P_{10} < (\frac{\gamma_{20}}{\gamma_{21}} - 1)/\gamma_{10}$, the expression in (C.10) can be written as

$$\max_{\tilde{\mathbf{p}}} \quad a \min\{f(P_{U1}, P_{U2}), \log(1+\gamma_{10}P_{10}+\gamma_{20}P_{20})\} + b\,\log(1+\gamma_{10}P_{10}). \tag{C.12}$$

Since $f(P_{U1}, P_{U2}) \geqslant \log(1+\gamma_{10}P_{10}+\gamma_{20}P_{20})$, (C.12) can be written as

$$\max_{\tilde{\mathbf{p}}} \quad a\,\log(1+\gamma_{10}P_{10}+\gamma_{20}P_{20}) + b\,\log(1+\gamma_{10}P_{10}). \tag{C.13}$$

The region resulting from (C.13) is the same as the conventional multiple access region. In the second case of (C.11), namely $P_{10} > (\frac{\gamma_{20}}{\gamma_{21}} - 1)/\gamma_{10}$, the problem in

(C.10) can be written as

$$\max_{\tilde{\mathbf{P}}} \quad a \min\left\{f(P_{U1}, P_{U2}), \log\left(1+\gamma_{10}P_{10}\right) + \log\left(1+\gamma_{21}P_{21}^{*}\right)\right\} + b \log\left(1+\gamma_{10}P_{10}\right). \tag{C.14}$$

The region resulting from solving (C.14) is the same as the region resulting from the constraint set in (C.4).

Therefore, given the containment arguments that gave rise to (C.6) and (C.9), the regions resulting from the case in which $P_{20} < (\frac{\gamma_{10}}{\gamma_{12}} - 1)/\gamma_{20}$ is contained in the convex hull of the conventional multiple access region and the region resulting from the constraint set in (C.4). Using similar arguments, it can be shown that the region resulting from solving Step 2 with $P_{10} < (\frac{\gamma_{20}}{\gamma_{21}} - 1)/\gamma_{10}$ is contained in the convex hull of the conventional multiple access region and the region resulting from the constraint set in (C.3).

Appendix D

Achievable Rate Region for The Half-Duplex Cooperative Multiple Access Scheme

Any block of symbols from node 1 will be received at the destination two times (exactly the same codeword but with different powers) on two orthogonal channels. In the first time block it will be sent by node 1 and will be received with power $\gamma_{10}P_{12}$. In the second time block it will be sent by both node 1 and node 2 and the signals will add coherently at the destination to produce a power of $\left(\sqrt{\gamma_{10}(Q_1^{(1)} - P_{12})} + \sqrt{\gamma_{20}Q_2^{(1)}}\right)^2$. If we let x denote an individual symbol from the codeword $B_1(n)$, the corresponding received signal at node 2 on the first channel is

$$y_2 = \sqrt{\gamma_{12}P_{12}}\, x + z_2, \tag{D.1}$$

where z_2 denotes the additive noise. The received signals at the destination node on the two orthogonal channels are

$$\mathbf{y}_0 = \mathbf{A}x + \mathbf{z}_0 \tag{D.2}$$

where $\mathbf{z}_0$ denotes the additive noise. Expanding the terms in (D.2) we have

$$\begin{pmatrix} y_0^{(1)} \\ y_0^{(2)} \end{pmatrix} = \begin{pmatrix} \sqrt{\gamma_{10}P_{12}} \\ \sqrt{\gamma_{10}(Q_1^{(1)} - P_{12})} + \sqrt{\gamma_{20}Q_2^{(1)}} \end{pmatrix} x + \begin{pmatrix} z_0^{(1)} \\ z_0^{(2)} \end{pmatrix}. \tag{D.3}$$

It is clear from equation (D.1) that in order for node 2 to be able to reliably decode the message sent from node 1, the rate of the message should satisfy

$$R_1 \leqslant \frac{r}{2}\log\Big(1 + \frac{\gamma_{12}P_{12}}{r/2}\Big). \tag{D.4}$$

In order for the destination node to be able to reliably decode the message of node 1, the rate of the message should also satisfy that $R_1 \leqslant I(x;\mathbf{y}_0)$. Calculating $I(x;\mathbf{y}_0)$, it can be shown that (for Gaussian signalling)

$$\begin{aligned} R_1 &\leqslant I(x;\mathbf{y}_0) && \text{(D.5a)} \\ &= H(\mathbf{y}_0) - H(\mathbf{y}_0|x) && \text{(D.5b)} \\ &= \log\big((2\pi e)^2 \det\big(E(\mathbf{y}_0\mathbf{y}_0^H)\big)\big) - \log\big((2\pi e)^2 \det\big(E(\mathbf{z}_0\mathbf{z}_0^H)\big)\big) && \text{(D.5c)} \\ &= \frac{r}{2}\log\left(1 + \frac{\gamma_{10}P_{12} + \Big(\sqrt{\gamma_{10}(Q_1^{(1)} - P_{12})} + \sqrt{\gamma_{20}Q_2^{(1)}}\Big)^2}{r/2}\right). && \text{(D.5d)} \end{aligned}$$

Hence, the minimum of the constraints in (D.4) and (D.5d) represent the constraint on the rate of the messages sent from node 1. This constraint can now be written as

$$\begin{aligned} R_1 &\leqslant \bar{R}_1 \\ &= \frac{r}{2}\min\left\{\log\left(1 + \tfrac{\gamma_{12}P_{12}}{r/2}\right), \log\left(1 + \frac{\gamma_{10}P_{12} + \Big(\sqrt{\gamma_{10}(Q_1^{(1)} - P_{12})} + \sqrt{\gamma_{20}Q_2^{(1)}}\Big)^2}{r/2}\right)\right\}. \end{aligned} \tag{D.6}$$

Similarly, we can obtain an analogous constraint on the rate of the messages of Node 2;

$$\begin{aligned} R_2 &\leqslant \bar{R}_2 \\ &= \frac{(1-r)}{2}\min\left\{\log\left(1 + \tfrac{\gamma_{21}P_{21}}{(1-r)/2}\right), \log\left(1 + \frac{\gamma_{20}P_{21} + \Big(\sqrt{\gamma_{20}(Q_2^{(2)} - P_{21})} + \sqrt{\gamma_{10}Q_1^{(2)}}\Big)^2}{(1-r)/2}\right)\right\}. \end{aligned} \tag{D.7}$$

Appendix E

Derivation of (3.37)

For given values of r and $\bar{R}_2$ we must choose values for P_{21}, $Q_1^{(2)}$ and $Q_2^{(2)}$ such that (3.36b) is satisfied. For the first term on the right hand side of (3.36b) to be satisfied with minimum power we should choose $P_{21} = \frac{(1-r)}{2\gamma_{21}}(2^{\frac{2\bar{R}_2}{1-r}} - 1)$ and for the second term on the right hand side of (3.36b) to be satisfied $Q_1^{(2)}$ and $Q_2^{(2)}$ should satisfy the following inequality

$$\gamma_{20}^2\left(Q_2^{(2)}\right)^2 - 2A_0\gamma_{20}Q_2^{(2)} - 2\gamma_{10}\gamma_{20}Q_1^{(2)}Q_2^{(2)} + (4\gamma_{10}\gamma_{20}P_{21} - 2A_0\gamma_{10})Q_1^{(2)} + \gamma_{10}^2\left(Q_1^{(2)}\right)^2 + \gamma_0 \leqslant 0, \tag{E.1}$$

where $A_0 = \frac{(1-r)}{2}(2^{\frac{2\bar{R}_2}{1-r}} - 1)$. Using the relations between $(Q_1^{(1)}, Q_2^{(1)})$ and $(Q_1^{(2)}, Q_2^{(2)})$, (E.1) becomes

$$\gamma_{20}^2\left(Q_2^{(1)}\right)^2 - B_0Q_2^{(1)} - 2\gamma_{10}\gamma_{20}Q_1^{(1)}Q_2^{(1)} + C_0Q_1^{(1)} + \gamma_{10}^2\left(Q_1^{(1)}\right)^2 + D_0 \leqslant 0, \tag{E.2}$$

where

$$\begin{aligned} B_0 &= 2\gamma_{10}\gamma_{20}P_1 + 2A_0\gamma_{20} - 2\gamma_{20}^2P_2, \\ C_0 &= 2\gamma_{10}\gamma_{20}P_2 + 2A_0\gamma_{10} - 4\gamma_{10}\gamma_{20}P_{21} - 2\gamma_{10}^2P_1, \\ D_0 &= A_0^2 + \gamma_{20}^2P_2^2 + \gamma_{10}^2P_1^2 - 2\gamma_{10}\gamma_{20}P_1P_2 - 2A_0\gamma_{20}P_2 \end{aligned}$$

$$- 2A_0\gamma_{10}P_1 + 4\gamma_{10}\gamma_{20}P_{21}P_1. \tag{E.3}$$

Now, equation (3.36a) can be written as

$$\begin{aligned} R_1 &\leqslant \bar{R}_1 \\ &= \frac{r}{2}\min\left\{\log\left(1+\frac{\gamma_{12}P_{12}}{r/2}\right), \log\left(1+\frac{\gamma_{10}Q_1^{(1)}+\gamma_{20}Q_2^{(1)}+2\sqrt{\gamma_{10}\gamma_{20}}\sqrt{Q_2^{(1)}(Q_1^{(1)}-P_{12})}}{r/2}\right)\right\}. \end{aligned} \tag{E.4}$$

The problem of maximizing $\bar{R}_1$ can now be written as

$$\max_{P_{12},Q_1^{(1)},Q_2^{(1)}} \quad \min\left\{\bar{R}_{11},\bar{R}_{12}\right\} \tag{E.5a}$$

$$\begin{aligned} \text{subject to} \quad & \gamma_{20}^2\left(Q_2^{(1)}\right)^2 - B_0Q_2^{(1)} - 2\gamma_{10}\gamma_{20}Q_1^{(1)}Q_2^{(1)} \\ & + C_0Q_1^{(1)} + \gamma_{10}^2\left(Q_1^{(1)}\right)^2 + D_0 \leqslant 0, \end{aligned} \tag{E.5b}$$

$$0 \leqslant Q_1^{(1)} \leqslant \bar{P}_1, \tag{E.5c}$$

$$0 \leqslant Q_2^{(1)} \leqslant \bar{P}_2, \tag{E.5d}$$

where $\bar{R}_{11}$ and $\bar{R}_{12}$ are the first and second terms on the right hand side of (E.4), respectively. This problem can be shown to be concave in P_{12}, $Q_1^{(1)}$ and $Q_2^{(1)}$ as follows. First, R_{11} is concave in P_{12}. The function inside the logarithm in R_{12} has a negative semi-definite Hessian, namely

$$\begin{aligned} &\frac{\sqrt{\gamma_{10}\gamma_{20}}}{2\left(Q_2^{(1)}\right)^{3/2}\left(Q_1^{(1)}-P_{12}\right)^{3/2}}\times \\ &\begin{pmatrix} -\left(Q_2^{(1)}\right)^2 & Q_2^{(1)}(Q_1^{(1)}-P_{12}) & \left(Q_2^{(1)}\right)^2 \\ Q_2^{(1)}(Q_1^{(1)}-P_{12}) & -(Q_1^{(1)}-P_{12})^2 & -Q_2^{(1)}(Q_1^{(1)}-P_{12}) \\ \left(Q_2^{(1)}\right)^2 & -Q_2^{(1)}(Q_1^{(1)}-P_{12}) & -\left(Q_2^{(1)}\right)^2 \end{pmatrix} \preceq 0. \end{aligned} \tag{E.6}$$

Since the logarithm is concave non-decreasing function, then $\bar{R}_{12}$ is a concave function and since the minimum of two concave functions is a concave function then the

objective function is concave. The first constraint can be shown to be convex by evaluating the Hessian. The Hessian is

$$\begin{pmatrix} 2\gamma_{10}^2 & -2\gamma_{10}\gamma_{20} \\ -2\gamma_{10}\gamma_{20} & 2\gamma_{20}^2 \end{pmatrix} \succeq 0, \tag{E.7}$$

which is positive semi-definite and hence the constraint is convex. The last three constraints are linear constraints, and hence the problem in (E.5) is convex and a global maximum can be efficiently obtained. However, as we show in the next paragraph, the variable P_{12} can be determined analytically.

We can solve the right hand side of (E.4) to obtain the value of P_{12} that maximizes the minimum of both equations in terms of $Q_1^{(1)}$ and $Q_2^{(1)}$. Since the term inside the first logarithm in (E.4) is linearly increasing in P_{12} and the term inside the second logarithm in (E.4) is concave decreasing in P_{12}, the intersection of these two curves is the target point. This will results in $P_{12}^* = f_1(Q_1^{(1)}, Q_2^{(1)})$, where

$$f_1(Q_1^{(1)}, Q_2^{(1)}) = \frac{\frac{\sigma_0^2 K_{12}^2}{\sigma_2^2}(K_{10}^2 Q_1^{(1)} + K_{20}^2 Q_2^{(1)}) - 4K_{10}^2 K_{20}^2 Q_2^{(1)}}{(\frac{\sigma_0^2 K_{12}^2}{\sigma_2^2})^2}$$
$$+ \frac{2K_{10}K_{20}\sqrt{\frac{\sigma_0^2 K_{12}^2}{\sigma_2^2} - K_{10}^2}\sqrt{\frac{\sigma_0^2 K_{12}^2}{\sigma_2^2} Q_1^{(1)} Q_2^{(1)} - (K_{20} Q_2^{(1)})^2}}{(\frac{\sigma_0^2 K_{12}^2}{\sigma_2^2})^2}. \tag{E.8}$$

By substituting the expression for $f_1(Q_1^{(1)}, Q_2^{(1)})$ into (E.5) we obtain (3.37). By evaluating the Hessian, it can be verified that $f_1(Q_1^{(1)}, Q_2^{(1)})$ is a concave function of $Q_1^{(1)}$ and $Q_2^{(1)}$. In the case that $\gamma_{12} Q_1^{(1)} \leqslant \gamma_{10} Q_1^{(1)} + \gamma_{20} Q_2^{(1)}$ the derivation simplifies in that $R_{11} \leqslant R_{12}$ for all admissible $Q_1^{(1)}$ and $Q_2^{(1)}$. In that case, the optimal value of P_{12} is $Q_1^{(1)}$ and $f_1(Q_1^{(1)}, Q_2^{(1)}) = Q_1^{(1)}$.

In Section 3.5 and the proof above, the parameter r was a bandwidth sharing parameter. However, it is easy to envision an equivalent time sharing system. In this paragraph we point out some minor adjustments to the formulation that are required

in the time sharing case. In the case of time sharing the average power transmitted by node i is $P_i = rQ_i^{(1)} + (1-r)Q_i^{(2)}$. Therefore, the constraints in (3.37d) should be changed to $\min(P_{1,\text{peak}}, \frac{\bar{P}_1}{r}) \geqslant Q_1^{(1)} \geqslant \max(0, \frac{\bar{P}_1 - (1-r)P_{1,\text{peak}}}{r})$, where $P_{1,\text{peak}}$ is the value of the peak power for the transmitter of node 1. Constraining $Q_1^{(1)}$ to be less than $\frac{\bar{P}_1}{r}$ guarantees that $Q_1^{(2)} = \frac{\bar{P}_1 - rQ_1^{(1)}}{1-r}$ will not take negative values, while constraining $Q_1^{(1)}$ to be greater than $\frac{\bar{P}_1 - (1-r)P_{1,\text{peak}}}{r}$ guarantees that $Q_1^{(2)}$ will not exceed the value of peak power for the transmitter of node 1. Using similar arguments, the constraint in (3.37d) should be changed to $\min(P_{2,\text{peak}}, \frac{\bar{P}_2}{r}) \geqslant Q_2^{(1)} \geqslant \max(0, \frac{\bar{P}_2 - (1-r)P_{2,\text{peak}}}{r})$. Moreover the rate constraints can be written as

$$R_1 \leqslant \bar{R}_1 = \frac{r}{2} \min \left\{ \log\left(1 + \gamma_{12} P_{12}\right), \log\left(1 + \gamma_{10} P_{12} + \left(\sqrt{\gamma_{10}(Q_1^{(1)} - P_{12})} + \sqrt{\gamma_{20} Q_2^{(1)}} \right)^2 \right) \right\}, \tag{E.9a}$$

$$R_2 \leqslant \bar{R}_2 = \frac{(1-r)}{2} \min \left\{ \log\left(1 + \gamma_{21} P_{21}\right), \log\left(1 + \gamma_{20} P_{21} + \left(\sqrt{\gamma_{20}(Q_2^{(2)} - P_{21})} + \sqrt{\gamma_{10} Q_1^{(2)}} \right)^2 \right) \right\}, \tag{E.9b}$$

where the rates $\bar{R}_1$ and $\bar{R}_2$ are both concave functions of the power components.

Appendix F

Proof of quasi-concavity of R_1 in r

Using the substitution $Q_1^{(2)} = \bar{P}_1 - Q_1^{(1)}$ and $Q_2^{(2)} = \bar{P}_2 - Q_2^{(1)}$, the second term on the right hand side of (3.36b) can be written as a function of P_{21}, $Q_1^{(1)}$ and $Q_2^{(1)}$. For given values of $Q_1^{(1)}$ and $Q_2^{(1)}$ we can solve the right hand side of (3.36a) to find the value of P_{12} that maximizes the minimum of the two equations in terms of $Q_1^{(1)}$ and $Q_2^{(1)}$. (A similar analysis led to (E.8).) Similarly we can solve the right hand side of (3.36b) for P_{21}. Hence, the constraints on R_1 and R_2 reduce to

$$R_1 \leqslant \bar{R}_1 = \frac{r}{2} \log \left(1 + \frac{f_1(Q_1^{(1)}, Q_2^{(1)})}{r/2} \right), \tag{F.1a}$$

$$R_2 \leqslant \bar{R}_2 = \frac{(1-r)}{2} \log \left(1 + \frac{f_2(Q_1^{(1)}, Q_2^{(1)})}{(1-r)/2} \right), \tag{F.1b}$$

where $f_1(Q_1^{(1)}, Q_2^{(1)})$ was defined in (E.8) and $f_2(Q_1^{(1)}, Q_2^{(1)})$ has a similar form. It can be shown that $f_1(Q_1^{(1)}, Q_2^{(1)})$ and $f_2(Q_1^{(1)}, Q_2^{(1)})$ are concave functions of $Q_1^{(1)}$ and $Q_2^{(1)}$ by evaluating the Hessian.

We will now show for a given target value of $\bar{R}_2$, $\bar{R}_1$ is quasi-concave in r by proving that the set of values of r such that $\bar{R}_1$ is greater than certain level $R_{1,\text{test}}$ is a convex set. For a given value of $\bar{R}_2$, say $R_{2,\text{tar}}$, if a value of r, say r_0, is to be

such that there exist transmission powers that provide a rate $\bar{R}_1$ that is greater than $R_{1,\text{test}}$, these powers must satisfy

$$f_1(Q_1^{(1)}, Q_2^{(1)}) \geqslant g_1(r), \tag{F.2a}$$

$$f_2(Q_1^{(1)}, Q_2^{(1)}) \geqslant g_2(r), \tag{F.2b}$$

for $r = r_0$, where $g_1(r) = \frac{r}{2}(2^{\frac{2R_{1,\text{test}}}{r}} - 1)$ and $g_2(r) = \frac{(1-r)}{2}(2^{\frac{2R_{2,\text{tar}}}{1-r}} - 1)$. The functions $g_1(r)$ and $g_2(r)$ can be shown to be convex functions in r for $r \in (0,1)$. Now, assume that there exist transmission powers $Q_1^{(1)} = X^{(1)}$ and $Q_2^{(1)} = Y^{(1)}$ such that (F.2) holds for $r = r_1$, and powers $Q_1^{(1)} = X^{(2)}$ and $Q_2^{(1)} = Y^{(2)}$ such that (F.2) holds for $r = r_2$. To complete the proof we need to show that for any $r_3 = \lambda r_1 + (1-\lambda) r_2$ with $\lambda \in [0,1]$ there exist transmission powers $Q_1^{(1)} = X^{(3)}$ and $Q_2^{(1)} = Y^{(3)}$ such that (F.2) holds for r_3.

Consider the powers $X^{(3)} = \lambda X^{(1)} + (1-\lambda) X^{(2)}$ and $Y^{(3)} = \lambda Y^{(1)} + (1-\lambda) Y^{(2)}$. For these powers,

$$f_1(X^{(3)}, Y^{(3)}) \geqslant \lambda f_1(X^{(1)}, Y^{(1)}) + (1-\lambda) f_1(X^{(2)}, Y^{(2)}) \tag{F.3a}$$

$$\geqslant \lambda g_1(r_1) + (1-\lambda) g_1(r_2) \tag{F.3b}$$

$$\geqslant g_1(r_3), \tag{F.3c}$$

where (F.3a) follows from concavity of $f_1(Q_1^{(1)}, Q_2^{(1)})$, (F.3b) follows from (F.2), and (F.3c) follows from the convexity of $g_1(r)$. A similar analysis shows that $f_2(X^{(3)}, Y^{(3)}) \geqslant g_2(r_3)$. That is, given $r_3 \in [r_1, r_2]$, we have constructed powers $X^{(3)}$ and $Y^{(3)}$ such that (F.2) holds for $r = r_3$. Therefore, the set of values of r for which $\bar{R}_1$ for a given $\bar{R}_2$ is greater than $R_{1,\text{test}}$ is convex, and hence $\bar{R}_1$ for a given $\bar{R}_2$ is a quasi-concave function in r.

Appendix G

Solving the weighted sum problem using the target rate approach

First we start by proving that if the achievable rates are convex functions of the power components for a given channel resource allocation parameter r, then the achievable rate regions achieved via jointly optimal power and channel resource allocation are convex. In order to prove that, we will prove that the rate achievable via time sharing between any two points that employ two different values for the resource allocation parameter r; say r_1 and r_2, can be achieved using a distinct value of r; say r_3.

In systems in which users transmit orthogonally in time, the achievable rates of the two source nodes can be represented as $\bar{R}_1 = r f_1(\mathcal{P})$ and $\bar{R}_2 = \hat{r} f_2(\mathcal{P})$, where $\mathcal{P}$ is a vector that contains the power components. The functions f_1 and f_2 have been shown to be concave in the power components for the orthogonal systems considered in Chapters 3 and 5. Now, consider the rate achievable via time sharing between two points using $(r_1, \mathcal{P}_1)$ and $(r_2, \mathcal{P}_2)$ with ratios α and $1-\alpha$, respectively. In that case the achievable rates can be written as:

$$R_1 = \alpha r_1 f_1(\mathcal{P}_1) + (1-\alpha) r_2 f_1(\mathcal{P}_2), \tag{G.1a}$$

$$R_2 = \alpha\hat{r}_1 f_2(\mathcal{P}_1) + (1-\alpha)\hat{r}_2 f_2(\mathcal{P}_2), \tag{G.1b}$$

where each of $(r_1, \mathcal{P}_1)$ and $(r_2, \mathcal{P}_2)$ satisfy the average power constraints. These power constraints can be written as $\mathbf{G}_1\mathcal{P}_1 \leqslant \bar{\mathcal{P}}$ and $\mathbf{G}_2\mathcal{P}_2 \leqslant \bar{\mathcal{P}}$,[1] where $\mathbf{G}_i$ is a matrix that adds the appropriate power components of the vector $\mathcal{P}_i$ with the appropriate ratios, and whose entries depend on r_i, and $\bar{\mathcal{P}}$ is a vector of the maximum average power for each user. Now, time sharing between $(r_1, \mathcal{P}_1)$ and $(r_2, \mathcal{P}_2)$ with ratios α and $1-\alpha$ is equivalent to allocating for the transmission of the message of user 1 a fraction of the time $r_3 = \alpha r_1 + (1-\alpha)r_2$ and an average power $\frac{\alpha r_1\mathcal{P}_1 + (1-\alpha)r_2\mathcal{P}_2}{r_3}$ and allocating for the transmission of the message of user 2 a fraction of the time $\hat{r}_3 = \alpha\hat{r}_1 + (1-\alpha)\hat{r}_2$ with an average power $\frac{\alpha\hat{r}_1\mathcal{P}_1 + (1-\alpha)\hat{r}_2\mathcal{P}_2}{\hat{r}_3}$. Now, we examine the rate achievable using r_3 and the average power for user 1

$$\begin{aligned} R_1(r_3) &= r_3 f_1\left(\frac{\alpha r_1\mathcal{P}_1 + (1-\alpha)r_2\mathcal{P}_2}{r_3}\right) && \text{(G.2a)} \\ &\geqslant r_3\left(\frac{\alpha r_1}{r_3} f_1(\mathcal{P}_1) + \frac{(1-\alpha)r_2}{r_3} f_1(\mathcal{P}_2)\right) && \text{(G.2b)} \\ &= \alpha r_1 f_1(\mathcal{P}_1) + (1-\alpha)r_2 f_1(\mathcal{P}_2), && \text{(G.2c)} \end{aligned}$$

The result in (G.2c) indicates that the rate achievable via time sharing can be achieved using a distinct value of r. A similar proof for $R_2(r_3)$ can be obtained using analogous steps. Therefore, the region obtained via jointly optimal power and channel resource allocation is convex. Since this achievable rate region represents the hypograph for the function $\bar{R}_1(\bar{R}_2)$, then this function is concave in $\bar{R}_2$ [5].

Next, we show that the weighted sum maximization problem is a convex problem. The weighted sum maximization problem can be written as:

$$\max \quad \mu_1\bar{R}_1 + \mu_2\bar{R}_2, \tag{G.3}$$

[1] These vector inequalities are element-wise inequalities.

and since $\bar{R}_1$ is a concave function of $\bar{R}_2$, the problem in (G.3) is a convex problem in $\bar{R}_2$. Therefore, it can be solved using efficient algorithms. One simple algorithm to solve this problem is to use the bisection search over $\bar{R}_2$, and in each step of the algorithm, the value of $\bar{R}_1(\bar{R}_2)$ is calculated using the target rate approach.

Appendix H

Concavity of the power allocation problem

The concavity of $h(x,y) = \sqrt{\frac{ax}{r} + \frac{bcxy}{r(r+bx+cy)}}$ in x and y for positive a, b, c, r and $x, y \geqslant 0$ can be shown by establishing the negative semi-definiteness of the Hessian of $h(x,y)$.

$$\nabla^2 h(x,y) = \begin{pmatrix} h_{xx} & h_{xy} \\ h_{yx} & h_{yy} \end{pmatrix}, \tag{H.1}$$

where $h_{wz} = \frac{\partial^2 f}{\partial w \partial z}$, for $w, z \in \{x, y\}$. It can be shown that

$$\begin{aligned} h_{xx} = -1/4\Big(&4a^2r^3bx + 4a^2r^3cy + 6a^2r^2b^2x^2 + 6a^2r^2c^2y^2 + 4a^2rb^3x^3 + a^2r^4 \\ &+ a^2b^4x^4 + a^2c^4y^4 + b^2c^4y^4 + 12a^2r^2bcxy + 2ar^3bcy + 6ar^2bc^2y^2 \\ &+ 12a^2rb^2x^2cy + 12a^2rbxc^2y^2 + 8ar^2b^2xcy + 16arb^2xc^2y^2 + 4a^2rc^3y^3 \\ &+ 2ac^4y^4b + b^2c^2y^2r^2 + 2b^2c^3y^3r + 6arc^3y^3b + 4a^2b^3x^3cy + 6a^2b^2x^2c^2y^2 \\ &+ 6ab^3x^2cyr + 6ab^3x^2c^2y^2 + 4a^2bc^3xy^3 + 8ab^2c^3xy^3 + 4xb^3c^3y^3 + 4xb^3rc^2y^2\Big) \end{aligned}$$

$$\times \left(x(ar + abx + acy + bcy)r(r + bx + cy)^3 \sqrt{\frac{x(ar + abx + acy + bcy)}{r(r + bx + cy)}} \right)^{-1}, \tag{H.2}$$

$$h_{yy} = -1/4 \frac{(b^2x + 4abx + 4bcy + br + 4acy + 4ar)(r + bx)xc^2b}{(ar + abx + acy + bcy)r(r + bx + cy)^3 \sqrt{\frac{x(ar+abx+acy+bcy)}{r(r+bx+cy)}}}, \tag{H.3}$$

and hence that

$$\det(\nabla^2 h(x, y)) = 1/4 \frac{(ab^2x^2 + abcxy + 2arbx + arcy + ar^2 + b^2rx + b^2xcy + bcyr)c^2b}{x(ar + abx + acy + bcy)r(r + bx + cy)^3}. \tag{H.4}$$

For positive values of the parameters (a, b, c, r) and non-negative x and y, the diagonal elements of (H.1) are negative and the determinant of $\nabla^2 h(x, y)$ is positive. Therefore, $\nabla^2 h(x, y)$ is negative semi-definite, which establishes the concavity of $h(x, y)$.

Appendix I

At least one of $\tilde{P}_{12}$ and $\tilde{P}_{21}$ will be zero at optimality

Since all the partial derivatives will be evaluated at the optimal point $(\tilde{P}_{11}^*, \tilde{P}_{21}^*)$, for simplicity, we will use $\frac{\partial f_i}{\partial \tilde{P}_{ij}}$ to refer to $\frac{\partial f_i(\tilde{P}_{11}^*, \tilde{P}_{21}^*)}{\partial \tilde{P}_{ij}}$. We are interested in the case in which both nodes have information to transmit, and hence $\tilde{P}_{11}^* > 0$, and $\tilde{P}_{21}^* < 2\bar{P}_2$. In that case it can be (analytically) shown that $\frac{\partial f_0}{\partial \tilde{P}_{i1}} < 0$, and that $\frac{\partial f_1}{\partial \tilde{P}_{i1}} > 0$.

Let us first consider the case in which $\lambda_4^* = 0$. From (4.12c) we have that $\frac{\partial f_0}{\partial \tilde{P}_{11}} + \lambda_1^* \frac{\partial f_1}{\partial \tilde{P}_{11}} \geqslant 0$, and hence $\lambda_1^* \geqslant -\frac{\partial f_0}{\partial \tilde{P}_{11}} / \frac{\partial f_1}{\partial \tilde{P}_{11}}$. Therefore,

$$\frac{\partial f_0}{\partial \tilde{P}_{21}} + \lambda_1^* \frac{\partial f_1}{\partial \tilde{P}_{21}} \geqslant \left(\frac{\partial f_0}{\partial \tilde{P}_{21}} \frac{\partial f_1}{\partial \tilde{P}_{11}} - \frac{\partial f_0}{\partial \tilde{P}_{11}} \frac{\partial f_1}{\partial \tilde{P}_{21}} \right) / \frac{\partial f_1}{\partial \tilde{P}_{11}}. \tag{I.1}$$

It can be shown that

$$\begin{aligned}
\frac{\partial f_0}{\partial \tilde{P}_{21}} \frac{\partial f_1}{\partial \tilde{P}_{11}} &= -\gamma_{10}\gamma_{20}\gamma_{12}\gamma_{21}\tilde{P}_{11}^*(r + \gamma_{12}\tilde{P}_{11}^*)(2\bar{P}_2 - \tilde{P}_{21}^*)(\hat{r} + 2\gamma_{21}\bar{P}_2 - \gamma_{21}\tilde{P}_{21}^*)/A \\
&= -\gamma_{10}\gamma_{20}\gamma_{12}\gamma_{21}\tilde{P}_{11}^*(2\bar{P}_2 r\hat{r} + 4\gamma_{21}\bar{P}_2^2 r - 4\gamma_{21}\bar{P}_2 r\tilde{P}_{21}^* - r\hat{r}\tilde{P}_{21}^* + \gamma_{21}r\tilde{P}_{21}^{*2} \\
&\quad + 2\gamma_{12}\hat{r}\tilde{P}_{11}^*\bar{P}_2 + 4\gamma_{21}\gamma_{12}\tilde{P}_{11}^*\bar{P}_2^2 - \hat{r}\gamma_{12}\tilde{P}_{11}^*\tilde{P}_{21}^* - 4\gamma_{21}\gamma_{12}\tilde{P}_{11}^*\tilde{P}_{21}^*\bar{P}_2 \\
&\quad + \gamma_{21}\gamma_{12}\tilde{P}_{11}^*\tilde{P}_{21}^{*2})/A,
\end{aligned}$$

where

$$\begin{aligned} A &= 4r\hat{r}(\hat{r}+\gamma_{21}(2\bar{P}_2-\tilde{P}_{21}^*)+\gamma_{10}(2\bar{P}_1-\tilde{P}_{11}^*))^2(r+\gamma_{20}\tilde{P}_{21}^*+\gamma_{12}\tilde{P}_{11}^*)^2 \\ &\quad\times\sqrt{\frac{\gamma_{10}\tilde{P}_{11}^*}{r}+\frac{\gamma_{20}\gamma_{12}\tilde{P}_{11}^*\tilde{P}_{21}^*}{r(r+\gamma_{20}\tilde{P}_{21}^*+\gamma_{12}\tilde{P}_{11}^*)}} \\ &\quad\times\sqrt{\frac{\gamma_{20}(2\bar{P}_2-\tilde{P}_{21}^*)}{\hat{r}}+\frac{\gamma_{10}\gamma_{21}(2\bar{P}_1-\tilde{P}_{11}^*)(2\bar{P}_2-\tilde{P}_{21}^*)}{\hat{r}(\hat{r}+\gamma_{21}(2\bar{P}_2-\tilde{P}_{21}^*)+\gamma_{10}(2\bar{P}_1-\tilde{P}_{11}^*))}}. \end{aligned}$$

It can also be shown that

$$\begin{aligned} -\frac{\partial f_0}{\partial\tilde{P}_{11}}\frac{\partial f_1}{\partial\tilde{P}_{21}} &= A^{-1}\left[\gamma_{10}(\underbrace{r+\gamma_{12}\tilde{P}_{11}^*}+\gamma_{20}\tilde{P}_{21}^*)^2+\gamma_{20}\gamma_{12}\tilde{P}_{21}^*(r+\gamma_{20}\tilde{P}_{21}^*)\right] \\ &\quad\times\Big[\gamma_{20}(\underbrace{\hat{r}+\gamma_{21}(2\bar{P}_2-\tilde{P}_{21}^*)}+\gamma_{10}(2\bar{P}_1-\tilde{P}_{11}^*))^2 \\ &\qquad+(\hat{r}+\gamma_{10}(2\bar{P}_1-\tilde{P}_{11}^*))(2\bar{P}_2-\tilde{P}_{21}^*)\gamma_{10}\gamma_{21}\Big] \\ &\geqslant_a \gamma_{10}\gamma_{20}(r+\gamma_{12}\tilde{P}_{11}^*)^2(\hat{r}+\gamma_{21}(2\bar{P}_2-\tilde{P}_{21}^*))^2/A \\ &= \gamma_{10}\gamma_{20}\gamma_{12}\gamma_{21}\tilde{P}_{11}^* \\ &\quad\times(8\bar{P}_2r\hat{r}+8\gamma_{21}\bar{P}_2^2r-8\gamma_{21}\bar{P}_2r\tilde{P}_{21}^*-4r\hat{r}\tilde{P}_{21}^*+2\gamma_{21}r\tilde{P}_{21}^{*2}+4\gamma_{12}\hat{r}\tilde{P}_{11}^*\bar{P}_2 \\ &\qquad+4\gamma_{12}\hat{r}\tilde{P}_{11}^*\bar{P}_2+4\gamma_{21}\gamma_{12}\tilde{P}_{11}^*\bar{P}_2^2-2\hat{r}\gamma_{12}\tilde{P}_{11}^*\tilde{P}_{21}^*-4\gamma_{21}\gamma_{12}\tilde{P}_{11}^*\tilde{P}_{21}^*\bar{P}_2 \\ &\qquad+\gamma_{21}\gamma_{12}\tilde{P}_{11}^*\tilde{P}_{21}^{*2})/A, \end{aligned}$$

where the right hand side of inequality a is obtained by retaining only the underbraced parts of the previous equation and ignoring the remaining terms, which are non-negative by construction. For the case of interest here, where both users have their own information to send, inequality a will be a strict inequality and hence we can write

$$\frac{\partial f_0}{\partial\tilde{P}_{21}}\frac{\partial f_1}{\partial\tilde{P}_{11}}-\frac{\partial f_0}{\partial\tilde{P}_{11}}\frac{\partial f_1}{\partial\tilde{P}_{21}} > 3r\hat{r}\tilde{P}_{11}^*(2\bar{P}_2-\tilde{P}_{21}^*)+\gamma_{12}\hat{r}\tilde{P}_{11}^{*2}(2\bar{P}_2-\tilde{P}_{21}^*)+\gamma_{21}r\tilde{P}_{11}^*(2\bar{P}_2-\tilde{P}_{21}^*)^2, \tag{I.2}$$

where the right hand side is positive because $\tilde{P}_{21}^*$ is required to satisfy the power

constraint $\tilde{P}_{21}^{*} \leqslant 2\bar{P}_2$. Using (I.1), and the positivity of (I.2) and $\frac{\partial f_1}{\partial \tilde{P}_{11}}$, we have that

$$\frac{\partial f_0}{\partial \tilde{P}_{21}} + \lambda_1^* \frac{\partial f_1}{\partial \tilde{P}_{21}} > 0. \tag{I.3}$$

Given (I.3) and (4.12b), in order for (4.12c) to be satisfied with $\lambda_4^* = 0$ we must have $\lambda_3^* > 0$. Using (4.12d), this implies that $\tilde{P}_{21} = 0$.

Using a similar strategy, we can show that if $\lambda_3^* = 0$, then

$$\frac{\partial f_0}{\partial \tilde{P}_{11}} + \lambda_1^* \frac{\partial f_1}{\partial \tilde{P}_{11}} < 0. \tag{I.4}$$

Given (I.4) and (4.12b), in order for (4.12c) to be satisfied with $\lambda_3^* = 0$ we must have $\lambda_4^* > 0$. Using (4.12d), this implies that $\tilde{P}_{11} = 2\bar{P}_1$ and hence that $\tilde{P}_{12} = 0$. Therefore, at optimality at least one of $\tilde{P}_{12}$ and $\tilde{P}_{21}$ equals zero.

Appendix J

Proof of $\bar{R}_2(\mathcal{P}', r) > \bar{R}_2(\mathcal{P}, r)$

The bounding argument below is based on the fact that for any non-negative and finite a, b, c and r

$$\frac{ab}{r+a+b} \leqslant a \qquad \text{and} \qquad \frac{\partial}{\partial a}\left(\frac{ab}{r+a+b}\right) \geqslant 0, \tag{J.1}$$

and that for $r > 0$

$$\frac{ab}{r+b+c} < a. \tag{J.2}$$

Now

$$\begin{aligned}
\bar{R}_2(\mathcal{P}', r) &= \frac{\hat{r}}{2}\log\left(1 + \frac{\gamma_{20}\tilde{P}'_{22}}{\hat{r}} + \frac{\gamma_{10}\gamma_{21}\tilde{P}'_{12}\tilde{P}'_{22}}{\hat{r}(\hat{r} + \gamma_{21}\tilde{P}'_{22} + \gamma_{10}(\tilde{P}_{12} - \tilde{\Delta}_1))}\right) \\
&= \frac{\hat{r}}{2}\log\left(1 + \frac{\gamma_{20}(\tilde{P}_{22} + \tilde{P}_{21})}{\hat{r}} + \frac{\gamma_{10}\gamma_{21}(\tilde{P}_{12} - \tilde{\Delta}_1)\tilde{P}'_{22}}{\hat{r}(\hat{r} + \gamma_{21}\tilde{P}'_{22} + \gamma_{10}(\tilde{P}_{12} - \tilde{\Delta}_1))}\right) \\
&= \frac{\hat{r}}{2}\log\Bigg(1 + \frac{\gamma_{20}\tilde{P}_{22}}{\hat{r}} + \frac{\gamma_{20}\tilde{P}_{21}}{\hat{r}} + \frac{\gamma_{10}\gamma_{21}\tilde{P}_{12}\tilde{P}'_{22}}{\hat{r}(\hat{r} + \gamma_{21}\tilde{P}'_{22} + \gamma_{10}(\tilde{P}_{12} - \tilde{\Delta}_1))} \\
&\qquad - \frac{\gamma_{10}\gamma_{21}\tilde{\Delta}_1\tilde{P}'_{22}}{\hat{r}(\hat{r} + \gamma_{21}\tilde{P}'_{22} + \gamma_{10}(\tilde{P}_{12} - \tilde{\Delta}_1))}\Bigg) \\
&>_a \frac{\hat{r}}{2}\log\left(1 + \frac{\gamma_{20}\tilde{P}_{22}}{\hat{r}} + \frac{\gamma_{20}\tilde{P}_{21}}{\hat{r}} + \frac{\gamma_{10}\gamma_{21}\tilde{P}_{12}\tilde{P}'_{22}}{\hat{r}(\hat{r} + \gamma_{21}\tilde{P}'_{22} + \gamma_{10}(\tilde{P}_{12} - \tilde{\Delta}_1))} - \frac{\gamma_{10}\tilde{\Delta}_1}{\hat{r}}\right) \\
&>_b \frac{\hat{r}}{2}\log\left(1 + \frac{\gamma_{20}\tilde{P}_{22}}{\hat{r}} + \frac{\gamma_{20}\tilde{P}_{21}}{\hat{r}} + \frac{\gamma_{10}\gamma_{21}\tilde{P}_{12}\tilde{P}'_{22}}{\hat{r}(\hat{r} + \gamma_{21}\tilde{P}'_{22} + \gamma_{10}(\tilde{P}_{12} - \tilde{\Delta}_1))} - \frac{\gamma_{20}\tilde{P}_{21}}{\hat{r}}\right)
\end{aligned}$$

$$
\begin{aligned}
&= \frac{\hat{r}}{2}\log\left(1+\frac{\gamma_{20}\tilde{P}_{22}}{\hat{r}}+\frac{\gamma_{10}\gamma_{21}\tilde{P}_{12}\tilde{P}'_{22}}{\hat{r}(\hat{r}+\gamma_{21}\tilde{P}'_{22}+\gamma_{10}(\tilde{P}_{12}-\tilde{\Delta}_1))}\right)\\
&>_c \frac{\hat{r}}{2}\log\left(1+\frac{\gamma_{20}\tilde{P}_{22}}{\hat{r}}+\frac{\gamma_{10}\gamma_{21}\tilde{P}_{12}\tilde{P}_{22}}{\hat{r}(\hat{r}+\gamma_{21}\tilde{P}_{22}+\gamma_{10}(\tilde{P}_{12}-\tilde{\Delta}_1))}\right)\\
&> \frac{\hat{r}}{2}\log\left(1+\frac{\gamma_{20}\tilde{P}_{22}}{\hat{r}}+\frac{\gamma_{10}\gamma_{21}\tilde{P}_{12}\tilde{P}_{22}}{\hat{r}(\hat{r}+\gamma_{21}\tilde{P}_{22}+\gamma_{10}\tilde{P}_{12})}\right)\\
&> \bar{R}_2(\mathcal{P},r),
\end{aligned}
$$

where inequality a is a consequence of (J.2) (assuming $\hat{r} > 0$), inequality b is obtained by applying the first inequality in (J.1) to (4.14), which yields $\gamma_{10}\tilde{\Delta}_1 \leqslant \gamma_{20}\tilde{P}_{21}$, and inequality c comes from the second inequality in (J.1).

Appendix K

Quasi-Concavity of the Resource Allocation Problem

Consider $r_1, r_2 \in \mathcal{S}_\beta$. Let x_1 and x_2 denote the maximizing values of $\tilde{P}_{21}$ corresponding to those values of r, respectively. Then the following pair of equations hold for $(r = r_1, \tilde{P}_{21} = x_1)$ and for $(r = r_2, \tilde{P}_{21} = x_2)$,

$$\frac{r}{2}\log\left(1 + \frac{2\gamma_{10}\bar{P}_1}{r} + \frac{2\gamma_{20}\gamma_{12}\bar{P}_1\tilde{P}_{21}}{r(r + \gamma_{20}\tilde{P}_{21} + 2\gamma_{12}\bar{P}_1)}\right) \geqslant R_{1,\text{test}}, \tag{K.1a}$$

$$\frac{\hat{r}}{2}\log\left(1 + \frac{\gamma_{20}}{\hat{r}}(2\bar{P}_2 - \tilde{P}_{21})\right) \geqslant R_{2,\text{tar}}. \tag{K.1b}$$

The inequalities in (K.1) can be rewritten as

$$f_1(r_1, x_1) \geqslant g_1(r_1), \qquad f_1(r_2, x_2) \geqslant g_1(r_2), \tag{K.2a}$$

$$f_2(r_1, x_1) \geqslant g_2(r_1), \qquad f_2(r_2, x_2) \geqslant g_2(r_2), \tag{K.2b}$$

where

$$f_1(r, x) = \sqrt{r^2 + 2\gamma_{10}\bar{P}_1 r + \frac{2\gamma_{20}\gamma_{12}\bar{P}_1 x r}{(r + \gamma_{20}x + 2\gamma_{12}\bar{P}_1)}}, \qquad g_1(r) = \sqrt{r^2 2^{\frac{2R_{1,\text{test}}}{r}}},$$

$$f_2(r, x) = \gamma_{20}(2\bar{P}_2 - x), \qquad g_2(r) = \hat{r}(2^{\frac{2R_{2,\text{tar}}}{\hat{r}}} - 1).$$

Examining the convexity properties of these functions, it can be seen that the function $f_2(r,x)$ is a linear function. That is $f_2(r,x)$ is concave in x and r. The second Differentiation of $g_1(r)$ with respect to r results in

$$\frac{d^2 g_1(r)}{dr^2} = \frac{2^{\frac{R_{1,\text{test}}}{r}} R_{1,\text{test}}^2 \ln(2)^2}{r^3} \geqslant 0. \tag{K.3}$$

Therefore, $g_1(r)$ is a convex function in r. With regard to the function $g_2(r)$, it can directly be shown to be convex decreasing in $\hat{r}$ by differentiating it with respect to $\hat{r}$. The first differentiation results in

$$\frac{dg_2(r)}{d\hat{r}} = \exp(2R_{2,\text{tar}} \ln(2)/\hat{r}) - 1 - \frac{2R_{2,\text{tar}} \ln(2)}{\hat{r}} \exp(2R_{2,\text{tar}} \ln(2)/\hat{r}). \tag{K.4}$$

Let $a = 2R_{2,\text{tar}} \ln(2)/\hat{r}$, then we have

$$\begin{aligned} \frac{dg_2(r)}{d\hat{r}} &= (1-a)\exp(a) - 1 && \text{(K.5a)} \\ &= (1-a)(1 + a + \frac{a^2}{2!} + \frac{a^3}{3!} + ..) - 1 && \text{(K.5b)} \\ &= \sum_{n=2}^{\infty} \frac{a^n}{(n-1)!}(\frac{1}{n} - 1) < 0. && \text{(K.5c)} \end{aligned}$$

The second differentiation with respect to $\hat{r}$ results in

$$\frac{d^2 g_2(r)}{d\hat{r}^2} = \frac{4R_{2,\text{tar}}^2 \ln(2)^2 2^{\frac{2R_{2,\text{tar}}}{\hat{r}}}}{\hat{r}^3} \geqslant 0. \tag{K.6}$$

Therefore, from (K.5c) and (K.6) we have that $g_2(r)$ is convex decreasing in $\hat{r}$. Furthermore, by obtaining an analytic expression for the Hessian of $f_1(r,x)$, it can be shown that the condition $2\gamma_{10}\bar{P}_1 \geqslant 1$ is sufficient for the Hessian to be negative semi-definite, and hence is sufficient for $f_1(r,x)$ to be concave in r and x.

Let $r_3 = \theta r_1 + (1-\theta) r_2$, for some $\theta \in [0,1]$, and let $x_3 = \theta x_1 + (1-\theta) x_2$. Then we have

$$f_1(r_3, x_3) \geqslant_a \theta f_1(r_1, x_1) + (1-\theta) f_1(r_2, x_2)$$

$$\geqslant \theta g_1(r_1) + (1-\theta) g_1(r_2) \geqslant_b g_1(r_3), \tag{K.7}$$

where inequality a follows from the concavity of $f_1(r, x)$ and inequality b follows from the convexity of $g_1(r)$. Similarly, we can show that

$$f_2(r_3, x_3) \geqslant g_2(r_3). \tag{K.8}$$

Hence, for any two values of r (namely, r_1 and r_2), if there exist values of x (namely, x_1 and x_2), such that the conditions in (K.1) are satisfied, then for any value of r that lies between r_1 and r_2 (namely, r_3), there exists a value for x that lies between x_1 and x_2 (namely, x_3), such that the conditions in (K.1) are satisfied. Therefore, $\mathcal{S}_\beta$ is a convex set, and hence the objective in (4.16) is quasi-concave in r. Following similar steps, it can be shown that the objective in (4.17) is quasi-concave in r if $2\gamma_{20}\bar{P}_2 \geqslant 1$.

Appendix L

Intersection of the Sets of r that Result from (4.16) and (4.17)

Here we will show that if $R_{1,\text{test}}$ is such that both $\mathcal{S}_\beta$ and $\mathcal{S}_\alpha$ are non-empty, then these two sets intersect. In doing so, we will show that if both sets are non-empty, then there exists a value of r, denoted r_3, such that a rate of at least $R_{1,\text{test}}$ can be achieved for Node 1 (and the target rate for Node 2 satisfied) using only direct transmission. Since direct transmission is a feasible solution for both (4.16) and (4.17), r_3 lies in both $\mathcal{S}_\beta$ and $\mathcal{S}_\alpha$, and hence these sets intersect.

Using the closed-form solution in (4.20) we have that

$$\beta(r) = \frac{r}{2}\log\left(1+\frac{2\bar{P}_1\gamma_{10}}{r}+\frac{2\bar{P}_1\gamma_{12}(2\bar{P}_2\gamma_{20}-\hat{r}(2^{\frac{2R_{2,\text{tar}}}{\hat{r}}}-1))}{r(r+(2\bar{P}_2\gamma_{20}-\hat{r}(2^{\frac{2R_{2,\text{tar}}}{\hat{r}}}-1))+2\bar{P}_1\gamma_{12})}\right) \quad \text{(L.1a)}$$

$$\alpha(r) = \frac{r}{2}\log\left(1+\frac{2\bar{P}_1\gamma_{10}}{r}-\frac{[2\bar{P}_2\gamma_{21}+\hat{r}][\hat{r}(2^{\frac{2R_{2,\text{tar}}}{\hat{r}}}-1)-2\bar{P}_2\gamma_{20}]}{r(2\bar{P}_2\gamma_{21}-[\hat{r}(2^{\frac{2R_{2,\text{tar}}}{\hat{r}}}-1)-2\bar{P}_2\gamma_{20}])}\right). \quad \text{(L.1b)}$$

Let $r_\beta \in \mathcal{S}_\beta$ and $r_\alpha \in \mathcal{S}_\alpha$. Since the constraints in (4.16b) and (4.17b) hold with equality at optimality, and since the power constraint must be satisfied, we have that

$$\hat{r}_\beta(2^{\frac{2R_{2,\text{tar}}}{\hat{r}_\beta}}-1) \leqslant 2\gamma_{20}\bar{P}_2, \quad \text{(L.2)}$$

and that

$$2\gamma_{20}\bar{P}_2 \leqslant \hat{r}_\alpha(2^{\frac{2R_{2,\text{tar}}}{\hat{r}_\alpha}} - 1) \leqslant 2(\gamma_{20}+\gamma_{21})\bar{P}_2. \tag{L.3}$$

Since $r_\beta \in \mathcal{S}_\beta$ and $r_\alpha \in \mathcal{S}_\alpha$ by assumption, $\beta(r_\beta) \geqslant R_{1,\text{test}}$ and $\alpha(r_\alpha) \geqslant R_{1,\text{test}}$. By substituting the expressions in (L.1) into these bounds, and using the inequalities in (L.2) and (L.3) we have

$$r_\beta\big(2^{\frac{2R_{1,\text{test}}}{r_\beta}} - 1\big) \leqslant 2\bar{P}_1\gamma_{10} + 2\bar{P}_2\gamma_{20} - \hat{r}_\beta\big(2^{\frac{2R_{2,\text{tar}}}{\hat{r}_\beta}} - 1\big), \tag{L.4a}$$

$$r_\alpha\big(2^{\frac{2R_{1,\text{test}}}{r_\alpha}} - 1\big) \leqslant 2\bar{P}_1\gamma_{10} + 2\bar{P}_2\gamma_{20} - \hat{r}_\alpha\big(2^{\frac{2R_{2,\text{tar}}}{\hat{r}_\alpha}} - 1\big). \tag{L.4b}$$

It can be shown that $r(2^{\frac{2R_{1,\text{test}}}{r}} - 1)$ is convex decreasing in r (see (K.5)), and hence for any $r_3 = \mu r_\beta + (1-\mu)r_\alpha$, we have

$$\begin{aligned}
r_3(2^{\frac{2R_{1,\text{test}}}{r_3}} - 1) &\leqslant \mu r_\beta(2^{\frac{2R_{1,\text{test}}}{r_\beta}} - 1) + (1-\mu)r_\alpha(2^{\frac{2R_{1,\text{test}}}{r_\alpha}} - 1) \\
&\leqslant \mu\Big(2\bar{P}_1\gamma_{10} + (2\bar{P}_2\gamma_{20} - \hat{r}_1(2^{\frac{2R_{2,\text{tar}}}{\hat{r}_1}} - 1))\Big) \\
&\quad + (1-\mu)\Big(2\bar{P}_1\gamma_{10} - [\hat{r}_2(2^{\frac{2R_{2,\text{tar}}}{\hat{r}_2}} - 1) - 2\bar{P}_2\gamma_{20}]\Big) \\
&= 2\bar{P}_1\gamma_{10} + 2\bar{P}_2\gamma_{20} - \Big(\mu\hat{r}_1(2^{\frac{2R_{2,\text{tar}}}{\hat{r}_1}} - 1) + (1-\mu)\hat{r}_2(2^{\frac{2R_{2,\text{tar}}}{\hat{r}_2}} - 1)\Big) \\
&\leqslant 2\bar{P}_1\gamma_{10} + 2\bar{P}_2\gamma_{20} - \hat{r}_3(2^{\frac{2R_{2,\text{tar}}}{\hat{r}_3}} - 1)
\end{aligned} \tag{L.5}$$

If we choose r_3 such that $\hat{r}_3(2^{\frac{2R_{2,\text{tar}}}{\hat{r}_3}} - 1) = 2\bar{P}_2\gamma_{20}$, i.e., $R_{2,\text{tar}} = \frac{\hat{r}_3}{2}\log(1+\frac{2\bar{P}_2\gamma_{20}}{\hat{r}_3})$,[1] then we have $r_3(2^{\frac{2R_{1,\text{test}}}{r_3}} - 1) \leqslant 2\bar{P}_1\gamma_{10}$, and hence $R_{1,\text{test}} \leqslant \frac{r_3}{2}\log(1+\frac{2\bar{P}_1\gamma_{10}}{r_3})$. That is, for the choice $r = r_3$, direct transmission from both nodes (i.e., $\tilde{P}_{12} = 0$ and $\tilde{P}_{21} = 0$) yields a rate for Node 1 that is at least $R_{1,\text{test}}$. (Actually, direct transmission yields the largest achievable rate for Node 1 for this value of r.) Since direct transmission is a feasible solution to both (4.16) and (4.17), r_3 is an element of both $\mathcal{S}_\beta$ and $\mathcal{S}_\alpha$, and hence these sets intersect.

[1]The existence of an r_3 such that $\hat{r}_\beta \geqslant \hat{r}_3 \geqslant \hat{r}_\alpha$ follows directly from (L.2) and (L.3) and the decreasing nature of the function $\hat{r}(2^{\frac{2R_{2,\text{tar}}}{\hat{r}}} - 1)$ in $\hat{r}$.

Appendix M

Proof of Proposition 5.1

Assume that the solutions to (5.7) with $r = r_\alpha$ and $r = r_\beta$ are both greater than certain target rate $C_{1,\text{tar}}$. Let x_α and x_β denote the corresponding optimal values of $\tilde{P}_{R1}$. Then we have that

$$\frac{r}{2}\min\Big\{\log(1+\frac{2\gamma_{1R}\bar{P}_1}{r}),\log(1+\frac{2\gamma_{10}\bar{P}_1+\gamma_{R0}P_{R1}}{r})\Big\} \;\geqslant\; C_{1,\text{tar}}, \qquad \text{(M.1a)}$$

$$\frac{\hat{r}}{2}\min\Big\{\log(1+\frac{\gamma_{2r}\bar{P}_2}{\hat{r}}),\log(1+\frac{2\gamma_{20}\bar{P}_2+\gamma_{R0}P_{R2}}{\hat{r}})\Big\} \;\geqslant\; C_{2,\text{tar}}, \qquad \text{(M.1b)}$$

for $(r = r_\alpha, \tilde{P}_{R1} = x_\alpha)$ and $(r = r_\beta, \tilde{P}_{R1} = x_\beta)$. The inequalities in (M.1) can be written as

$$f_1(x_\alpha) \geqslant g_1(r_\alpha), \qquad f_1(x_\beta) \geqslant g_1(r_\beta), \qquad \text{(M.2a)}$$

$$f_2(x_\alpha) \geqslant g_2(r_\alpha), \qquad f_2(x_\beta) \geqslant g_2(r_\beta), \qquad \text{(M.2b)}$$

where

$$f_1(x) = \min\big\{2\gamma_{1R}\bar{P}_1, 2\gamma_{10}\bar{P}_1+\gamma_{R0}x\big\}, \qquad g_1(r) = r\big(2^{\frac{2C_{1,\text{tar}}}{r}}-1\big),$$

$$f_2(x) = \min\big\{2\gamma_{2r}\bar{P}_2, 2\gamma_{20}\bar{P}_2+\gamma_{R0}(2\bar{P}_R-x)\big\}, \qquad g_2(r) = \hat{r}\big(2^{\frac{2C_{2,\text{tar}}}{\hat{r}}}-1\big).$$

Examining these functions, we observe that $f_1(x)$ and $f_2(x)$ are both concave functions. By differentiating $g_1(r)$ twice with respect to r we obtain

$$\frac{d^2 g_1(r)}{dr^2} = \frac{4C_{1,\text{tar}}^2 \ln(2)^2 2^{\frac{2C_{1,\text{tar}}}{r}}}{r^3} \geqslant 0, \tag{M.3}$$

and hence, $g_1(r)$ is a convex function in r. Similarly, we can show that $g_2(r)$ is convex in r.

Now, if we consider $r_\gamma = \mu r_\alpha + \hat{\mu} r_\beta$ and $x_\gamma = \mu x_\alpha + \hat{\mu} x_\beta$, where $\mu \in [0,1]$ and $\hat{\mu} = 1 - \mu$, then

$$\begin{aligned} f_1(x_\gamma) &\geqslant_a \mu f_1(x_\alpha) + \hat{\mu} f_1(x_\beta) && \text{(M.4)} \\ &\geqslant \mu g_1(r_\alpha) + \hat{\mu} g_1(r_\beta) && \text{(M.5)} \\ &\geqslant_b g_1(r_\gamma), && \text{(M.6)} \end{aligned}$$

where a follows from the concavity of $f_1(x)$ and b follows from the convexity of $g_1(r)$. Similarly, it can be shown that

$$f_2(x_\gamma) \geqslant g_2(r_\gamma). \tag{M.7}$$

Hence, for any two values of r (namely, r_α and r_β), if there exist values of x (namely, x_α and x_β), such that the conditions in (M.1) are satisfied, then for any value of r that lies between r_α and r_β (namely, $r_\gamma = \mu x_\alpha + \hat{\mu} x_\beta$), there exists a value for x that lies between x_α and x_β (namely, $x_\gamma = \mu x_\alpha + \hat{\mu} x_\beta$) such that the conditions in (M.1) are satisfied. Therefore, the set of values of r for which the solution of the problem in (5.7) is greater than a certain target rate $C_{1,\text{tar}}$ is a convex set. Hence, the problem in (5.7) is quasi-concave in r.

Appendix N

Proof of Proposition 5.2

We begin by showing that the function $\frac{r}{2}\log\left((1+\frac{a}{r})(1+\frac{bx}{r})\right)$ is quasi-concave in the variables r and x, where a and b are non-negative constants. To do so, we assume that the pairs (r_α, x_α) and (r_β, x_β) satisfy

$$\frac{r}{2}\log\left(\left(1+\frac{a}{r}\right)\left(1+\frac{bx}{r}\right)\right) \geqslant M, \tag{N.1}$$

where M is a non-negative constant. We can write (N.1) as

$$f_0(r,x) \geqslant g_0(r), \tag{N.2}$$

where

$$f_0(r,x) = r + bx \qquad \text{and} \qquad g_0(r) = \frac{r^2 2^{\frac{2M}{r}}}{r+a}.$$

The function $f_0(r,x)$ is a linear function, while the function $g_0(r)$ can be shown to be convex function using the fact that

$$\frac{d^2 g_0(r)}{dr^2} = \frac{2a^2 2^{\frac{2a}{r}}(r^2(1-\ln(2))^2 + 2ar\ln(2)(2\ln(2)-1) + \ln(2)^2(r^2+2a^2))}{(r+a)^3 r^2} \geqslant 0. \tag{N.3}$$

Now, if we consider $r_\gamma = \mu r_\alpha + \hat{\mu} r_\beta$ and $x_\gamma = \mu x_\alpha + \hat{\mu} x_\beta$, where $\mu \in [0,1]$ and $\hat{\mu} = 1-\mu$, then

$$\begin{aligned} f_0(r_\gamma, x_\gamma) &= \mu f_0(r_\alpha, x_\alpha) + \hat{\mu} f_0(r_\beta, x_\beta) && \text{(N.4)} \\ &\geqslant \mu g_0(r_\alpha) + \hat{\mu} g_0(r_\beta) && \text{(N.5)} \\ &\geqslant_a g_0(r_\gamma), && \text{(N.6)} \end{aligned}$$

where a follows from the convexity of $g_1(r)$. Therefore, the set of pairs (r,x) that satisfy (N.1) is a convex set, and hence the function $\frac{r}{2}\log\big((1+\frac{a}{r})(1+\frac{bx}{r})\big)$ is quasi-concave in the variables r and x.

By obtaining its second derivative, it is straight forward to show that $\frac{r}{2}\log(1+\frac{2\gamma_{1R}\bar{P}_1}{r})$ is concave in r. Since the minimum of a concave function and a quasi-concave function is a quasi-concave function, then we can say that the function

$$\frac{r}{2}\min\left\{\log\left(1+\frac{2\gamma_{1R}\bar{P}_1}{r}\right), \log\left(1+\frac{2\gamma_{10}\bar{P}_1}{r}\right)+\log\left(1+\frac{\gamma_{R0}\tilde{P}_{R1}}{r}\right)\right\}$$

is quasi-concave in r and P_{R1}. Similarly, the function

$$\frac{\hat{r}}{2}\min\left\{\log\left(1+\frac{2\gamma_{2r}\bar{P}_2}{\hat{r}}\right), \log\left(1+\frac{2\gamma_{20}\bar{P}_2}{\hat{r}}\right)+\log\left(1+\frac{\gamma_{R0}(2\bar{P}_R-\tilde{P}_{R1})}{\hat{r}}\right)\right\}$$

can be shown to be quasi-concave in r and P_{R1}. Therefore, the problem in (5.9) is quasi-concave in r and P_{R1}. That is, the set of all pairs (r, P_{R1}) for which the solution of the problem (5.9) is greater than a target rate $C_{1,\text{tar}}$, i.e., the set of all pairs that satisfy

$$\frac{r}{2}\min\left\{\log\left(1+\frac{2\gamma_{1R}\bar{P}_1}{r}\right), \log\left(1+\frac{2\gamma_{10}\bar{P}_1}{r}\right)+\log\left(1+\frac{\gamma_{R0}\tilde{P}_{R1}}{r}\right)\right\} \geqslant C_{1,\text{tar}}, \quad \text{(N.7a)}$$

$$\frac{\hat{r}}{2}\min\left\{\log\left(1+\frac{2\gamma_{2r}\bar{P}_2}{\hat{r}}\right), \log\left(1+\frac{2\gamma_{20}\bar{P}_2}{\hat{r}}\right)+\log\left(1+\frac{\gamma_{R0}\tilde{P}_{R2}}{\hat{r}}\right)\right\} \geqslant C_{2,\text{tar}}, \quad \text{(N.7b)}$$

is a convex set.

Appendix O

Proof of Proposition 5.3

Consider the function

$$f(r,x) = r\log\left(1+\frac{a}{r}+\frac{bcx}{r(r+b+cx)}\right), \tag{O.1}$$

where a, b and c are positive constants and $(r,x) \in (0,1)\times\mathbb{R}_{++}$. We will avoid the cases where $r=0$ or $r=1$ because these cases correspond to scenarios in which one of the source nodes does not transmit. In those scenarios, the problem is easy to solve because all the relay power and all the channel resource will be allocated to the transmission of the message of the other source node. We will show that $f(r,x)$ is quasi-convex using the the second-order condition for the quasi-convexity which states that [5]: For any vector $\mathbf{z}$ such that $\mathbf{z}^T\nabla f = 0$, if the function f satisfies $\mathbf{z}^T\nabla^2 f\mathbf{z} < 0$, then f is quasi-concave.

For the function f, we denote the gradient as $\nabla f = [f_r,\ f_x]^T$, where $f_w = \frac{\partial f}{\partial w}$. Since $\nabla f \in \mathbb{R}^2$, the subspace orthogonal to ∇f will be a one dimensional subspace. Since the vector $\mathbf{z} = [-f_x,\ f_r]^T$ is orthogonal to ∇f, then all the vectors in the subspace orthogonal to ∇f are parallel to the vector $\mathbf{z}$. Examining the quantity

$\mathbf{z}^T\nabla^2 f\mathbf{z}$, we have that

$$\mathbf{z}^T\nabla^2 f\mathbf{z} = -A\frac{f(r,x)^2}{r^2} + B\frac{f(r,x)}{r} - C, \tag{O.2}$$

where A, B and C are positive quantities that depend on the constants a, b and c and the variables r and x. Equation (O.2) can be written as

$$\mathbf{z}^T\nabla^2 f\mathbf{z} = -\left[\left(\sqrt{A}\frac{f(r,x)}{r} - \sqrt{C}\right)^2 + \left(2\sqrt{AC} - B\right)\frac{f(r,x)}{r}\right]. \tag{O.3}$$

From (O.3), it can be seen that it is sufficient that $2\sqrt{AC} > B$ for the quantity $\mathbf{z}^T\nabla^2 f\mathbf{z}$ to be negative and consequently for the function $f(r,x)$ to be quasi-concave in (r,x). Since both the quantities $2\sqrt{AC}$ and B are positive, we can examine the quantities $4AC$ and B^2. In particular, it can be shown that

$$\begin{aligned} 4AC - B^2 \;=\; & 4(\underbrace{5abcxr^2 - bcxr^3} + \underbrace{3ab^2r^2 - b^2r^3} + \underbrace{abr^3 - br^4} + 4ab^3cx + 10ab^2cxr \\ & + 2b^3cxr + 2a^2c^2x^2r + 6a^2b^2r + 6a^2br^2 + 2a^2r^3 + 2a^2b^3 + 4bac^2x^2r \\ & + 4ab^2c^2x^2 + b^2r^2cx + 2a^2bc^2x^2 + 4a^2r^2cx + 8a^2bcxr + 4a^2b^2cx \\ & + 2arb^3 + 2b^2c^2x^2r + 2b^3c^2x^2)r^2b^3c^4(b+r)^2(b+cx+r)^{-4} \\ & \times(rb + rcx + r^2 + ab + acx + ar + bcx)^{-5}. \end{aligned} \tag{O.4}$$

The underbraced terms in (O.4) contain the negative terms in (O.4), each paired with a corresponding positive term. It can be seen that if $a \geqslant r$ then each of these underbraced terms is non-negative. Therefore, $a \geqslant 1$ is a sufficient condition for $4AC > B^2$, and hence is a sufficient condition for the function $f(r,x)$ to be quasi-concave.

By making the substitutions $a = 2\gamma_{10}\bar{P}_1$, $b = 2\gamma_{1R}\bar{P}_1$, $c = \gamma_{R0}$, and $x = P_{R1}$, the sufficient condition becomes $2\gamma_{10}\bar{P}_1 \geqslant 1$. That is, if the maximum achievable SNR of the direct channel of Node 1 is at least -3 dB, then the function $\frac{r}{2}\log\left(1 + \frac{2\gamma_{10}\bar{P}_1}{r} + \frac{2\gamma_{1R}\gamma_{R0}\bar{P}_1\bar{P}_{R1}}{r(r+2\gamma_{1R}\bar{P}_1+\gamma_{R0}\bar{P}_{R1})}\right)$ is quasi-concave in (r, P_{R1}). Similarly, we can

obtain that $2\gamma_{20}\bar{P}_2 \geqslant 1$ is a sufficient condition for the function

$$\frac{\hat{r}}{2}\log\left(1+\frac{2\gamma_{20}\bar{P}_2}{\hat{r}}+\frac{2\gamma_{2r}\gamma_{R0}\bar{P}_2\tilde{P}_{R2}}{\hat{r}(\hat{r}+2\gamma_{2r}\bar{P}_2+\gamma_{R0}\tilde{P}_{R2})}\right)$$

to be quasi-concave in $(\hat{r}, P_{R2})$. Therefore, the problem in (5.10) is quasi-concave in (r, P_{R1}) if the maximum achievable SNR of the direct channel of both nodes is at least -3dB.

Appendix P

Proof of Proposition 5.4

Following a similar proof to that in Appendix O, consider the function

$$f(r,x) = r\log\left(1+\frac{a}{r}+\frac{bc(a+r)x}{r(r^2+(a+b)r+c(a+r)x)}\right), \tag{P.1}$$

where a, b and c are positive constants and $(r,x) \in (0,1)\times\mathbb{R}_{++}$. Define $\mathbf{z}$ to be the vector orthogonal to the gradient subspace of the function $f(r,x)$, i.e., $\mathbf{z} = [-f_x,\ f_r]^T$. Examining the quantity $\mathbf{z}^T\nabla^2 f\mathbf{z}$, we have that

$$\begin{aligned}\mathbf{z}^T\nabla^2 f\mathbf{z} &= -\frac{A}{r^2}f(r,x)^2+\frac{B}{r}f(r,x)-C,\\ &= -\left[\left(\sqrt{A}\frac{f(r,x)}{r}-\sqrt{C}\right)^2+\left(2\sqrt{AC}-B\right)\frac{f(r,x)}{r}\right],\end{aligned} \tag{P.2}$$

where, of course A, B and C are different positive functions of a, b, c, r and x than those in Appendix O.

From (P.2) it can be seen that it is sufficient that $2\sqrt{AC} > B$ for $\mathbf{z}^T\nabla^2 f\mathbf{z}$ to be negative, and consequently for the function $f(r,x)$ to be quasi-concave in (r,x). Since both $2\sqrt{AC}$ and B are positive, we can examine

$$4AC-B^2 = 4b^3c^4r^5(\underbrace{20ba^3r^4-3bar^6}+\underbrace{18b^2a^3r^3-2b^2ar^5}+\underbrace{20bcxa^2r^4-bcxr^6}$$

$$
\begin{aligned}
&+ \underbrace{8b^2a^2r^4 - b^2r^6} + \underbrace{7ba^5r^2 - br^7} + 12a^2r^2b^2c^2x^2 + 2r^5cxb^2 + 2r^4c^2x^2b^2 \\
&+ 4ar^4bc^2x^2 + 2a^2r^4c^2x^2 + 2r^4cxb^3 + 10ar^4b^2cx + 2a^2r^6 + 24a^2r^3b^2cx \\
&+ 8ar^3b^2c^2x^2 + 11a^5bcxr + 10a^4xcrb^2 + 8a^5r^3 + 2a^6r^2 + 16a^2r^3bc^2x^2 \\
&+ 3a^3xcrb^3 + 37a^4r^2cxb + 16a^4x^2c^2rb + 9b^2r^2a^4 + 5a^2xcr^2b^3 + 2a^6x^2c^2 \\
&+ a^2r^2b^4 + 8a^3x^2c^2rb^2 + 26a^3b^2cxr^2 + 4a^2br^5 + 4a^2r^5cx + 24a^3br^2c^2x^2 \\
&+ 44a^3br^3cx + 8x^2c^2a^3r^3 + 12a^4r^2c^2x^2 + 24a^4r^3cx + 5b^3r^3a^2 + ar^5bcx \\
&+ 16a^3r^4cx + 12a^4r^4 + 4ar^3b^3cx + 8a^3r^5 + 2a^4x^2c^2b^2 + 4a^6rcx \\
&+ 8a^5c^2x^2r + 4a^5x^2c^2b + 16a^5r^2cx + 5b^3r^2a^3 + 21a^4r^3b) \\
&\times (2ar + r^2 + a^2 + ab + rb)^{-2}(cx + r)^{-4}(acx + rcx + ar + rb + r^2)^{-5}
\end{aligned}
\tag{P.3}
$$

The underbraced terms of (P.3) contain the negative terms in (P.3), each paired with a corresponding positive terms. It can be seen that if $a \geqslant r$, each of these underbraced terms is non-negative. Therefore, $a \geqslant 1$ is a sufficient condition for $4AC > B^2$, and hence for the function $f(r, x)$ to be quasi-concave.

Making the substitutions $a = 2\gamma_{10}\bar{P}_1$, $b = 2\gamma_{1R}\bar{P}_1$, $c = \gamma_{R0}$, and $x = P_{R1}$, the sufficient condition becomes $2\gamma_{10}\bar{P}_1 \geqslant 1$. That is, if the maximum achievable SNR of the direct channel of Node 1 is at least -3 dB, then the function $\frac{r}{2}\log\left(1 + \frac{2\gamma_{10}\bar{P}_1}{r} + \frac{2\gamma_{1R}\gamma_{R0}\bar{P}_1(2\gamma_{10}\bar{P}_1 + r)\bar{P}_{R1}}{r(r^2 + 2(\gamma_{10}+\gamma_{1R})\bar{P}_1 r + \gamma_{R0}(2\gamma_{10}\bar{P}_1 + r)\bar{P}_{R1})}\right)$ is quasi-concave in (r, P_{R1}). Similarly, we can obtain that $2\gamma_{20}\bar{P}_2 \geqslant 1$ is a sufficient condition for the function $\frac{\hat{r}}{2}\log\left(1 + \frac{2\gamma_{20}\bar{P}_2}{\hat{r}} + \frac{2\gamma_{2R}\gamma_{R0}\bar{P}_2(2\gamma_{20}\bar{P}_2 + \hat{r})\bar{P}_{R2}}{\hat{r}(\hat{r}^2 + 2(\gamma_{20}+\gamma_{2R})\bar{P}_2\hat{r} + \gamma_{R0}(2\gamma_{20}\bar{P}_2 + \hat{r})\bar{P}_{R2})}\right)$ to be quasi-concave in $(\hat{r}, P_{R2})$. Therefore, the problem in (5.12) is quasi-concave in (r, P_{R1}) if the maximum achievable SNR of the direct channel of both nodes is at least -3dB.

Bibliography

[1] P. A. Anghel, M. Kaveh, and Z. Q. Luo, "Optimal relayed power allocation in interference-free non-regenerative cooperative systems," in *Proc. IEEE 5th Workshop Signal Processing Advances in Wireless Commun.*, Lisbon, July 2004, pp. 21–25.

[2] ——, "An efficient algorithm for optimum power allocation in decode-and-forward cooperative system with orthogonal transmissions," in *Proc. IEEE Int. Conf. Acoustics, Speech, Signal Processing*, May 2006, pp. IV–685– IV–688.

[3] R. Annavajjala, P. C. Cosman, and L. B. Milstein, "Statistical channel knowledge-based optimum power allocation for relaying protocols in the high SNR regime," *IEEE J. Select. Areas Commun.*, vol. 25, no. 2, pp. 292–305, Feb. 2007.

[4] K. Azarian, H. El Gamal, and P. Schniter, "On the achievable diversity-multiplexing tradeoff in half-duplex cooperative channels," *IEEE Trans. Inform. Theory*, vol. 51, no. 12, pp. 4152–4172, Dec. 2005.

[5] S. Boyd and L. Vandenberghe, *Convex Optimization.* Cambridge University Press, 2004.

[6] A. B. Carleial, "Multiple-access channels with different generalized feedback signals," *IEEE Trans. Inform. Theory*, vol. 28, no. 6, p. 841, Nov. 1982.

[7] D. Chen and J. N. Laneman, "Modulation and demodulation for cooperative diversity in wireless systems," *IEEE Trans. Wireless Commun.*, vol. 5, no. 7, pp. 1785–1794, July 2006.

[8] S. T. Chung and A. J. Goldsmith, "Degrees of freedom in adaptive modulation: a unified view," *IEEE Trans. Commun.*, vol. 49, no. 9, pp. 1561–1571, Sept. 2001.

[9] T. M. Cover and J. A. Thomas, *Elements of information theory.* New York: Wiley, 1991.

[10] T. M. Cover and A. El Gamal, "Capacity theorems for the relay channel," *IEEE Trans. Inform. Theory*, vol. 25, no. 5, Sept. 1979.

[11] T. M. Cover and C. S. K. Leung, "An achievable rate region for the multiple-access channel with feedback," *IEEE Trans. Inform. Theory*, vol. 27, no. 3, May 1981.

[12] A. del Coso and C. Ibars, "The amplify-based multiple-relay multiple-access channel: capacity region and MAC-BC duality," in *Proc. IEEE Wkshp Inform. Theory for Wireless Networks*, July 2007, pp. 1–5.

[13] Y. Ding and K. M. Wong, "The amplify-and-forward half-duplex cooperative system: Pairwise error probability and precoder design," *IEEE Trans. Signal Processing*, vol. 55, no. 2, pp. 605–617, 2007.

[14] A. El Gamal and S. Zahedi, "Capacity of a class of relay channels with orthogonal components," *IEEE Trans. Inform. Theory*, vol. 51, no. 5, pp. 1815–1817, May 2005.

[15] H. E. Gamal, G. Caire, and M. O. Damen, "On the optimality of lattice space-time (LAST) coding," in *Proc. IEEE Int. Symp. Inform. Theory*, June 2004, p. 96.

[16] ——, "On the optimality of incremental redundancy last coding," in *Proc. Int. Conf. Wireless Networks, Communications, Mobile Computing*, Maui, HI, June 2005.

[17] M. Gastpar, G. Kramer, and P. Gupta, "The multiple-relay channel: coding and antenna-clustering capacity," in *Proc. IEEE Int. Symp. Inform. Theory*, Lausanne, Switzerland, July 2002, p. 136.

[18] M. Gastpar and M. Vetterli, "On the capacity of large gaussian relay networks," *IEEE Trans. Inform. Theory*, vol. 51, no. 3, pp. 765–779, Mar. 2005.

[19] A. J. Goldsmith and S. G. Chua, "Adaptive coded modulation for fading channels," *IEEE Trans. Commun.*, vol. 46, no. 5, pp. 595 – 602, May 1998.

[20] P. Gupta and P. R. Kumar, "Towards and information theory of large networks: An achievable rate region," *IEEE Trans. Inform. Theory*, vol. 49, pp. 1877–1894, Aug. 2003.

[21] A. Høst-Madsen, "On the capacity of wireless relaying," in *Proc. IEEE Veh. Technol. Conf.*, Sept. 2002, pp. 1333–1337.

[22] A. Høst-Madsen and J. Zhang, "Capacity bounds and power allocation for wireless relay channels," *IEEE Trans. Inform. Theory*, vol. 51, no. 6, pp. 2020–2040, June 2005.

[23] T. E. Hunter and A. Nosratinia, "Coded cooperation under slow fading, fast fading, and power control," in *Proc. Asilomar Conf. Signals, Systems, Computers*, Pacific Grove, CA, 2002, pp. 118–122.

[24] ——, "Cooperative diversity through coding," in *Proc. IEEE Int. Symp. Inform. Theory*, June/July 2002, p. 220.

[25] ——, "Performance analysis of coded cooperation diversity," in *Proc. IEEE Int. Conf. Commun.*, Anchorage, AK, May 2003, pp. 2688–2692.

[26] ——, "Diversity through coded cooperation," *IEEE Trans. Wireless Commun.*, vol. 5, no. 2, pp. 283–289, Feb. 2006.

[27] O. Ileri, S.-C. Mau, and N. B. Mandayam, "Pricing for enabling forwarding in self-configuring ad hoc networks," *IEEE J. Select. Areas Commun.*, vol. 23, no. 1, pp. 151–162, Jan. 2005.

[28] S. A. Jafar and K. S. Gomadam, "Duality and capacity region of AF relay MAC and BC," arXiv:0608060v1 [cs.IT].

[29] M. Janani, A. Hedayat, T. E. Hunter, and A. Nosratinia, "Coded cooperation in wireless communications: space-time transmission and iterative decoding," *IEEE Trans. Signal Processing*, vol. 52, no. 2, pp. 362–371, Feb. 2004.

[30] O. Kaya and S. Ulukus, "Power control for fading multiple access channels with user cooperation," in *Proc. Int. Conf. Wireless Networks, Communications, Mobile Computing*, Maui, HI, June 2005.

[31] ——, "Power control for fading cooperative multiple access channels," *IEEE Trans. Wireless Commun.*, vol. 6, no. 8, pp. 2915–2923, 2007.

[32] B. Khoshnevis, W. Yu, and R. Adve, "Grassmannian beamforming for MIMO amplify-and-forward relaying," arxiv:0710.5758v1 [cs.IT].

[33] R. C. King, "Multiple access channels with generalized feedback," ph.D. thesis, Stanford Univ., Stanford, CA, March 1978.

[34] G. Kramer, M. Gastpar, and P. Gupta, "Cooperative strategies and capacity theorems for relay networks," *IEEE Trans. Inform. Theory*, vol. 51, no. 9, pp. 3037–3063, Sept. 2005.

[35] G. Kramer and A. J. van Wijngaarden, "On the white Gaussian multiple-access relay channel," in *Proc. IEEE Int. Symp. Inform. Theory*, Sorrento, Italy, June 25–30 2000.

[36] L. Lai, K. Liu, and H. El Gamal, "The three node wireless network: Achievable rates and cooperation strategies," *IEEE Trans. Inform. Theory*, vol. 52, no. 3, pp. 805–828, Mar. 2006.

[37] J. N. Laneman, "Cooperative diversity in wireless networks: algorithms and architectures," ph.D. thesis, Massachusetts Institute of Technology, Cambridge, MA, September 2002.

[38] J. N. Laneman, D. N. C. Tse, and G. W. Wornell, "Cooperative diversity in wireless networks: Efficient protocols and outage behavior," *IEEE Trans. Inform. Theory*, vol. 50, no. 12, pp. 3062–3080, Dec. 2004.

[39] E. G. Larsson and Y. Cao, "Collaborative transmit diversity with adaptive radio resource and power allocation," *IEEE Communication Letters*, vol. 9, no. 6, pp. 511–513, June 2005.

[40] Y. Liang and G. Kramer, "Rate regions for relay broadcast channels," *IEEE Trans. Inform. Theory*, vol. 53, no. 10, pp. 3517–3535, Oct. 2007.

[41] Y. Liang and V. V. Veeravalli, "Gaussian orthogonal relay channels: optimal resource allocation and capacity," *IEEE Trans. Inform. Theory*, vol. 51, no. 9, pp. 3284–3289, Sept. 2005.

[42] ——, "Cooperative relay broadcast channels," *IEEE Trans. Inform. Theory*, vol. 53, no. 3, pp. 900–928, Mar. 2007.

[43] I. Maric and R. D. Yates, "Bandwidth and power allocation for cooperative strategies in Gaussian relay networks," in *Proc. Asilomar Conf. Signals, Systems, Computers*, Nov. 2004, pp. 1907–1911.

[44] ——, "Forwarding strategies for Gaussian parallel-relay networks," in *Proc. IEEE Int. Symp. Inform. Theory*, 27 June–2 July 2004, p. 270.

[45] W. Mesbah and T. N. Davidson, "Joint power and resource allocation for orthogonal amplify-and-forward pairwise user cooperation," To appear in *IEEE Trans. Wireless Commun.*

[46] ——, "Optimal power allocation for full-duplex cooperative multiple access," in *Proc. IEEE Int. Conf. Acoustics, Speech, Signal Processing*, Toulouse, May 2006, pp. 689–692.

[47] ——, "Optimal power and resource allocation for half-duplex cooperative multiple access," in *Proc. IEEE Int. Conf. Commun.*, Istanbul, June 2006, pp. 4469–4473.

[48] ——, "Joint power and resource allocation for orthogonal amplify-and-forward pairwise user cooperation," in *Proc. IEEE Int. Conf. Acoustics, Speech, Signal Processing*, Las Vegas, NV, March 30– April 4 2008.

[49] ——, "Optimization of a modified orthogonal amplify-and-forward pairwise user cooperation," in *Proc. IEEE Wireless Commun. Network. Conf.*, Las Vegas, NV, 31 March– 3 April 2008.

[50] ——, "Optimized power allocation for pairwise cooperative multiple access," *IEEE Trans. Signal Processing*, vol. 56, no. 7, pp. 2994–3008, July 2008.

[51] ——, "Power and resource allocation for orthogonal multiple access relay systems," *EURASIP Journal of Advanced Signal Processing. Special Issue on Cooperative Wireless Networks*, May 2008.

[52] ——, "Power and resource allocation for orthogonal multiple access relay systems," in *Proc. IEEE Int. Symp. Inform. Theory*, Toronto, ON, July 2008.

[53] R. U. Nabar, H. Bolcskei, and F. W. Kneubuhler, "Fading relay channels: performance limits and space-time signal design," *IEEE J. Select. Areas Commun.*, vol. 22, no. 6, pp. 1099–1109, Aug. 2004.

[54] T. C.-Y. Ng and W. Yu, "Joint optimization of relay strategies and resource allocations in cooperative cellular networks," *IEEE J. Select. Areas Commun.*, vol. 25, no. 2, pp. 328–339, Feb. 2007.

[55] C. Pan, Y. Cai, and Y. Xu, "Relay MAC channels: Capacity and resource allocation," in *Proc. IEEE Vehicular Tech. Conf.*, Dublin, Apr. 2007, pp. 2900–2904.

[56] T. Q. S. Quek, M. Z. Win, H. Shin, and M. Chiani, "Optimal power allocation for amplify-and-forward relay networks via conic programming," in *Proc. IEEE Int. Conf. Commun.*, Glasgow, June 2007, pp. 5058–5063.

[57] P. Razaghi and W. Yu, "Parity forwarding for multiple relay networks," submitted to the *IEEE Transactions on Information Theory, November 2007.*

[58] ——, "Bilayer low-density parity-check codes for decode-and-forward in relay channels," *IEEE Trans. Inform. Theory*, vol. 53, no. 10, pp. 3723–3739, Oct. 2007.

[59] A. Reznik, S. Kulkarni, and S. Verdu, "Capacity and optimal resource allocation in the degraded Gaussian relay channel with multiple relays," in *Proc. Allerton Conf. Commun., Control, Computing*, Monticello, IL, Oct. 2002.

[60] L. Sankaranarayanan, G. Kramer, and N. B. Mandayam, "Capacity theorems for the multiple-access relay channels," in *Proc. 42nd Ann. Allerton Conf. Commun., Control, Computing*, Monticello, IL, Sept. 2004.

[61] ——, "Hierarchical sensor networks: capacity bounds and cooperative strategies using the multiple-access relay channel model," in *Proc. IEEE Sensor Ad Hoc Commun. Networks Conf.*, Santa Clara, CA, Oct. 2004, pp. 191–199.

[62] ——, "Cooperation vs. hierarchy: an information-theoretic comparison," in *Proc. IEEE Int. Symp. Inform. Theory*, Adelaide, Australia, Sept. 2005, pp. 411–415.

[63] H. Sato, "Information transmission through a channel with relay," the Aloha System, University of Hawaii, Honolulu, Tech. Rep. B76–7, Mar. 1976.

[64] B. Schein and R. G. Gallager, "The Gaussian parallel relay network," in *Proc. IEEE Int. Symp. Inform.Theory*, Sorrento, Italy, 2000, p. 22.

[65] K. Seddik, A. K. Sadek, W. Su, and K. J. R. Liu, "Outage analysis and optimal power allocation for multi-node amplify-and-forward relay networks," *IEEE Signal Processing Letters*, vol. 14, no. 6, pp. 377–380, June 2007.

[66] A. Sendonaris, E. Erkip, and B. Aazhang, "User cooperation diversity—Part I: System description," *IEEE Trans. Commun.*, vol. 51, no. 11, pp. 1927–1938, Nov. 2003.

[67] ——, "User cooperation diversity—Part II: Implementation aspects and performance analysis," *IEEE Trans. Commun.*, vol. 51, no. 11, pp. 1939–1948, Nov. 2003.

[68] S. Serbetli and A. Yener, "Relay assisted F/TDMA ad hoc networks: Node classification, power allocation and relaying strategies," *IEEE Trans. Commun.*, vol. 56, no. 6, pp. 937–947, June 2008.

[69] C. E. Shannon, "Communication in the presence of noise," in *Proc. IRE*, vol. 18, 1949, pp. 10 – 21.

[70] A. Stefanov and E. Erkip, "Cooperative coding for wireless networks," *IEEE Trans. Commun.*, vol. 52, no. 9, pp. 1470–1476, Sept. 2004.

[71] E. Telatar, "Capacity of multi-antenna gaussian channels," *European Trans. Telecommun.*, vol. 10, no. 6, pp. 585–596, 1999.

[72] K. Tourki, D. Gesbert, and L. Deneire, "Cooperative diversity using per-user power control in multiuser MAC channel," in *Proc. IEEE Int. Symp. Inform. Theory*, Nice, June 2007, pp. 1911–1915.

[73] D. N. C. Tse, P. Viswanath, and L. Zheng, "Diversity-multiplexing tradeoff in multiple-access channels," *IEEE Trans. Inform. Theory*, vol. 50, no. 9, pp. 1859–1874, Sept. 2004.

[74] D. N. C. Tse and P. Viswanath, *Fundamentals of wireless communication.* Cambridge University Press, 2005.

[75] E. Van Der Meulen, "Transmission of information in a T-terminal discrete memoryless channel," ph.D. dissertation, Dep. of Statistics, University of California, Berkeley, 1968.

[76] ——, "Three terminal communication channels," *Adv. Appl. Probability*, vol. 3, pp. 120–154, 1971.

[77] ——, "A survey of multi-way channels in information theory: 1961-1976," *IEEE Trans. Inform. Theory*, vol. 23, no. 2, Jan. 1977.

[78] F. M. J. Willems, "The discrete memoryless multiple access channel with partially cooperating encoders," *IEEE Trans. Inform. Theory*, vol. 29, no. 3, pp. 441–445, May 1983.

[79] F. M. J. Willems and E. Van Der Meulen, "Partial feedback for the discrete memoryless multiple access channel," *IEEE Trans. Inform. Theory*, vol. 29, no. 2, pp. 287–290, Mar. 1983.

[80] ——, "The discrete memoryless multiple access channel with cribbing encoders," *IEEE Trans. Inform. Theory*, vol. 31, no. 3, pp. 313–327, Mar. 1985.

[81] F. M. J. Willems, E. Van Der Meulen, and J. P. M. Schalkwijk, "An achievable rate region for the multiple access channel with generalized feedback," in *Proc.*

Allerton Conf. Commun., Control, Computing, Monticello, IL, 1983, pp. 284–292.

[82] A. Wyner and J. Ziv, "The rate-distortion function for source coding with side information at the decoder," *IEEE Trans. Inform. Theory*, vol. 22, no. 1, Jan. 1976.

[83] L. Xie and X. Zhang, "TDMA and FDMA based resource allocations for quality of service provisioning over wireless relay networks," in *Proc. IEEE Wireless Commun. Networking Conf.*, Hong Kong, Mar. 2007, pp. 3153–3157.

[84] J. Yang and D. R. Brown III, "The effect of channel state information on optimum energy allocation and energy efficiency of cooperative wireless transmission systems," in *Proc. Conf. Inform. Sci. Syst.*, Princeton, NJ, Mar. 2006, pp. 1044–1049.

[85] M. Yuksel and E. Erkip, "Multi-antenna cooperative wireless systems: A diversity-multiplexing tradeoff perspective," *IEEE Trans. Inform. Theory*, vol. 53, no. 10, pp. 3371–3393, Oct. 2007.

[86] B. Zhao and M. Valenti, "Distributed turbo coded diversity for the relay channel," *IEE Electron. Lett.*, vol. 39, no. 10, pp. 786–787, May 2003.

[87] L. Zheng and D. N. C. Tse, "Diversity and multiplexing: a fundamental tradeoff in multiple antenna channels," *IEEE Trans. Inform. Theory*, vol. 49, pp. 1073–1096, May 2003.